

Norwegian University  
of Life Sciences

**Master's Thesis 2020 60 ECTS**

Faculty of Chemistry, Biotechnology and Food Science  
Morten Kjos

# **Using CRISPR interference to study novel biofilm-associated genes in *Staphylococcus aureus***

Marita Torrissen Mårli  
Biotechnology



## **Acknowledgements**

This master thesis was completed as part of the Master program in Biotechnology at the University of Life Sciences (NMBU). The work was conducted in the Molecular Microbiology research group at the Faculty of Chemistry, Biotechnology and Food Science (KBM) in the period from August 2019 to June 2020.

First and foremost, I would like to thank my main supervisor, Dr. Morten Kjos, for his guidance through each stage of the process. Thank you for always taking your time to answer any questions and for helping me both in the lab and during the writing process. I would also like to thank my co-supervisor Dr. Christian Kranjec for help and guidance in the lab.

A big thank you to everyone in the Molecular Microbiology group for support and guidance, and for providing an excellent work environment and many fun moments to look back on. An extra thanks to Zhian Salehian for always lending a helping hand with troublesome PCR reactions and guidance in the lab whenever needed. I would also like to thank both Zhian Salehian and Dr. Danae Morales Angeles for helping me finish my last projects when the university closed down for students due to covid-19.

Thanks to my fellow master students Anette, Ingvild and Jeanette for social support during this year, and for always having someone to complain to. And thank you to my co-student Eirin for being there through all the stressful times with lab reports and exams, and for always being supportive.

Lastly, a huge thank you to my friends and family who have kept up with me, and always supported me.

Marita Torrissen Mårli

Ås, June 2020



## Abstract

The opportunistic pathogen *S. aureus* causes biofilm-associated infections which are often chronic and difficult to eradicate. As *S. aureus* is often resistant to multiple antibiotics, understanding the underlying processes of biofilm formation and regulation is crucial to identify novel treatment strategies. Although many genes have already been implicated to be involved in *S. aureus* biofilm formation, much is still unknown. Functional studies of genes by deletion or inactivation is time-consuming and restricted to non-essential genes. In this work, knockdown of gene expression by CRISPR interference (CRISPRi) was explored as a method to identify new biofilm-associated genes in *S. aureus*.

Initially it was shown that CRISPRi can be used as a fast and simple method to study biofilm-associated genes in *S. aureus* in two different biofilm model systems, namely the crystal violet microtiter plate assay and the macrocolony formation assay. Thereafter, several new putative biofilm-associated genes were identified. By CRISPRi-based knockdown of gene expression for a selection of genes, we identified three WalRK regulated genes involved in biofilm formation in the crystal violet microtiter plate assay. While two of the genes, *atl* and *sle1* have already been associated with biofilm formation, we also discovered an uncharacterized gene *SAOUHSC\_00671* whose role in biofilm formation is still unknown. *SAOUHSC\_00671* depleted cells showed a reduction in biofilm formation and increased clustering when analyzed by confocal microscopy. *SAOUHSC\_00671* harbors LysM domains and a CHAP domain, suggesting that this protein might be a cell wall hydrolase, whose role in *S. aureus* biofilm needs to be further investigated.

A genome wide CRISPRi library was used to screen for novel biofilm genes using a macrocolony formation assay. With this approach, several genes of the central metabolic pathways were found to affect the wrinkling and structuring of *S. aureus* macrocolonies. These include PckA, involved in gluconeogenesis, and FumC and SucA, both involved in the TCA cycle. Furthermore, depletion of *ubiE* and *hemE*, encoding enzymes involved in the synthesis of menaquinone and heme, respectively, resulted in macrocolonies with a loss of structure and surface wrinkling. Based on these data, we propose a link between macrocolony formation and respiratory metabolism in *S. aureus*. Finally, in the same screen, a putative methyltransferase was also shown to be important for *S. aureus* macrocolony structuring, and the molecular function of this gene needs to be further investigated.



## Sammendrag

*S. aureus* er en opportunistisk bakterie som forårsaker biofilm-relaterte infeksjoner som ofte er kroniske og vanskelig å behandle. Siden *S. aureus* også ofte er resistent mot flere antibiotika, er det viktig å finne nye behandlingsmetoder. For å kunne gjøre dette er det nødvendig å forstå prosessene som ligger til grunn for biofilm dannelse- og regulering. Selv om mange gener allerede har blitt beskrevet i *S. aureus* biofilm, er det fortsatt mye som er ukjent. Det å studere gen-funksjonalitet i *S. aureus* er en tidkrevende prosess som også er begrenset til å studere ikke-essensielle gener. I dette arbeidet har vi undersøkt om nedregulering av genekspresjon ved CRISPR interferens (CRISPRi) kan brukes som en metode for å identifisere nye biofilm-relaterte gener i *S. aureus*.

Det ble innledningsvis vist at CRISPRi kan brukes som en rask og enkel metode for å studere gener involvert i biofilm dannelse i *S. aureus* ved hjelp av to ulike modell systemer, krystallfiolett-mikrotiterassayet og et makrokoloniassay. Deretter ble det identifisert flere nye gener som potensielt er involvert i biofilm dannelse. Ved å slå ned genekspresjon ved bruk av CRISPRi for en rekke gener, identifiserte vi tre gener under regulering av WalRK som var involvert i biofilmdannelse i krystallfiolett-mikrotiterassayet. Selv om to av disse genene, *atl* og *sle1*, allerede har blitt assosiert med biofilmdannelse, identifiserte vi et gen, *SAOUHSC\_00671*, hvis rolle i biofilmdannelse fortsatt er ukjent. Celler hvor *SAOUHSC\_00671* ekspresjon var slått ned viste en reduksjon av biofilm. Uvanlige klynger av celler ble observert ved bruk av konfokal mikroskopi. *SAOUHSC\_00671* har flere LysM domener i tillegg til et CHAP domene, noe som indikerer at dette proteinet potensielt er involvert i hydrolyse av cellevegg. Rollen til dette proteinet i biofilmdannelse krever videre undersøkelser.

Ved bruk av et CRISPRi bibliotek ble det gjennomført et genomskala makrokoloniassayeksperiment for å lete etter nye gener involvert i biofilmdannelse. Genene *pckA*, som er involvert i glukoneogenesen, samt *fumC* og *sucA* som er involvert i TCA syklusen viste seg å påvirke struktureringen av makrokolonier. Videre viste det seg at mangelen på UbiE og HemE, enzymer som er involvert i henholdsvis syntese av menaquinone (vitamin K<sub>2</sub>) og heme, resulterte i makrokolonier med tap av struktur og rynker. Basert på disse resultatene foreslår vi en forbindelse mellom makrokolonidannelse og respirasjon i *S. aureus*. Avslutningsvis fant vi, i den samme screeningen, en potensiell metyltransferase som også viste seg å være viktig for strukturering av makrokolonier i *S. aureus*. De molekylære funksjonene til dette genet krever videre studier.



# Index

<b>1</b>	<b>Introduction.....</b>	<b>1</b>
1.1	<i>Staphylococcus aureus</i> .....	1
1.1.1	Clinical impact and antibiotic resistance.....	1
1.1.2	Pathogenesis.....	3
1.1.3	Virulence factors .....	4
1.1.4	Metabolism.....	5
1.2	Biofilm formation in <i>S. aureus</i> .....	7
1.2.1	Stages of biofilm development.....	8
1.2.2	Regulation of <i>S. aureus</i> biofilm formation.....	11
1.3	<i>In vitro</i> model systems in <i>S. aureus</i> biofilm research.....	13
1.3.1	The microtiter plate assay .....	13
1.3.2	Confocal laser scanning microscopy.....	14
1.3.3	The macrocolony biofilm model .....	15
1.4	Functional genetics using CRISPR interference .....	15
1.4.1	Genetic engineering in <i>S. aureus</i> .....	15
1.4.2	CRISPR/Cas9 and CRISPR interference for transcriptional knockdown.....	16
1.5	Aim of the study .....	20
<b>2</b>	<b>Materials .....</b>	<b>21</b>
2.1	Strains and plasmids .....	21
2.2	Primers.....	22
2.3	Enzymes and chemicals.....	23
2.4	Kits and equipment.....	24
2.5	Growth medium, buffers and solutions .....	25
<b>3</b>	<b>Methods.....</b>	<b>27</b>
3.1	Growth and storage of <i>E. coli</i> and <i>S. aureus</i> .....	27
3.2	Plasmid isolation.....	27
3.3	Isolation of genomic DNA .....	28
3.4	The polymerase chain reaction .....	28
3.4.1	Colony PCR screening .....	30
3.5	Agarose gel electrophoresis.....	31

3.5.1	Extraction of DNA from agarose gels.....	32
3.6	Restriction digestion and ligation.....	33
3.7	Targeted gene sequencing .....	35
3.8	Generation of <i>S. aureus</i> genetically modified strains.....	35
3.8.1	Transformation in <i>E. coli</i> .....	35
3.8.2	Transformation in <i>S. aureus</i> .....	36
3.8.3	Blue white screening.....	37
3.8.4	Construction of a NCTC8325-4 <i>SAOUCHS_00671</i> knockout mutant .....	38
3.8.5	Construction of a NCTC8325-4 SA00671 overexpression mutant.....	40
3.8.6	Construction of a NCTC8325-4 $\Delta$ SAOUHSC_00671 complementation strain .....	41
3.8.7	Construction of a Newman $\Delta$ <i>ubiE::spc</i> allelic exchange plasmid.....	41
3.8.8	Construction of <i>S. aureus</i> CRISPRi strains.....	42
3.9	Growth curves.....	43
3.10	Biofilm assays.....	44
3.10.1	The crystal violet microtiter plate assay.....	44
3.10.2	Macrocolony formation.....	45
3.10.3	Screening a pooled CRISPRi library for genes involved in macrocolony formation .....	45
3.10.4	Confocal laser scanning microscopy.....	46
<b>4</b>	<b>Results .....</b>	<b>47</b>
4.1	Using CRISPR interference to study biofilm formation in <i>S. aureus</i> .....	47
4.1.1	Construction of a <i>S. aureus</i> CRISPR interference strain collection for knockdown of proposed biofilm-related genes.....	47
4.1.2	Using CRISPR interference and the crystal violet microtiter plate assay to study <i>S. aureus</i> biofilm formation .....	48
4.1.3	Using CRISPR interference to study <i>S. aureus</i> macrocolony formation .....	55
4.2	Screening for WalRK regulated genes involved in biofilm formation.....	58
4.3	SAOUHSC_00671 is involved in <i>S. aureus</i> biofilm formation .....	60
4.4	Identification of novel genes involved in <i>S. aureus</i> macrocolony formation using a CRISPR interference pooled library.....	67
4.5	Impaired respiration alters <i>S. aureus</i> macrocolony formation.....	70
4.6	Lack of the putative methyltransferase NWMN_RS14065 alters macrocolony formation .....	72
<b>5</b>	<b>Discussion.....</b>	<b>75</b>

5.1	CRISPRi can be used to study biofilms of <i>S. aureus</i> model strains in two different assays .....	75
5.2	The crystal violet microtiter assay to study genes involved in biofilm by CRISPRi ..	77
5.3	SAOUHSC_00671 is a potential new biofilm associated protein regulated by the WalRK system .....	80
5.4	Macrocolony formation can be used as a simple biofilm model in screening for novel biofilm associated genes using a pooled CRISPRi library .....	82
5.5	Fully functional gluconeogenesis and TCA cycle are needed for proper macrocolony formation .....	84
5.6	A functional respiration is needed for proper macrocolony formation .....	85
5.7	A putative methyltransferase seems to be important for macrocolony formation .....	87
<b>6</b>	<b>Concluding remarks and future research.....</b>	<b>89</b>
	<b>References .....</b>	<b>91</b>
	<b>Appendix .....</b>	<b>103</b>



# 1 Introduction

## 1.1 *Staphylococcus aureus*

The first reports on staphylococci date from the early 1880's in a series of clinical observations and laboratory studies published by the surgeon Alexander Ogston. He observed micrococci clustering together like grapes, resulting in the organism being named *Staphylococcus* from the Greek words *Staphyle* and *kokkos* meaning “bunch of grapes” and “berries”, respectively (Lowy, 1998; Ogston, 1881; Ogston, 1882). Still, almost 140 years later, *Staphylococcus aureus* remains a major cause of human disease and is the best-studied staphylococcal species together with *Staphylococcus epidermidis*.

### 1.1.1 Clinical impact and antibiotic resistance

*S. aureus* is a frequent cause of infections in both the community and in hospitals. The European Centre for Disease Control (ECDC) estimates in a point prevalence study that 3.2 million people acquire a healthcare associated infection (HAI) annually in acute care hospitals in the European Union (EU) and the European Economic Area (EEA) (ECDC, 2013). *S. aureus* is among the most prevalent pathogens that are associated with HAIs (Khan et al., 2015), with the ECDC estimating that approximately 12.3% of HAIs in the EU/EEA are being caused by *S. aureus*. In the United States, *S. aureus* is the most frequently occurring bacterial pathogen among clinical isolates from hospital inpatients, and the second most occurring bacterial pathogen among clinical isolates from outpatients (Naber, 2009; Styers et al., 2006).

*S. aureus* is also a common colonizer of the skin and nostrils of healthy humans, with approximately 30% being persistently colonized (Lindsay, 2014). Infections with *S. aureus* begins when the microorganism enters through a breach in the skin or mucosa and can cause local infections or spread to distant organs. *S. aureus* can cause a large range of infections, including skin and soft tissue infections (SSTIs), muscle and visceral abscesses, septic arthritis, osteomyelitis, endocarditis, pneumonia, brain abscesses, meningitis and bacteremia, as well as sepsis, toxic shock syndrome, and food poisoning (Lowy, 1998; Tong et al., 2015).

Acquisition of new DNA by horizontal gene transfer (HGT) has been important for the adaptation of *S. aureus* to different environments and for its success as both a colonizer and a pathogen. Through HGT *S. aureus* dramatically alter the ability to evade antibiotics, colonize new hosts and

## 1 Introduction

adapt to new environments (Lindsay, 2014), making *S. aureus* especially capable to adapt to the greatest challenge of the microbial world: the introduction of antibiotics in the late 1920's (Bagnoli et al., 2018). *S. aureus* is naturally susceptible to virtually every antibiotic that has ever been developed, but only few years after the introduction of penicillin, penicillin-resistant strains of *S. aureus* was identified (Chambers & Deleo, 2009). Penicillin is a  $\beta$ -lactam antibiotic that acts on the penicillin binding proteins (PBPs) of the *S. aureus* cell wall, and penicillin-resistant strains isolated early after the beginning of the widespread use of penicillin expressed a  $\beta$ -lactamase that hydrolyze the  $\beta$ -lactam ring of penicillin, which is essential for the antimicrobial activity of the drug (Chambers & Deleo, 2009; Foster, 2017).

The antibiotics methicillin and the more stable derivative oxacillin were developed as  $\beta$ -lactamase-stable derivatives of penicillin (Foster, 2017). However, shortly after the introduction of methicillin, methicillin-resistant *S. aureus* (MRSA) strains were isolated from hospitals (Jevons, 1961). Methicillin resistance is due to the acquisition of a new gene, *mecA*, that codes for an additional alternative PBP, PBP2a, which has a lower affinity for  $\beta$ -lactam antibiotics (Bagnoli et al., 2018; Pantosti et al., 2007). Unlike  $\beta$ -lactamase-mediated resistance, which is narrow in its spectrum of activity, methicillin resistance is broad, resulting in resistance to most of the  $\beta$ -lactam class of antibiotics (Chambers & Deleo, 2009; Peacock & Paterson, 2015). Despite the broad-spectrum resistance to  $\beta$ -lactams, some newly developed  $\beta$ -lactams have been found effective against MRSA (Peacock & Paterson, 2015). The *mecA* gene is found on a mobile genetic element designated the staphylococcal chromosome cassette SCCmec, and can thus be transferred horizontally, potentially contributing to the spread of MRSA strains, together with chromosomal mutations and antibiotic selection (Chambers & Deleo, 2009; Ito et al., 2003).

MRSA strains are often more multidrug resistant than methicillin susceptible *S. aureus* (MSSA) strains, being resistant also to macrolides, aminoglycosides and/or fluoroquinolones (Pantosti et al., 2007). The ever-increasing burden of MRSA in hospitals in the 1970's and 1980's led to the increased use of vancomycin, the last remaining antibiotic to which MRSA strains were reliably susceptible. This intensive selection pressure has resulted in the emergence of vancomycin-intermediate *S. aureus* (VISA) and vancomycin-resistant *S. aureus* (VRSA) (Chambers & Deleo, 2009; Pantosti et al., 2007).

### 1.1.2 Pathogenesis

*S. aureus* is often considered to be an opportunistic pathogen. Despite its role as a pathogen in intensive care units and the community, causing life-threatening diseases, the interaction between *S. aureus* and humans are in most circumstances benign (Feng et al., 2008). *S. aureus* colonizes the skin and mucosa of humans and several animal species. Although multiple body sites can be colonized in humans, the anterior nares of the nose is the most frequent carriage site for *S. aureus* (Wertheim et al., 2005; Williams, 1963). From longitudinal studies, it has been shown that 10-35% of individuals carry *S. aureus* persistently, while 20-75% carry *S. aureus* intermittently and 5-50% never carry *S. aureus* (Armstrong-Esther, 1976; Feng et al., 2008). Besides asymptomatic carriage of the nares, other less frequently colonized sites include the mucosa in the oropharynx, the skin, the axillae, the perineum, and the vagina (Lowy, 1998; Williams, 1963).

Depending on the predispositions of the host and on virulence-associated traits of the bacterium, *S. aureus* can cause a variety of infections in both animals and humans. In healthy individuals in the community, *S. aureus* frequently causes minor skin and soft tissue infections such as impetigo and cutaneous abscesses, or more severe infections such as necrotizing fasciitis (Balasubramanian et al., 2017). In a nosocomial setting, *S. aureus* can initiate chronic infections at surgical sites or on implanted medical devices including artificial heart valves, catheters, prosthetic joints and orthopedic implants, which are infections generally associated with *S. aureus* biofilm formation (Balasubramanian et al., 2017; Lister & Horswill, 2014; Tong et al., 2015). Biofilm-related infections are associated with increased morbidity and mortality, with infected medical devices often requiring surgical removal and increased durations of hospitalization (Moormeier & Bayles, 2017) (See **section 1.2** for details on biofilm). During bacteremia, which can be caused by cells dispersing from an established biofilm, *S. aureus* circulates in blood and can seed vital organs resulting in disseminated infections such as endocarditis, osteomyelitis and descending urinary tract infections (Balasubramanian et al., 2017; Wertheim et al., 2005). Besides being an important human pathogen, *S. aureus* also causes a variety of infections in animals, ranging from superficial skin diseases to bacteremia (Peton & Le Loir, 2014). *S. aureus* infections in animals are most commonly reported to cause mastitis in cows but have also been reported in a wide range of other animals, including sheep, goats, pigs and birds (Haag et al., 2019; Peton & Le Loir, 2014).

## 1 Introduction

In humans, most *S. aureus* infections are derived from colonizing flora, and individuals that are asymptomatic carriers are at higher risk to develop invasive infections such as bacteremia (von Eiff et al., 2001). In approximately 80% of *S. aureus* bacteremia cases, a relation between the nasal *S. aureus* strain and the infecting strain have been found, with the strains often sharing the same phage type or genotype (von Eiff et al., 2001). Studies have shown that eradication of *S. aureus* carriage in the nares can be effective in reducing the incidence of *S. aureus* infection (Bode et al., 2010; Kluytmans et al., 1996; von Eiff et al., 2001), thus being a potential target for prevention of *S. aureus* infection.

### 1.1.3 Virulence factors

The versatility of *S. aureus* as both a commensal and a pathogen result from *S. aureus* strains possessing a variety of virulence factors (Otto, 2014). The commensal and invasive lifestyles of *S. aureus* are radically different, and it is therefore likely that the bacterium undergoes extensive adaptation while transitioning between the two states (Balasubramanian et al., 2017). The expression of many virulence factors is therefore controlled by several different signaling systems, including the two-component systems (TCS) *agr*, *sae*, *srr* and *arl* (Balasubramanian et al., 2017; Novick, 2003). These complex regulatory systems sense environmental signals which ultimately act to regulate gene expression. In addition to external stimuli, *S. aureus* responds to cell density by means of an auto induced quorum sensing signal (Balasubramanian et al., 2017).

For *S. aureus*, colonization of the human nose presents a significant challenge that requires not only adherence to nasal epithelial cells, but also an ability to cope with the host defense and competing resident microorganisms (Liu, 2009). The attachment of *S. aureus* to the host cell surface initiating the colonization process is mediated by several adhesins, collectively termed microbial surface components recognizing adhesive matrix molecules (MSCRAMMs) (Liu, 2009), which are described in more detail in **section 1.2**.

When the mucosal surface or skin is breached by *S. aureus*, the organism is met by the host immune system, whose primary defense against *S. aureus* infection is the innate immunity provided by neutrophils (Foster, 2005). *S. aureus* deploys multiple strategies to avoid neutrophil killing, one being the secretion of chemotaxis inhibitory protein of *S. aureus* (CHIPS) and extracellular adherence protein (Eap) (Foster, 2005; Liu, 2009). CHIPS is secreted to prevent chemotaxis of neutrophils to the site of infection (Bien et al., 2011) while binding of Eap to intercellular adhesion

## 1 Introduction

molecule-1 (ICAM-1) on the surface of endothelial cells blocks neutrophil binding (Foster, 2005). Another strategy used by *S. aureus* is to avoid opsonization by antibodies and complement, which directly or indirectly leads to killing of *S. aureus* or uptake by phagocytes. *S. aureus* evades opsonophagocytosis by expressing capsule, clumping factor A (ClfA), protein A and a number of complement inhibitors on its surface (Foster, 2005; Liu, 2009).

Another fundamental feature of *S. aureus* is the ability to secrete toxins that damages the membranes of the host cells. Cytolytic toxins form  $\beta$ -barrel pores in the plasma membrane of eukaryotic cells, causing leakage and, ultimately, lysis (Otto, 2014). *S. aureus* secrete several cytolytic toxins, among them  $\alpha$ -toxin,  $\gamma$ -toxin, leucocidin, and Panton-Valentine leucocidin (PVL) (Bien et al., 2011; Foster, 2005; Otto, 2014).  $\gamma$ -toxin lyses both erythrocytes and leukocytes, while PVL is toxic only to leukocytes (Foster, 2005). *S. aureus* can also produce additional exotoxins, which cause toxic shock syndrome and food poisoning (Bien et al., 2011; Holtfreter & Bröker, 2004).

Another critical virulence mechanisms of *S. aureus* is the ability to form biofilms, which allows the bacterium to persist on surfaces and resist host defenses and antibiotics (Foster, 2005). This is described in further detail in **section 1.2**.

### 1.1.4 Metabolism

*S. aureus* colonizes various niches that have different oxygen availability. Oxygen concentrations vary between healthy and infected or necrotic tissues, as well as in wounds where oxygen levels are estimated to be below 1% (hypoxic) or completely lacking (anoxic). While aerobic growth is generally favourable when considering resources spent for the amount of energy obtained, *S. aureus* is often exposed to conditions that do not allow aerobic growth (Bagnoli et al., 2018). In the absence or limited levels of oxygen, *S. aureus* utilizes either anaerobic respiration with nitrate as an electron acceptor, or fermentative pathways to generate energy (Mashruwala et al., 2017a). To allow for regulation of respiratory activity and metabolic pathways, *S. aureus* utilizes different two-component regulatory systems, including SrrAB, NreCBA, and AirRS (Bagnoli et al., 2018).

Unlike the respiratory system of *Escherichia coli* and *Bacillus subtilis*, that of staphylococci is not very well characterized (Götz & Mayer, 2013). In glycolysis, *S. aureus* uses a nearly universal set of enzymes to convert glucose to pyruvate, with the simultaneous formation of some ATP. However, the bulk of ATP is formed when pyruvate, as well as other compounds, is oxidized to

## 1 Introduction

CO<sub>2</sub> and H<sub>2</sub>O during the tricarboxylic acid (TCA) cycle followed by the electron transport chain. In the TCA cycle, pyruvate, lipids and amino acids can be oxidized to produce the reducing agents NADH and FADH<sub>2</sub> (McNamara & Proctor, 2000).

NADH and FADH<sub>2</sub> donate electrons to the electron transport chain to generate the potential energy required to form ATP (**Figure 1.1**). Electrons cannot exist in aqueous solutions and their transfer from NADH and FADH<sub>2</sub> to O<sub>2</sub> therefore requires a set of carrier proteins embedded in the cell membrane (McNamara & Proctor, 2000). In *S. aureus*, menaquinone (MK) and the prosthetic group heme are required for the transfer of electrons. Menaquinones are the sole isoprenoid quinones in staphylococci, and is the first electron acceptor in the chain of molecules that receives electrons from FADH<sub>2</sub> or the NADH oxidase complex (Götz & Mayer, 2013; McNamara & Proctor, 2000). Heme is the component of cytochromes that receives electrons from menaquinone. Both menaquinone and heme are synthesized using several enzymes encoded by the *men* and *hem* operons, respectively (McNamara & Proctor, 2000). Studies of the staphylococcal cytochromes suggests that staphylococci possess a branched respiratory system of two alternative terminal oxidases, cytochrome *aa<sub>3</sub>* and cytochrome *bd*, (Götz & Mayer, 2013; Hammer et al., 2013) in addition to a nitrate reductase when nitrate is used as a terminal electron acceptor (Rudra & Boyd, 2020). A consequence of the transfer of electrons through menaquinone and the cytochromes is the simultaneous transfer of protons from within the cell to the outside of the cell, generating a proton motive force. This proton motive force then provides the energy needed to drive the formation of ATP from ADP by the F<sub>0</sub>F<sub>1</sub>-ATPase complex (Götz & Mayer, 2013; McNamara & Proctor, 2000).

When heme, MK, or terminal electron acceptors are absent, *S. aureus* generates energy through fermentation. Fermentation employs substrate-level phosphorylation, which produces acid end products, to generate ATP and maintain the redox balance of the cell (Mike et al., 2013). The major fermentative end products produced are L-lactate, D-lactate, formate, ethanol, and 2,3-butanediol, all of which are generated through different fermentative pathways. These products are formed by reduction of pyruvate, and these reactions serve to recycle NAD<sup>+</sup> for use in the glycolytic pathway (Fischetti et al., 2019).

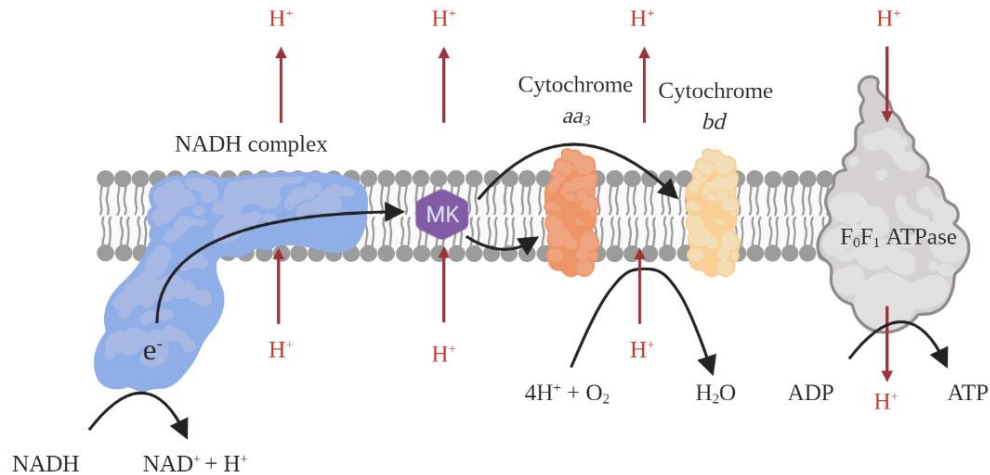


**Figure 1.1 Proposed electron transport in *S. aureus* during aerobic growth.** Electrons are transferred from NADH or FADH<sub>2</sub> (not shown) to oxygen via a series of electron carriers embedded in the cell membrane. Electrons are funneled to menaquinone (MK) either from the NADH complex or directly from FADH<sub>2</sub>, before being transferred to one of two terminal oxidases present in *S. aureus*, cytochrome *bd* and cytochrome *aa<sub>3</sub>*, in which O<sub>2</sub> is reduced to H<sub>2</sub>O. The transfer of electrons drives the generation of a proton motive force through the simultaneous transport of protons across the membrane (in red). The proton motive force drives the formation of ATP from the F<sub>0</sub>F<sub>1</sub> ATPase.

## 1.2 Biofilm formation in *S. aureus*

A biofilm can be defined as a microbially-derived sessile community in which cells are attached to a surface or to other cells and embedded in a protective extracellular polymeric matrix (Archer et al., 2011; Donlan & Costerton, 2002; Lister & Horswill, 2014). The composition of the biofilm matrix, also called extracellular matrix (ECM) varies depending on the strain and on environmental conditions, but in general contain host factors, polysaccharides, proteins, and extracellular DNA (eDNA) (Balasubramanian et al., 2017; Flemming & Wingender, 2010; Lister & Horswill, 2014).

The multilayered, high-density structured biofilm protects *S. aureus* from antibiotics and the human immune system (Foster, 2005). *S. aureus* biofilms decrease the efficiency of antimicrobial peptides of the innate host defense, and inhibit uptake and killing by phagocytes (Otto, 2013; Scherr et al., 2015; Thurlow et al., 2011). The increased tolerance to antibiotics by *S. aureus* in biofilms is an example of adaptive resistance where cells that are taken from a biofilm generally recover their original susceptibility when brought back to the planktonic state (de la Fuente-Núñez et al., 2013). This adaptive resistance can be achieved through the altered gene expression of biofilms, or by reduced diffusion of some antibiotics, which are unable to penetrate the ECM (Lister & Horswill, 2014; Singh et al., 2010). An alternative proposal is that increased antibiotic tolerance is achieved through the development of physiologically dormant persister cells. Persister cells are

metabolically inactive, with the antimicrobial targets or the cellular need for these targets being shut down (Waters et al., 2016).

### 1.2.1 Stages of biofilm development

Biofilm developmental stages have been defined by many and can be divided into at least three major events: initial attachment, biofilm maturation, and dispersal (Lister & Horswill, 2014; Otto, 2008; Otto, 2013). Moormeier and Bayles (2017) have proposed to include two additional stages, ultimately resulting in the five stages (i) attachment, (ii) multiplication, (iii) exodus, (iv) maturation, and (v) dispersal (**Figure 1.2**).

The first step of biofilm formation is the initial **attachment**, which can occur on both biotic and abiotic surfaces. Initial attachment to biotic surfaces (e.g., host tissues or artificial surfaces coated with host matrix proteins) is mediated by a variety of cell-wall anchored (CWA) proteins specific for different host matrix substrates (Moormeier & Bayles, 2017). Attachment to abiotic surfaces, such as directly to the surface of indwelling medical devices, is mostly dependent on the physiochemical characteristics of the device and the bacterial surface (Moormeier & Bayles, 2017). The net charge of teichoic acids have been shown to play a role in the initial attachment during biofilm formation (Gross et al., 2001) as well as some surface proteins, such as the major autolysin of *S. aureus*, Atl, which is important for daughter cell separation during cell division (Biswas et al., 2006; Houston et al., 2011). Atl has been shown to be important for attachment to polystyrene fibrinogen and vitronectin (Hirschhausen et al., 2012).

Part of the well-characterized group of CWA proteins are the microbial surface components recognizing adhesive matrix molecules (MSCRAMMs), several of which share a common cell wall targeting motif (LPXTG) but have different binding specificities for host matrix components, such as fibronectin, fibrinogen and collagen (Foster et al., 2014; Moormeier & Bayles, 2017). Many different proteins have been implicated in binding host matrix components to initiate cell adherence and/or biofilm development, some of which include fibronectin-binding proteins (FnBPA and FnBPB), serine-aspartate repeat family proteins (SdrC, SdrD and SdrE), clumping factors (ClfA and ClfB), *S. aureus* surface protein G (SasG) and multiple others (Corrigan et al., 2007; Moormeier & Bayles, 2017).

Following attachment, *S. aureus* cells divide and accumulate in step two of biofilm formation, **multiplication**. At this stage in biofilm development, *S. aureus* produces a variety of factors that

## 1 Introduction

help stabilize cell-to-cell interactions. Some of these proteins have dual roles in both attachment and multiplication, such as the MSCRAMMs FnBPA, FnBPB, ClfB and SdrC, while other CWA proteins, like protein A and SasC have been shown to be important for biofilm multiplication (Moormeier & Bayles, 2017). The **exodus** stage of biofilm development is an early dispersal event where subpopulations of cells are released from the biofilm resulting in microcolony formation and restructuring of the biofilm (Moormeier & Bayles, 2017). This stage occurs through regulated nuclease-dependent degradation of eDNA and marks a shift from the biofilm being reliant mainly on proteins for integrity, to a dependence on both eDNA and proteins (Moormeier & Bayles, 2017).

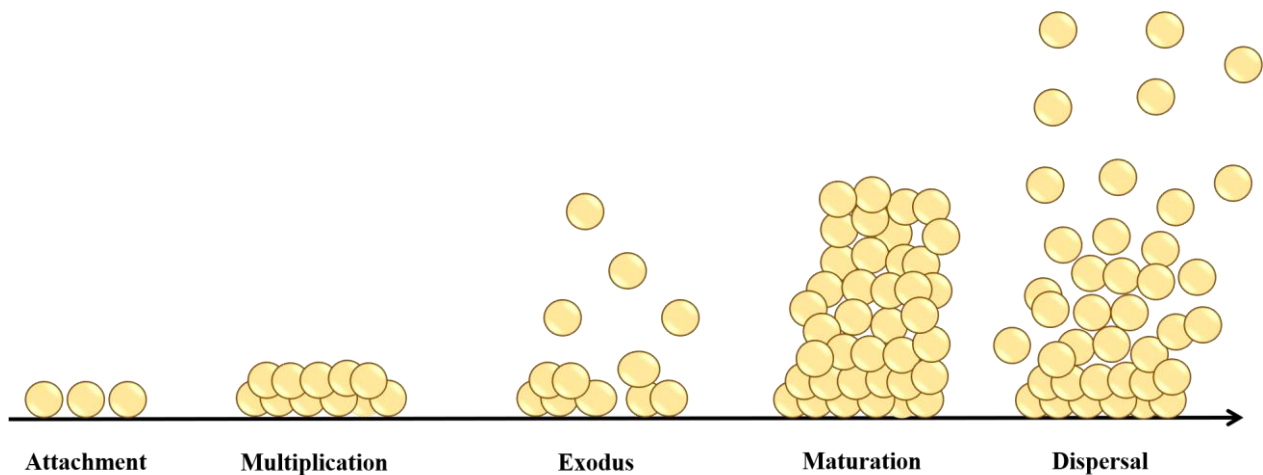


**Figure 1.2 The five stages of *S. aureus* biofilm development.** *S. aureus* attaches to biotic or abiotic surfaces. The biofilm then develops into a ‘mat’ of cells encased in an extracellular matrix composed of proteins and extracellular DNA (eDNA). This is followed by a period of exodus in which subpopulations of cells are released from the biofilm. During maturation, cells are linked together by adhesive forces, and the bulk of the extracellular matrix is formed. Regulatory systems initiate dispersal of cells via protease activation and/or PSM production, allowing dispersal of cells to distant sites, potentially seeding new sites of biofilm development. Figure is adapted from Moormeier & Bayles, 2017.

Biofilm **maturation** comprises adhesive processes that link bacteria together during proliferation, in addition to disruptive processes that form channels in the biofilm structure (Otto, 2013). This is the stage in which the bulk of the ECM is produced, which encapsulates the cells of the biofilm in a three-dimensional structure (Moormeier et al., 2014). One very important adhesive biofilm molecule, which has been demonstrated to be necessary for biofilm formation in many cases, is the exopolysaccharide poly-N-acetylglucosamine (PNAG) also known as polysaccharide intercellular adhesin (PIA), which is encoded by the *icaADBC* genes (Archer et al., 2011; Otto, 2013). Expression of the *icaADBC* genes is negatively regulated at the transcriptional level by the *ica* regulator (*icaR*) gene product, which is divergently transcribed from *icaADBC* (Jefferson et al., 2003). Although the majority of clinical *S. aureus* isolates contain the *ica* operon, *ica*-independent

## 1 Introduction

biofilm strategies have been discovered by the lack of correlation between *ica*-expression and biofilm formation (Fitzpatrick et al., 2005). *ica*-independent biofilm development mechanisms can include cell surface components such as teichoic acids and MSCRAMMs. Houston et al. (2011) have identified *ica*-independent clinical isolates which are Atl-dependent and FnBP-dependent.

During the last step of biofilm formation, **dispersal**, the ECM becomes partially degraded by nucleases and proteases to facilitate dissemination of cells from the biofilm (Boles & Horswill, 2011; Lister & Horswill, 2014). Detached biofilm bacteria may establish secondary biofilm infections elsewhere or cause acute, non-biofilm related infections, such as sepsis (Otto, 2013). Dispersal of *S. aureus* biofilm has largely been shown to be under control of the *agr* quorum sensing system (Moormeier & Bayles, 2017) (see **section 1.2.2** for *agr*).

Throughout the biofilm, the access of nutrients, oxygen and other electron acceptors will be variable, and thus the formation of mature biofilm does not only include matrix formation, but also requires structuring (Le et al., 2019; Otto, 2013). Structuring of the biofilm results in the formation of channels important for nutrient delivery throughout the biofilm, while it also contributes to detachment and dispersal (Le et al., 2019). Structuring of the biofilm have been linked both to degradation of biofilm matrix molecules, predominantly by proteases, and to the surfactant phenol-soluble modulins (PSM) peptides (Boles & Horswill, 2011; Le et al., 2019; Periasamy et al., 2012). The PSM family consists of PSM $\alpha$ 1-4, PSM $\beta$ 1-2 and the RNAPIII-encoded  $\delta$ -toxin (Cheung et al., 2014). PSMs are thought to function as surfactants disrupting molecular interactions within the biofilm matrix, mediating dispersal (Moormeier & Bayles, 2017; Otto, 2013; Periasamy et al., 2012). Contradictory, PSMs have also been implicated to form long fibers which potentially contribute to biofilm integrity (Schwartz et al., 2012).

Another important component of the staphylococcal biofilm is extracellular DNA (eDNA). Although eDNA was initially thought to be a residual material from lysed cells, its importance as an integral part of the ECM has become increasingly accepted (Flemming & Wingender, 2010), and it is thought to be released from cells through regulated autolysis, in part by the autolysin Atl (Bose et al., 2012; Foulston et al., 2014). Due to the negative charge of the DNA polymer, eDNA potentially act as an electrostatic polymer that anchors cells to a surface, to host factors, and to each other (Lister & Horswill, 2014). The importance of eDNA in biofilm formation has been demonstrated by the observation that DNaseI can decrease biofilm formation (Archer et al., 2011;

Whitchurch et al., 2002). In *S. aureus*, cell death and lysis have been shown to be controlled by the *cid* and *lrg* operons, which have opposing effects on murein hydrolase activity. CidA has been shown to promote cell lysis and the subsequent release of DNA during the development of biofilm (Rice et al., 2007). Further, Mann et al. (2009) propose that cell lysis and DNA release must occur early in attachment for proper biofilm formation to occur.

### 1.2.2 Regulation of *S. aureus* biofilm formation

Although a biofilm can arise from a single cell, biofilm communities contain distinct micro niches that result in metabolic heterogeneity and variability in gene expression (Moormeier et al., 2014). Gradients in oxygen, nutrients and electron acceptors can cause heterogenous gene expression throughout the biofilm, resulting in a biofilm containing aerobically growing cells, fermentatively growing cells, dead cells and dormant cells (Archer et al., 2011; Beenken et al., 2004; Rani et al., 2007). Several global regulators, such as the *agr* quorum sensing system, sigma factor B ( $\sigma^B$ ), and SarA, have strong connections to *S. aureus* biofilms (Paharik & Horswill, 2016).

The **accessory gene regulator (*agr*)** system is a peptide quorum sensing system which functions by sensing extracellular levels of an autoinducing peptide (AIP) that is produced by staphylococci during growth (Paharik & Horswill, 2016). Besides AIP, *agr* can also be regulated by several other regulators such as SarA or by environmental factors such as glucose or pH (Kavanaugh & Horswill, 2016; Le & Otto, 2015; Regassa et al., 1992). The *agr* locus encodes the components of an autoregulatory quorum-sensing system that control the expression of the regulatory RNA molecule RNAIII (Koenig et al., 2004). AIP is released outside the cell where it accumulates and, at a given concentration, binds the surface-exposed histidine kinase AgrC. This results in phosphorylation of the response regulator AgrA, which in turn induces expression of RNAIII (Koenig et al., 2004; Paharik & Horswill, 2016). RNAIII regulates translation initiation rates and/or mRNA stability of at least nine *S. aureus* transcripts directly, including master transcription factors Rot and MgrA and the phenol-soluble modulins (PSMs) PSM $\alpha$  and PSM $\beta$  in addition to hundreds of genes that are believed to be indirectly controlled via RNAIII-dependent regulation of global transcription factors (Koenig et al., 2004; Queck et al., 2008; Svenningsen, 2018). The *agr* quorum-sensing system also includes the precursor for AIP, AgrD, and a secretory protein (AgrB) responsible for export and processing of AgrD (Koenig et al., 2004).

## 1 Introduction

The general picture is that induction of the *agr* quorum sensing system represses the expression of cell surface proteins used to adhere to host tissue, form biofilm and evade the host immune system, while simultaneously activating the expression of exotoxins and superantigens (Paharik & Horswill, 2016; Svenningsen, 2018). Moormeier et al. (2014) hypothesize that *agr* is downregulated during biofilm attachment, and that increased attachment of *agr* mutant strains is the result of decreased production of PSMs, which potentially act as strong surfactants preventing hydrophobic interactions between the cell surface and the polystyrene surface. As the biofilm develops, small subpopulations experience *agr* re-activation, which positively regulates proteases and PSMs, causing detachment and dispersal of the biofilm (Lister & Horswill, 2014; Paharik & Horswill, 2016; Peschel & Otto, 2013).

Another global regulator implicated in *S. aureus* biofilm formation is the **staphylococcal accessory regulator (*sarA*)**. The *sar* locus encodes the DNA-binding protein SarA which binds to conserved regions termed Sar boxes within promoter regions of genes encoding cell surface proteins, exoproteins, and also the promoters of the *agr* locus. By binding to the *agr* locus, SarA increases transcription of both the *icaADBC* genes and RNAlII, thus partially having a regulatory role via its effect on *agr* (Dunman et al., 2001; Paharik & Horswill, 2016; Rehtin et al., 1999). Expression of *sarA* is generally associated with increased expression of *agr*, however SarA also directly regulates several other genes that affect biofilm formation, and has an opposing role to *agr* when it comes to biofilm formation (Beenken et al., 2010), indicating that this regulation is finely balanced. Where *agr* induces production of proteases and nucleases, *sarA* represses their production, while positively regulating *fnbA* and *fnbB*. Thus, *agr* expression is implicated in limiting biofilm formation, while expression of *sarA* has been shown to promote biofilm formation (Beenken et al., 2010).

Additional levels of control are accomplished through the ***sigB* operon product  $\sigma^B$** .  $\sigma^B$  is an alternative sigma factor of RNA polymerase that is activated in stress response and leads to global changes in promoter specificity, and thus gene expression (Paharik & Horswill, 2016). Factors necessary for the early stages of biofilm formation, including the adhesive factors ClfA and FnBPA, are up-regulated by  $\sigma^B$  (Archer et al., 2011; Entenza et al., 2005). In addition, factors associated with biofilm dispersal and a planktonic mode of life, including proteases, are repressed

by  $\sigma^B$  (Martí et al., 2010). Notably, *agr* RNAIII levels are elevated in *sigB* mutants, implicating that  $\sigma^B$  is an antagonist of *agr* (Beenken et al., 2010; Lauderdale et al., 2009).

### 1.3 *In vitro* model systems in *S. aureus* biofilm research

There is an increasing interest in the study of biofilm formation due to its profound impact in clinical settings, both in humans and in animals. Acquiring a greater understanding of the biofilm as a whole and at a single cell level will provide new insights into methods to control biofilms, e.g., in clinical settings like *S. aureus* biofilm on indwelling medical devices. Since staphylococcal biofilms are formed by different strains with various surfaces and conditions, choosing the experimental platform for biofilm experiments is critical. To study *S. aureus* biofilm formation *in vitro* and extract reliable data, scientists need model systems that provide reproducible conditions (Azeredo et al., 2017).

#### 1.3.1 The microtiter plate assay

Biofilm formation in microtiter plates is by far the most commonly used method for studying biofilm. It was one of the first methods standardized for quantification of biofilm and was originally used by Madilyn Fletcher to investigate bacterial attachment in polystyrene petri dishes, and was later developed to study biofilm formation in microtiter plates (typically 96-well plates) for a wide range of bacterial species (Azeredo et al., 2017; Christensen et al., 1985; Fletcher, 1977; O'Toole & Kolter, 1998). In the biofilm microtiter plate assay, bacterial cells are grown in wells of a polystyrene microtiter plate or on coupons placed in the wells of a microtiter plate. At different timepoints, ranging from 1 hour to 24 hours, the planktonic cells are removed and washed, before staining the biomass attached to the surface of the polystyrene wells (Azeredo et al., 2017; Coenye & Nelis, 2010; Merritt et al., 2005).

One of the major advantages of the microtiter plate biofilm assay is that it allows for a large number of strains to be tested simultaneously, enabling screens for biofilm-defective mutants or evaluation of the effect of different treatments and compounds on biofilm attachment and/or formation. It also allows for a variety of growth conditions including growth media, temperature, humidity, CO<sub>2</sub> and O<sub>2</sub> to be tested (Coenye & Nelis, 2010; Fletcher, 1977; O'Toole & Kolter, 1998). Several external factors could induce *S. aureus* biofilm formation in the microtiter plate assay, with sodium chloride (NaCl) and glucose being the most common supplements to either tryptic soy broth (TSB) or brain heart infusion (BHI) media, but other supplements like citrate and yeast extract can also be used

(Chen et al., 2012). The mechanisms behind the different supplements are not entirely known, but glucose is thought to lower the pH of the medium, thereby inhibiting the *agr* quorum sensing system (Regassa et al., 1992). Additionally, it has been shown that supplementing the media or coating the wells of the microtiter plate with human plasma promotes the formation of robust biofilms, possibly through the promotion of biofilm attachment to plasma proteins (e.g., fibrinogen) (Beenken et al., 2003; Chen et al., 2012). Subinhibitory concentrations of some antibiotics has also been shown to increase biofilm formation, due to increased autolysin-dependent release of eDNA (Kaplan et al., 2012).

On the other hand, a potential drawback of the microtiter plate assay is that the biofilm mass is assessed by measuring all attached biomass. Part of this biomass may be the result of cells that have sedimented to the wells becoming embedded in the biofilm, and the measured biofilm will not solely be a result of a biofilm forming process. Approaches to overcome this issue have been developed, such as the Calgary biofilm device where biofilms are grown on pegs immersed in the media (Azeredo et al., 2017; Ceri et al., 1999; Coenye & Nelis, 2010).

Biofilm biomass and viability in microtiter plates can be assessed by different methods. Determination of colony forming units (CFU) on agar media is common, however the fraction of detached cells may not be representative of the initial biofilm population nor does it allow for recovery of viable but non-culturable organisms (Azeredo et al., 2017; Coenye & Nelis, 2010). For quantification of total biofilm mass, crystal violet (CV) staining is widely used. CV stains both live and dead cells as well as some components present in the biofilm matrix. (Azeredo et al., 2017; Christensen et al., 1985).

### **1.3.2 Confocal laser scanning microscopy**

Confocal Laser Scanning Microscopy (CLSM) has proven to be a valuable microscopic technique to study biofilm structure. In CLSM the focal plane is collected with a high resolution, and multi acquisition of such planes at different depths in the sample makes it possible to obtain a three-dimensional image of the biofilm structure. This allows for evaluation of for example biofilm thickness and roughness (Azeredo et al., 2017). Biofilm CLSM imaging can be performed with a range of fluorescent probes, with SYTO9 and SYBR-Green being the most widely used dyes. By coupling the green SYTO9 with the red propidium iodide in LIVE/DEAD staining, cell viability of the biofilm can be assessed (Azeredo et al., 2017; Coenye & Nelis, 2010). CLSM can also be

used qualitatively by staining of different biofilm matrix components like polysaccharide, eDNA, proteins and lipids (Schlafer & Meyer, 2017).

### 1.3.3 The macrocolony biofilm model

Another model system used to study biofilms is the macrocolony biofilm model, which is based on biofilms growing on a nutrient agar surface (Serra & Hengge, 2014). Studying biofilm macrocolonies can give an insight into processes that are related to the three-dimensional organization of biofilms, in addition to providing a method to identify and characterize bacterial strains with altered biofilm phenotypes, and to investigate the impact of environmental conditions on biofilm formation (Ray et al., 2012; Serra & Hengge, 2014). Macrocolony biofilm formation has been used to study a variety of bacteria such as *B. subtilis* and *E. coli* (Branda et al., 2001; Serra et al., 2015), and has also been used to study macrocolony formation in *S. aureus* (Wermser & Lopez, 2018). Macrocolony biofilms are characterized by an intricate macroscopic morphology with wrinkles, elongated folds, ridges and/or concentric ring patterns (Serra et al., 2015). In *Pseudomonas aeruginosa*, wrinkling of the biofilm macrocolony is linked to the intracellular redox state, and it is thought that the wrinkled surface increases the surface-to-volume ratio of the macrocolony, maximizing oxygen accessibility (Dietrich et al., 2013).

In the macrocolony biofilm model developed for *S. aureus*, the complex medium agar is supplemented with magnesium, which trigger the aggregation of cells into a structured macrocolony (Koch et al., 2014). Chronic staphylococcal infections due to biofilm formation often occur at sites containing high concentrations of  $Mg^{2+}$  (e.g., joints and bones) (García-Betancur et al., 2017; Koch et al., 2014). In the *S. aureus* macrocolony model,  $Mg^{2+}$  from the medium binds to *S. aureus* cell wall teichoic acids resulting in an increased cell wall stability and rigidity. This increase in cell wall rigidity promotes the expression of the stress-induced alternative sigma factor  $\sigma^B$ , which in turn represses *agr* quorum sensing, ultimately de-repressing biofilm-related genes (García-Betancur et al., 2017; Koch et al., 2014; Wermser & Lopez, 2018).

## 1.4 Functional genetics using CRISPR interference

### 1.4.1 Genetic engineering in *S. aureus*

The diverse features of different *S. aureus* strains come from its diverse genetic background. *S. aureus* has a ~3.0 Mbp chromosome and in many cases more than one plasmid. The chromosome is composed of the core-genome which is shared in many *S. aureus* strains, the core-variable region

shared by restricted lineage(s) and mobile genetic elements transferred between cells (Sato'o et al., 2018). The combination of these latter elements has resulted in great genetic variation. The genetic variation of different *S. aureus* strains and lineages is reflected by a large number of frequently used laboratory strains, such as Newman, COL, USA300, UAMS-1 and the NCTC8325-derived strains SH1000, NCTC8325-4, SA113 and RN4220 (Prax et al., 2013). These strains differ when it comes to transcriptional regulators, activity of the *agr* quorum sensing system, physiological fitness, availability and activity of virulence factors or genetic amenability and robustness (Prax et al., 2013). Our understanding of these *S. aureus* traits relies on our ability to study functions of the *S. aureus* genes. A major barrier to the genetic manipulation of staphylococci is the inability to transform DNA into the majority of clinical isolates due to a strong restriction modification (RM) barrier, and genetic manipulations in *S. aureus* is therefore rather time-consuming and laborious (Monk & Foster, 2012).

Conventionally, gene function in *S. aureus* have been studied through gene knockouts, which directly deletes or disrupts a gene, or through gene knockdown, which represses gene expression but does not destroy the gene. Allelic exchange is the most commonly used technique to construct gene knockout mutants in *S. aureus*, but this happens at a relatively low rate and extensive screening is necessary to screen for desired mutants, making it a time consuming process (Zhao et al., 2017). Furthermore, gene knockout cannot be used to study essential genes, as these are lethal to the cell.

### 1.4.2 CRISPR/Cas9 and CRISPR interference for transcriptional knockdown

New tools for gene editing as well as for knocking down the expression of individual genes in a variety of organisms have been developed based on the CRISPR (clustered regulatory interspaced short palindromic repeats) / Cas9 (CRISPR associated protein 9) technology. In this work, CRISPR interference (CRISPRi) (Qi et al., 2013) is used to knock down expression of genes. CRISPR systems are naturally found in ~50% of all bacteria, where they help cells prevent infection by bacteriophages through CRISPR RNA (crRNA)-based DNA recognition and Cas nuclease-mediated DNA cleavage (Guzzo et al., 2020; Zhang et al., 2014).

The CRISPR locus consists of a series of conserved repeated sequences interspaced by distinct nonrepetitive protospacers derived from phage (**Figure 1.3**). In the CRISPR/Cas system, invading foreign DNA is processed by Cas nuclease into small DNA fragments, which are then incorporated

## 1 Introduction

into the CRISPR locus of host genomes as protospacers (Zhang et al., 2014). For type II CRISPR systems, the protospacers and repeats are expressed as a single RNA, with the individual spacers (crRNA) being cut out and loaded onto a Cas9 protein. Invariable target-independent trans-activating crRNA (tracrRNA), which is a unique noncoding RNA with homology to the repeat sequences, is also transcribed from the locus and contributes to the processing of pre-crRNA (Guzzo et al., 2020; Jiang & Doudna, 2017; Kim & Kim, 2014). The Cas9 protein forms a complex with both the crRNA and the tracrRNA to form an active DNA endonuclease. The resulting endonuclease target a 23-bp target DNA sequence that is composed of the 20-bp sequence of the crRNA (i.e., the protospacer) and the sequence (5'-NGG-3' or 5'-NAG-3') known as protospacer adjacent motif (PAM), which is recognized by Cas9 itself (Guzzo et al., 2020; Kim & Kim, 2014; Mir et al., 2018). The PAM sequence is located immediately downstream of the protospacer and is important both for spacer acquisition and for target recognition and cleavage (Chylinski et al., 2014). Cas9 then cleaves incoming phage DNA, by generating a double-stranded break in the target DNA to prevent phage infection (Mir et al., 2018; Zhang et al., 2014).

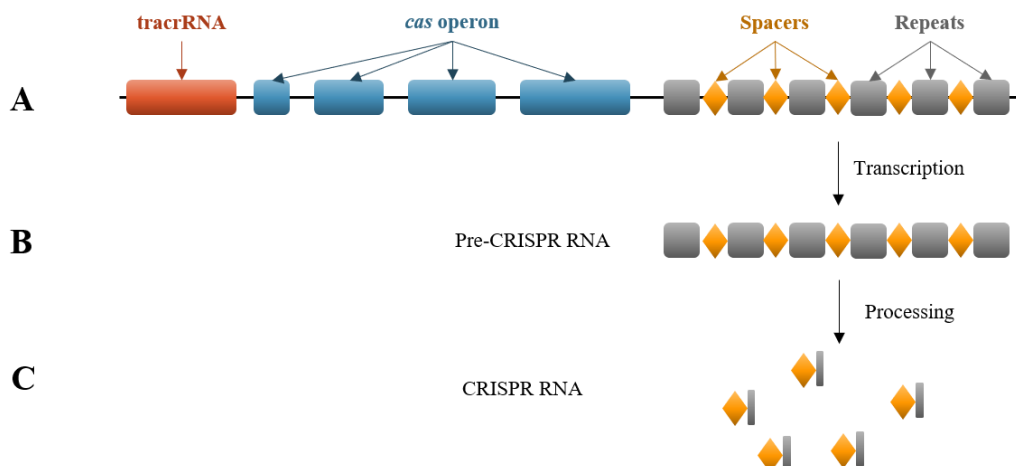


**Figure 1.3 General overview of a CRISPR locus in a type II CRISPR-Cas system.** (A) The locus comprises an array of repetitive sequences (repeats, grey) interspaced by short stretches of non-repetitive sequences (spacers, yellow), as well as a set of CRISPR-associated (*cas*) genes (blue). Preceding the *cas* operon is the *trans* activating CRISPR RNA gene (*tracrRNA*, red) which encodes a unique noncoding RNA with homology to the repeat sequences. (B) The spacers and repeats are transcribed into a precursor RNA (pre-CRISPR). The *tracrRNA* is transcribed separately. (C) CRISPR RNA maturation.

Although discovered as an immune system in bacteria, CRISPR/Cas has been developed as a useful genetic tool. Most well-known is CRISPR/Cas9-based genetic engineering to make knock-out or knock-ins. These approaches relies on cellular DNA repair mechanisms, including nonhomologous end-joining (NHEJ) repair and homology-directed repair (HDR) (Zhang et al., 2014). In engineered

## 1 Introduction

systems, the crRNA and tracrRNA is fused into a single-guide RNA (sgRNA) with a designed hairpin which mimics the tracrRNA-crRNA complex (Mir et al., 2018; Qi et al., 2013). The CRISPR/Cas9 genetic tool is thus relatively simple and only relies on two parts; the Cas9 and the sgRNA.

In 2013, Qi et al., showed that CRISPR/Cas9 could be repurposed for genome regulation instead of genome editing, by so-called CRISPR interference (CRISPRi). With CRISPRi the nuclease Cas9 is substituted for a catalytically inactive Cas9 (dead Cas9 or dCas9) protein. Unlike the wild-type Cas9 which introduces double-stranded breaks in DNA, dCas9 does not have endonuclease activity, but still has an intact DNA-binding capability (Qi et al., 2013). The CRISPRi system is based on the dCas9 being co-expressed with a sgRNA designed with a 20 base pair complementary region, which targets the dCas9 to the 5' region of a gene of interest. At the target site, dCas9 serves as a transcriptional roadblock for RNA polymerase, hence downregulating transcription (Qi et al., 2013).

CRISPRi knockdowns are reversible, and has been shown to have low off-target effects, although this needs to be verified for different species (Qi et al., 2013; Zhao et al., 2017). Another advantage of CRISPRi as opposed to other conventional gene knockdown methods is that, by using CRISPRi, new genes can be easily targeted in a single cloning step. To target new genes, only the 20-nucleotide base pairing region of the sgRNA construct needs to be modified, allowing for easy construction of large libraries of sgRNA strains (Cui et al., 2018; Kjos, 2019; Liu et al., 2017). The CRISPRi system can also be used to knock down multiple genes simultaneously, allowing the study of processes which involves a series of genes by expressing multiple sgRNAs together (Zhao et al., 2017). Also important, CRISPRi allows functional studies of both essential and non-essential genes. Despite all of the advantages with CRISPRi, a disadvantage with the system is the polar effects when targeting genes within an operon, most likely blocking transcription of all downstream genes within an operon (Kjos, 2019), in addition to some leaky effect of CRISPRi in the absence of induction (Zhao et al., 2017).

CRISPRi has been used for transcriptional knockdown in multiple different species, including *Streptococcus pneumoniae* (Liu et al., 2017) and *B. subtilis* (Peters et al., 2016). In *S. aureus*, an inducible CRISPR/dCas9 interference system have been developed by Stamsås et al. (2018), where CRISPRi is achieved through a two-plasmid system in which the dCas9 is expressed on one

## 1 Introduction

plasmid behind an inducible IPTG-promoter, and the sgRNA is expressed on a separate plasmid behind a constitutive promoter (**Figure 1.4**). Upon addition of IPTG, dCas9 will be expressed and the dCas9-sgRNA-complex formation will result in a transcription block and knockdown of the target gene. Without induction with IPTG, dCas9 will not be expressed, and transcription will proceed as normal.

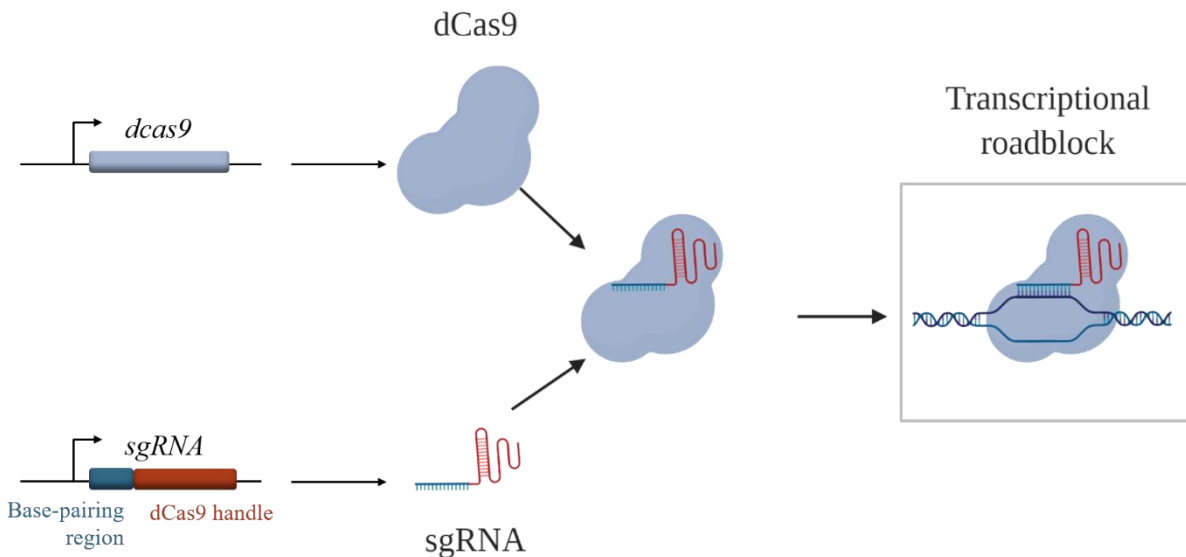


**Figure 1.4 CRISPRi in *S. aureus*.** The dCas9 protein is expressed from an IPTG-inducible promoter on one plasmid, while the sgRNA is constitutively expressed on a separate plasmid. With addition of IPTG, dCas9 is expressed and guided to the target site by the sgRNA. Binding of dCas9 to the 5' end of the coding sequence of its target gene functions as a transcriptional roadblock, blocking transcription elongation. Figure is adapted from Peters et al., 2016 and Liu et al., 2017

## **1.5 Aim of the study**

The biofilm mode of growth utilized by *S. aureus* makes the infections caused by this Gram-positive bacterium especially difficult to treat. To be able to identify new treatment strategies to combat *S. aureus* biofilm-associated infections, a greater understanding of the genes and processes underlying biofilm formation and regulation is needed. Most methods used to study gene function in *S. aureus* involves chromosomal inactivation commonly achieved through transposon mutagenesis or gene knock out. To overcome these time-consuming methods, we wanted to explore the use of CRISPR interference for knockdown of gene expression to study biofilm-associated genes in *S. aureus*. As a proof of concept, gene expression of a selection of genes previously described to be involved in biofilm formation was knocked down using CRISPRi and used to study biofilm formation using the crystal violet microtiter plate assay and the macrocolony formation assay. Furthermore, we wanted to investigate whether CRISPRi could be used in these two model systems to identify novel genes or pathways involved in *S. aureus* biofilm formation. This was done by screening a collection of CRISPRi strains, targeting selected genes for knockdown of gene expression in the microtiter plate assay, and by utilizing a CRISPRi pooled library composed of a mixture of strains harboring sgRNAs targeting all transcriptional units of the *S. aureus* genome in the macrocolony formation assay.

## 2 Materials

### 2.1 Strains and plasmids

**Table 2.1** List of plasmids used in this work with a short description of relevant characteristics

<b>Plasmid</b>	<b>Description<sup>1</sup></b>	<b>Source or reference</b>
pVL2336	<i>E. coli/S. aureus</i> shuttle plasmid vector, amp <sup>R</sup> , ery <sup>R</sup> , cam <sup>R</sup>	Unpublished
pCG248	<i>E. coli/S. aureus</i> shuttle vector, amp <sup>R</sup> , cam <sup>R</sup>	Helle et al. (2011)
pCN55	<i>E. coli/S. aureus</i> shuttle vector, spc <sup>R</sup>	Charpentier et al. (2004)
pMAD	X-GAL, vector for allelic replacement in Gram-positive bacteria, amp <sup>R</sup> , ery <sup>R</sup>	Arnaud et al. (2004)
pMAD-GG	pMAD, but BsaI restriction sites in MCS, compatible with golden gate cloning, amp <sup>R</sup> , ery <sup>R</sup>	Dr. Danae Morales, unpublished
pLOW	Plasmid for IPTG-inducible expression of proteins in <i>S. aureus</i> , amp <sup>R</sup> , ery <sup>R</sup>	Liew et al. (2011)

<sup>1</sup> amp; ampicillin, ery; erythromycin, spc; spectinomycin, cam; chloramphenicol

**Table 2.2** List of parental strains used in this work, with a short description of their relevant genotype and characteristics

<b>Strain</b>	<b>genotype and characteristics<sup>1</sup></b>	<b>Source or reference</b>
IM08B	DH10B, $\Delta dcm$ , P <sub>help</sub> - <i>hsdMS</i> , P <sub>N25</sub> - <i>hsdS</i> (strain expressing the <i>S. aureus</i> CC8 specific methylation genes)	Monk et al. (2015)
SH1000	<i>rsbU</i> + derivative strain of NCTC8325-4	Horsburgh et al. (2002)
NCTC8325-4	NCTC8325 cured for $\phi 11$ , $\phi 12$ , and $\phi 13$	Novick (1967)
Newman	Human clinical isolate	Duthie and Lorenz (1952)

All remaining strains used or constructed for this work are listed in **appendix A1 and A2**.

## 2.2 Primers

**Table 2.3** List of primers used in this work

<b>Name</b>	<b>Sequence 5'-3', reference<sup>1</sup></b>
Primers for validation of sgRNA plasmids	
mk25_pCG248_R_check	AAATCTCGAAAATAATAGAGGGA, Dr. Morten Kjos
mk26_pCG248_F_check	GGATAACCGTATTACCGCCT, Dr Morten Kjos
Primers for construction and validation of pMAD deletion vectors	
im156_pMAD_check_F	AATCTAGCTAATGTTACGTTACA, Ine Storaker Myrbråten
mk177_pMAD_check_R	GATGCCGCCGGAAGCGAG, Dr. Morten Kjos
mk188_aad_up_F	ATTGGGCCACCTAGGATC, Dr. Morten Kjos
mk189_aad_down_R	ACTATGCGGCCGCTCGAG, Dr. Morten Kjos
mk389_seq_in_aad_R	ACCGTTAGCGTTTAAGTACATC, Dr. Morten Kjos
mm7_00671_up_F_GG	TATGGGGGTCTCCCTATGCAAATTTAACAAGAGCGAATCGT
mm8_00671_up_R	GATCCTAGGTGGGCCCAATCTAGCAATTCACATCATGTGAGATTG
mm9_00671_down_F	CTCGAGCGGCCGCATAGTAGGGACTCCTCCTTAAATTATGT
mm10_00671_down_R_GG	TATGGGGGTCTCCCTGCCTAACTTATGACAATCGCTCCA
mm11_00671_check_up_F	CTGAAGGCTCATTTGGAGTG
mm12_00671_check_down_R	TAACTTATGACAATCGCTCCAG
mm13_01487_up_F_GG	GCATTGGGTCTCGCTATCATAAATACTACGTGTTTCTTGAACCC
mm14_01487_up_R_GG	GCATTGGGTCTCGTCGTGGCAAAGTTAAACATGAAC
mm15_aad_up_F_GG	GCATTGGGTCTCCACGATTGGGCCACCTAGGATC
mm16_aad_down_R_GG	GCATTGGGTCTCCTCACTATGCGGCCGCTCGAG
mm17_01487_down_F_GG	GCATTGGGTCTCGGTGACGCGTTTTCTCCATACTTTATG
mm18_01487_down_R_GG	GCATTGGGTCTCGCTGCGGAACATTCATTGTTTAAAGCGTTC
mm19_00671_check_in_F	CTGCGTTACCAGCCCAATAC
mm20_00671_check_in_R	GAAGCTTGTGCATCATGATGC
mm21_01487_check_in_F	GCTTCTTCAAACATGCGCTTC
mm22_01487_check_in_R	GGGACGAAAGCATTAGATGTTTG
mm25_01487_check_up_F	CCACTTTATGTATCCCCCTGTG
mm26_01487_check_down_R	GCTGGTAAAGCATTAAAAGATGCTG
Primers for construction and validation of pLOW expression vector	
im110_seq-pLOW_up ermC	TTGGTTGATAATGAACTGTGCT, Ine Storaker Myrbråten
im134_pLOW_down_check_R	TGTGCTGCAAGGCGATTAAG, Ine Storaker Myrbråten
mm23_00671_F_SalI	CAGTGTCGACTAAGGAGGAGTCCCTATGAAAAAATTAG
mm24_00671_R_NotI	GCTAGCGGCCGCGATGTGAATTGCTAGTATATATCAGTAC

<sup>1</sup> No reference is indicated for the primers made for this work

## 2.3 Enzymes and chemicals

**Table 2.4** List of enzymes and chemicals used in this work

<b>Compound</b>	<b>Product number</b>	<b>Supplier</b>
1 kb DNA ladder		New England BioLabs
Acetic acid, CH <sub>3</sub> COOH	1.00063.1011	Merck
Agar powder		Merck
Agarose	15510-027	Invitrogen
Alkaline Phosphatase, Calf Intestinal (CIP)	M0290	New England BioLabs
Ampicillin	A-9518	Sigma-Aldrich
BamHI, FastDigest	FD0055	ThermoFisher Scientific
Bacto™ Brain Heart Infusion	237200	BD Diagnostics
Bacto™ Tryptic Soy Broth	286220	BD Diagnostics
Bacto™ Yeast Extract		BD Diagnostics
BglII, FastDigest	FD0083	ThermoFisher Scientific
BsaI-HF	R3535	New England BioLabs
BsmBI	R0580	New England BioLabs
Chloramphenicol, C <sub>11</sub> H <sub>12</sub> Cl <sub>2</sub> N <sub>2</sub> O <sub>5</sub>	C0378	Sigma-Aldrich
Crystal Violet	340244K	BDH Laboratory Supplies
dNTPs	N0447	New England BioLabs
EDTA, C <sub>10</sub> H <sub>16</sub> N <sub>2</sub> Na <sub>2</sub> O <sub>8</sub> •2H <sub>2</sub> O	20 296.360	VWR
Erythromycin, C <sub>37</sub> H <sub>67</sub> NO <sub>13</sub>	E6376	Sigma-Aldrich
Glucose, C <sub>6</sub> H <sub>12</sub> O <sub>6</sub>	10117gK	VWR
Glycerol, C <sub>3</sub> H <sub>8</sub> O <sub>3</sub>	1.04094.1000	Merck
Hydrochloric acid, HCl	30721	Riedel-De Haën
IPTG, Isopropyl-β-D-thiogalactosidase		Sigma-Aldrich
Isopropanol		VWR
Lysostaphin		Sigma-Aldrich
Lysozyme		Sigma-Aldrich
Magnesium chloride hexahydrate, Cl <sub>2</sub> Mg•6H <sub>2</sub> O	63072	Fluka
N,N,N',N'-tetramethylethane-1,2-diamine (TEMED), C <sub>6</sub> H <sub>16</sub> N <sub>2</sub>	T9281	Sigma-Aldrich
NotI-HF	R3189	New England BioLabs
peqGreen	PEQL37-501	Saveen Werner
Phusion® High-Fidelity DNA polymerase	M0530	New England BioLabs
PstI, FastDigest	FD0614	ThermoFisher Scientific
RedTaq® ReadyMix™	R2523	Sigma-Aldrich
RNase A		Sigma-Aldrich
SalI-HF	R3138	New England BioLabs
Sodium chloride (NaCl)	1.06464.1000	Merck
Sodium dodecyl sulphate (SDS)		Merck
Sodium hydroxide, NaOH	1.06469.1000	Merck
Spectinomycin, C <sub>14</sub> H <sub>24</sub> N <sub>2</sub> O <sub>7</sub> • 2HCl • 5H <sub>2</sub> O	S9007	Sigma-Aldrich
Sucrose, C <sub>12</sub> H <sub>22</sub> O <sub>11</sub>	102745C	BHD
T4 DNA ligase	M0202L	New England BioLabs
Tryptone		BD Biosciences
X-Gal		Sigma-Aldrich
Yeast extract	1.04086.0250	Merck

## 2.4 Kits and equipment

**Table 2.5** List of kits and laboratory equipment used in this work

<b>Kit / Equipment</b>	<b>Model / Product number</b>	<b>Supplier</b>
96-well polystyrene microtiter plates	82.1581.001	Sarstedt
Chambered coverglass	155409PK	ThermoFisher Scientific
E.Z.N.A.® Plasmid Mini Kit I	D6943-02	Omega Bio-Tek
Filmtracer™ LIVE/DEAD™ Biofilm Viability Kit	L10316	Invitrogen
Gel imager	GelDoc-1000	BioRad
Laser scanning confocal microscope	LSM700	Zeiss
Microplate reader	Synergy H1 Hybrid Reader	BioTek®
NEB® Golden Gate Assembly Kit (BsaI-HF®v2)	E1601L	New England Biolabs
NucleoSpin® Gel and PCR Clean-up	740609.250	Machnery-Nagel
PCR machine	ProFlex PCR systems	Applied Biodynamics
Spectrophotometer	NanoDrop 2000	Thermo-Fischer Scientific
Stereomicroscope	AxioZoom. V16	Zeiss

## 2.5 Growth medium, buffers and solutions

**Table 2.6** List of pre-made buffers and solutions used in this work

<b>Compound</b>	<b>Product number</b>	<b>Supplier</b>
5x Phusion High Fidelity buffer	B0518S	New England BioLabs
10x FastDigest Green Buffer	B72	ThermoFisher
10x NEBuffer™ 3.1	B7203S	New England BioLabs
Gel Loading Dye Purple (6x)	B7025S	New England BioLabs
Nuclei Lysis Solution	A7941	Promega
Protein Precipitation Solution	A7951	Promega
T4 ligase reaction buffer (10x)	B0202S	New England Biolabs

### 1 kb DNA ladder (50 mg/ml)

50 µl 1 kb ladder, 200 µl 10x loading buffer, 750 µl dH<sub>2</sub>O

### 10x TEN-buffer

100 mM Tris-HCl, 10 mM EDTA, 1 M NaCl

### 50x TAE-buffer

424 g Tris base, 57.1 ml Acetic acid, 100 ml 0.5 M EDTA, pH 8.0

Adjusted to 1 L with dH<sub>2</sub>O

### Lysogeny broth (LB)

Autoclaved: 10 g/L NaCl, 10 g/L Tryptone, 5 g/L Yeast extract

### S.O.C medium

Autoclaved: 2.0 g Tryptone, 0.5 g Yeast extract, 333.3 µl 3 M NaCl, 83.3 µl 3 M KCl, 96 ml dH<sub>2</sub>O

After autoclaving, add sterile filtrated: 2 ml 1 M MgCl<sub>2</sub>, 1 ml 2 M glucose

### Staphylococcus lysis buffer

40 mM NaOH, 0.2 % SDS



## 3 Methods

### 3.1 Growth and storage of *E. coli* and *S. aureus*

Experiments were performed in the *S. aureus* strains SH1000, NCTC8325-4 and Newman (all constructs are listed in **appendix A1** and **A2**). *E. coli* IM08B were used for cloning. All *E. coli* strains were grown in lysogeny broth (LB) or on lysogeny agar (LA) supplemented with ampicillin (100 µg/ml) for selection. *S. aureus* strains were grown in brain heart infusion (BHI) medium or tryptic soy broth (TSB) or on BHI agar or TSB agar. Agar plates were prepared with 1.5% (w/v) agar. Selective medium was supplemented with erythromycin (5 µg/ml) and IPTG (300 µM) for *S. aureus* overexpression constructs and complementation constructs, with erythromycin (5 µg/ml), chloramphenicol (10 µg/ml) and IPTG (300 µM) for *S. aureus* CRISPRi constructs, and with spectinomycin (100 µg/ml) for *S. aureus* knockout constructs. Frozen stocks for long term storage were prepared by adding glycerol to a final concentration of 17% to both *E. coli* and *S. aureus* cultures. Frozen stocks were stored at -80 °C.

### 3.2 Plasmid isolation

Plasmids were isolated using E.Z.N.A.® Plasmid Mini Kit I per the manufacturers protocol. This protocol was used for plasmid isolation from both *E. coli* and *S. aureus*. Before plasmid isolation, E.Z.N.A HiBind® DNA mini columns were equilibrated by adding 50 µl equilibration buffer to the column and centrifuging at 13,000 x g for 1 minute. For plasmid isolation from *E. coli*, cells were harvested from 1-5 ml overnight culture by centrifugation. The cell pellet was resuspended in 250 µl solution I (resuspension buffer). RNase A was added to the solution to degrade RNA. Cells were further lysed by addition of 250 µl solution II, an alkaline lysis buffer. After obtaining a clear lysate, 350 µl solution III was added to neutralize the acidic pH, resulting in precipitation of chromosomal DNA and cellular debris, while plasmid DNA remains in solution. The precipitate was removed by centrifugation and the clear supernatant was transferred to an equilibrated HiBind® mini column. HBC buffer was added to the column, resulting in plasmid DNA binding the silica column. The bound plasmid DNA was subsequently washed using the supplied wash buffer. After washing, the empty column was centrifuged to dry of any residual ethanol from the wash buffer. The plasmid DNA was eluted using 30-100 µl elution buffer. Isolated plasmids were stored at -20 °C.

### 3 Methods

*S. aureus* is a Gram-positive which can be difficult to lyse only using the lysis step of commercially available plasmid isolation kits. *S. aureus* has been found to be completely resistant to lysozyme, due to a modification in the peptidoglycan wall with an O-acetylation at the C-6 position of the *N*-acetyl muramic acid (Bera et al., 2007). As such, *S. aureus* is particularly hard to lyse, as many bacterial nucleic acid isolation techniques involve the use of lysozyme (Huff & Silverman, 1968). Therefore, another lytic enzyme, lysostaphin, is used for *S. aureus*. Lysostaphin cleaves cross-linking pentaglycine bridges, which are abundant in the cell walls of staphylococci (Huff & Silverman, 1968). Harvested *S. aureus* cells were resuspended in 250 µl solution I with addition of 1 µl lysostaphin (10 mg/ml) and 5 µl lysozyme (100 mg/ml). The solution was incubated at 37 °C for 30 minutes before continuing with the plasmid isolation protocol as described above.

#### **3.3 Isolation of genomic DNA**

To isolate genomic DNA (gDNA) from *S. aureus*, cells were harvested from 10 ml overnight culture by centrifugation for 2 minutes at maximum speed. The cell pellet was resuspended in 200 µl EDTA, 5 µl lysozyme (100 mg/ml) and 1 µl lysostaphin (10 mg/ml) and incubated at 37 °C for 30 minutes. After incubation, 600 µl Nuclei Lysis Solution (Promega) was added, followed by a 5-minute incubation at 80 °C. The cell lysate was subsequently cooled to room temperature before degrading RNA by the addition of 5 µl RNase A (10 mg/ml) at 37 °C for 30 minutes. After cooling the lysate to room temperature, 200 µl Protein Precipitation Solution (Promega) was added, followed by a 5-minute incubation on ice. The precipitate was removed by centrifugation and the clear supernatant was transferred to a tube containing 600 µl isopropanol to precipitate the DNA, mixing by inverting the tube. The gDNA was pelleted by centrifugation at max speed for 5 minutes. Subsequently, 600 µl 70% ethanol was added for washing, followed by a second centrifugation for 10 minutes. Residual ethanol was dried off by incubating the tube with the lid open at 55 °C for 15-30 minutes. The pellet was resuspended in dH<sub>2</sub>O and gDNA was verified by agarose gel electrophoresis (see **section 3.5**) and concentration was determined by NanoDrop. Isolated gDNA was stored at -20 °C.

#### **3.4 The polymerase chain reaction**

The polymerase chain reaction (PCR) is an *in vitro* method used to amplify large numbers of specific DNA-fragments from a sample. The PCR consists of three temperature-specific steps which are repeated in cycles: thermal denaturation of the target DNA, primer annealing of synthetic

### 3 Methods

oligonucleotide primers, and extension of the annealed primers by a DNA polymerase. Each cycle is repeated 25-30 times, and for each cycle the number of DNA fragments approximately doubles. The components of the PCR includes the DNA template and primers annealing to each end of the target sequence, the four deoxynucleotide triphosphates (dNTPs) dATP, dCTP, dGTP and dTTP, appropriate salts and buffers, and a thermostable DNA polymerase (Lo & Chan, 2006).

The first step of the PCR, denaturation, involves heating the reaction mixture to 94-98 °C. This results in separation of the two strands of DNA. At these temperatures the hydrogen bonds holding the two DNA strands together are broken. During annealing, the temperature is typically lowered to somewhere between 40-65 °C at which the synthetic oligonucleotide primers bind to their complementary sites on the single stranded DNA molecule. The temperature and length of time required for primer annealing depends on the melting temperature ( $T_m$ ) of the primers, which is dependent on their length and GC content (Lo & Chan, 2006; Ramesh et al., 1992). The primers used in this work have been designed to have a  $T_m$  of approximately 58-60 °C. The extension phase is typically carried out at 72 °C. In this step the DNA polymerase attaches to and elongates the DNA from the free 3' OH end of the primers. The time and temperature of extension depends on the type of DNA polymerase used. At the end of each cycle, the newly synthesized extension product serves as a template for the next cycle, resulting in exponential accumulation of DNA (Lo & Chan, 2006; Ramesh et al., 1992).

In this work, two different DNA polymerases were used: Phusion® High-Fidelity (HF) and RedTaq®. The Phusion® HF polymerase comprises a DNA-binding domain fused to a *Pyrococcus*-like proofreading polymerase, resulting in a polymerase generating PCR products with very high accuracy and speed, working at approximately 30 seconds per kilobase (New England BioLabs, 2020b). This polymerase was used for sequencing and cloning due to its proofreading capacity. For PCR where the accuracy of the end-product was not as important, RedTaq® polymerase, which has less proofreading capacity, was used.

For PCR using Phusion® HF polymerase the enzyme was mixed with the DNA template, appropriate primers, dNTPs and a 5x Phusion® HF buffer. For difficult PCRs, additional  $Mg^{2+}$ , in the form of  $MgCl_2$  was added to the reaction mix to ensure optimal activity of the Phusion® HF polymerase. The volumes and reagents used are listed in **table 3.1**. Primers used in this work are found in **section 2.2**.

**Table 3.1** Components of the Phusion® High-Fidelity PCR

Component	Final concentration/Volume
5x Phusion® HF Buffer	1x
10 mM dNTPs	200 µM
10 µM Forward Primer	0.5 µM
10 µM Reverse Primer	0.5 µM
Template DNA	< 250 ng
MgCl <sub>2</sub> (optional)	1 µl
Phusion® HF Polymerase	1 unit/50 µl PCR
dH <sub>2</sub> O	To a final volume of 50 µl

The thermocycling conditions was adjusted based on the length of the DNA template, the efficiency of the DNA polymerase and the  $T_m$  of the primers. The standard program for Phusion® HF PCR is listed in **table 3.2**.

**Table 3.2** Standard thermocycling conditions for Phusion® High-Fidelity PCR

Step	Temperature	Time	Cycles
Initial denaturation	98 °C	5-10 minutes	1x
Denaturation	98 °C	30 seconds	25-30x
Annealing	45-72 °C <sup>1</sup>	30 seconds	
Elongation	72 °C	30 seconds/kilobase	
Final extension	72 °C	5-10 minutes	1x
Hold	4 °C	∞	

<sup>1</sup> The annealing temperature was adjusted based on the  $T_m$  of the primers. The primers used in this work had a  $T_m$  of approximately 58-60 °C

If DNA-fragments were difficult to amplify, touch down PCR was utilized. In a touch down PCR the annealing temperature is initially set to a high temperature, but gradually lowered after a certain number of cycles. In this work the touch down PCR was programmed with annealing temperatures as following: 5 cycles at 60 °C, 5 cycles at 58 °C and 30 cycles at 52 °C.

### 3.4.1 Colony PCR screening

Colony screening with PCR is a rapid initial screen to determine the presence of a DNA insert after transformation. Colony PCR involves lysing the bacteria and amplifying DNA with either insert-specific or plasmid-specific primers, depending on the experiment. Using a combination of specific

primers, the orientation of the insert can be verified. Before setting up the PCR reaction, *E. coli* colonies were lysed by picking one colony or 2-4  $\mu\text{l}$  overnight culture in 10  $\mu\text{l}$  dH<sub>2</sub>O and microwaving at maximum power for 2 minutes. The lysate was subsequently cooled on ice for ~5 minutes before proceeding with the PCR protocol, adding the PCR components to the lysate. As described in **section 3.2**, *S. aureus* cells can be difficult to lyse. As an alternative strategy, *S. aureus* colonies or 2-4  $\mu\text{l}$  overnight culture was therefore added to 30  $\mu\text{l}$  Staphylococcus lysis buffer (40 mM NaOH, 0.2% SDS) and incubated at 95 °C for 5 minutes, followed by cooling for 5 minutes on ice and subsequent dilution in 100  $\mu\text{l}$  dH<sub>2</sub>O. 2-4  $\mu\text{l}$  of the diluted lysate was added to the PCR reaction. For colony screening RedTaq® ReadyMix™ PCR reaction mix was used. This contains buffer, dNTPs, the *Taq* DNA polymerase and an inert loading dye (Sigma-Aldrich, 2020). On ice, the Readymix™ was mixed with appropriate primers, DNA template and dH<sub>2</sub>O as described in **table 3.3**. The PCR reaction was added to the thermocycler as described for Phusion® polymerase, only that the extension time of RedTaq polymerase is approximately one minute per kilobase and that it is slightly less thermostable, so the denaturation steps were conducted at 94 °C.

**Table 3.3** Components of the RedTaq® ReadyMix™ PCR

Component	Final concentration/Volume
RedTaq® ReadyMix™ PCR reaction mix <sup>1</sup>	5 $\mu\text{l}$
10 $\mu\text{M}$ Forward primer	0.2 $\mu\text{M}$
10 $\mu\text{M}$ Reverse primer	0.2 $\mu\text{M}$
DNA template	2-4 $\mu\text{l}$
dH <sub>2</sub> O	To a final volume of 10 $\mu\text{l}$

<sup>1</sup> The RedTaq® ReadyMix™ PCR reaction mix contains the buffer, dNTPs, the *Taq* polymerase and an inert loading dye (Sigma-Aldrich, 2020).

### 3.5 Agarose gel electrophoresis

Agarose gel electrophoresis is a method used for the separation of DNA based on the size of the DNA fragments. When heated in a buffer and allowed to cool, agarose polymers associate non-covalently and form a network of bundles whose pore sizes are determined by the concentration of agarose (Lee et al., 2012). To separate DNA using agarose gel electrophoresis, the DNA sample is loaded into small wells at the top of the agarose gel and a current is applied. The phosphate backbone of the DNA molecule is negatively charged so that when an electric field is applied DNA fragments will migrate to the positively charged anode. DNA has a uniform mass/charge ratio, resulting in the DNA molecules being separated by size within an agarose gel. Smaller DNA

### 3 Methods

fragments will travel faster through the gel than larger DNA fragments (Lee et al., 2012). To visualize the DNA fragments after separation, a fluorescent dye is added to the gel before casting. In this work, the DNA binding dye peqGREEN, which fluoresces under UV, was used.

Agarose gel electrophoresis was used to analyze PCR fragments and gDNA. In this work, a 1% (w/v) agarose gel was used. The agarose gel was prepared by dissolving agarose in TAE (40 mM Tris-Acetate, 1 mM EDTA) buffer by boiling. After melting the agarose, peqGREEN (1  $\mu$ l/50 ml) was added to the gel solution. The agarose gel solution was poured into a cast, and a comb was placed in the gel to create the wells. The gel was allowed to set at room temperature before being moved to a gel electrophoresis chamber and covered with TAE buffer. DNA samples were mixed with a 6x loading buffer to a final concentration of 1x. The loading dye contains glycerol which simplifies loading of the sample, and the dye bromophenol blue which makes the samples visible when loading. In the case of PCR products resulting from using RedTaq® polymerase, a loading dye was already present in the PCR mix. A 1 kb DNA ladder with DNA-fragments of known sizes was applied to the gel, allowing for determination of approximate size of the fragments in the sample. The gel electrophoresis was conducted at 90V until the DNA fragments were sufficiently separated, approximately 25-35 minutes. The fragments were visualized under UV light in a GelDoc-1000 (BioRad).

#### **3.5.1 Extraction of DNA from agarose gels**

For separated DNA fragments that were going to be used further, the fragments were isolated from the agarose gel and purified using the Nucleospin® Gel and PCR Clean-up Kit (Machery-Nagel). The DNA band at the correct size was excised from the agarose gel and completely dissolved in buffer NTI (~200  $\mu$ l buffer per 100 mg agarose gel) at 55 °C. The dissolved gel was transferred to a Nucleospin® Gel and PCR Clean-up Column and centrifuged at 11,000 x g for 30 seconds. Buffer NTI contains chaotropic salts, and in the presence of chaotropic salts the DNA from the sample binds to the silica membrane of the Nucleospin® column. Following this, contaminants were removed by washing the column with 700  $\mu$ l buffer NT3. After washing, a second centrifugation with an empty column was done to dry of any residual ethanol from buffer NT3. The DNA was eluted in a clean Eppendorf tube under low salt conditions using 15-30  $\mu$ l of the slightly alkaline elution buffer NE (5 mM Tris-HCl, pH 8.5). The column was incubated at room temperature with the elution buffer for 1 minute before centrifugation. The eluted DNA was stored at -20 °C.

### 3.6 Restriction digestion and ligation

Restriction digestion takes advantage of naturally occurring enzymes that cleave double stranded DNA at specific sequences, either leaving behind blunt or sticky ends. Restriction digestion and ligation was used for the construction of sgRNA plasmids, allelic exchange plasmids and an expression plasmid. A standard restriction digestion reaction is presented in **table 3.4**.

**Table 3.4** Components used in a standard restriction digestion reaction

Component	Final concentration/Volume
DNA	1 µg
10x supplied reaction buffer	5 µl/1x
Restriction enzyme(s) <sup>1</sup>	1 µl of each enzyme
dH <sub>2</sub> O	To a final volume of 50 µl

<sup>1</sup> In the case of a double digestion, 1 µl of each enzyme is added to the reaction

The restriction digestions were incubated at the optimum temperature for the given restriction enzyme for 1-2 hours. In this work, restriction digestions carried out with BsmBI was incubated at 55 °C, while all other restriction digestions were carried out at 37 °C. For restriction digestions of destination vectors, 1 µl CIP (Alkaline Phosphatase, Calf Intestinal) was added to the reaction after ~ 1 hour of incubation, followed by a subsequent incubation for ~ 30 minutes. CIP nonspecifically catalyzes the dephosphorylation of 5' and 3' ends of DNA phosphomonoesters, preventing re-ligation of the empty vector. Digested DNA was verified using agarose gel electrophoresis and purified either from the agarose gel (**Section 3.5**) or directly from the digestion reaction using 200 µl buffer NT1 per 100 µl reaction.

In this work, the construction of CRISPRi sgRNA plasmids was conducted using the type IIS restriction enzyme BsmBI, while allelic exchange plasmids were constructed using the type IIS restriction enzyme BsaI using golden gate cloning (Engler et al., 2009). Type IIS restriction enzymes bind to their recognition site but cut the DNA downstream from the recognition site in a non-sequence specific way but based on position, also allowing a final construct in which the restriction site is absent (**Figure 3.1**). BsmBI has the recognition site 5'-CGTCTC-3' and cuts one base downstream on the top strand and five bases downstream on the bottom strand (N<sub>1</sub>/N<sub>5</sub>), leaving a 4 bp overhang, while BsaI recognizes the sequence 5'-GGTCTC-3' and cuts in a N<sub>1</sub>/N<sub>5</sub> manner. Since type IIS restriction enzymes cut in a non-sequence specific way, the overhang they create varies from one recognition site to another and recognition sites can therefore be designed to generate DNA fragments with unique overhangs.

### 3 Methods

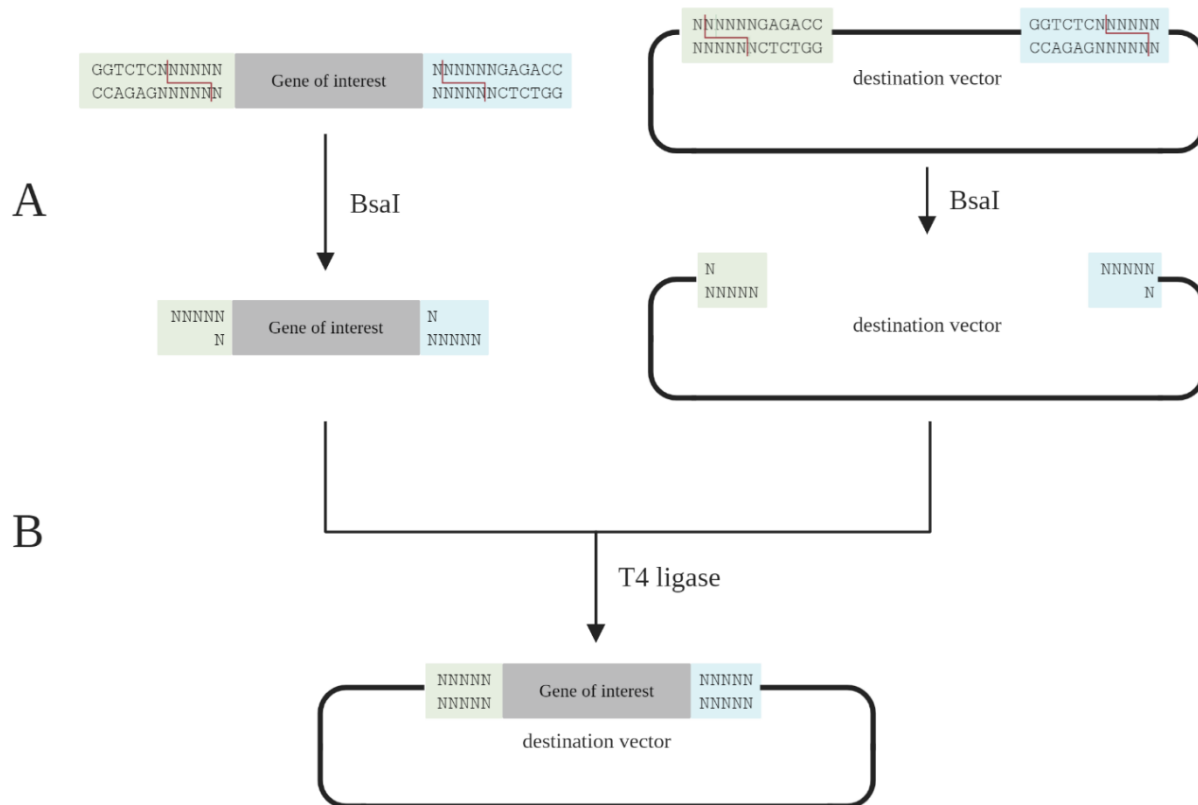


**Figure 3.1 Golden Gate cloning.** Gene of interest is amplified by PCR using primers introducing the specific type IIS restriction sites. Destination vector harbors type IIS restriction sites. **(A)** Both amplicon and destination vector are cleaved using a type IIS restriction enzyme (BsaI is used as an example). The restriction enzyme leaves 4 bp overhangs in the amplicon and destination vector complementary to each other, allowing for directional insert of the amplicon into the vector. **(B)** Restriction digested amplicon and destination vector is ligated using T4 ligase.

For the construction of CRISPRi double-sgRNA plasmids, the restriction enzymes BglIII, PstI and BamHI were used for BglBrick cloning (**Section 3.8.8**), while the restriction enzymes NotI and SalI were used for the construction of a *SAOUHSC\_00671* expression plasmid by standard restriction digestion and ligation (**Section 3.8.5**).

Digested inserts and plasmids were joined by the formation of a phosphodiester bond between the 5' phosphate and 3' hydroxyl termini, which is catalyzed by T4 ligase. The components of the reaction were mixed with a molar insert:vector ratio of 10:1 or 3:1. The reaction volume was 20  $\mu$ l, using 2  $\mu$ l of the supplied 10x reaction buffer and 1  $\mu$ l T4 DNA ligase. Ligation reactions were carried out overnight at 16  $^{\circ}$ C. Ligation reactions were stored at -20  $^{\circ}$ C or directly transformed into the desired host.

### **3.7 Targeted gene sequencing**

Targeted gene sequencing by Sanger sequencing was performed to verify correct construction of plasmids. This was done for plasmids isolated from both *E. coli* and *S. aureus*. For targeted gene sequencing 5 µl plasmid DNA with a concentration of 80-100 ng/µl was mixed with 2 µl of the sequencing primer (10 µM) and 3 µl dH<sub>2</sub>O and sent for sequencing. If plasmid was isolated from *S. aureus* strains harboring more than one plasmid, the gene of interest was amplified by PCR and verified by agarose gel electrophoresis, as described in **sections 3.4** and **3.5**, using the PCR amplicon for the sequencing reaction. This method usually gives a read of approximately 1000 base pairs. If the gene of interest was larger than this, multiple primers were used to get complete coverage of the sequence. Targeted gene sequencing was performed by GATC, Eurofins Genomics.

### **3.8 Generation of *S. aureus* genetically modified strains**

#### **3.8.1 Transformation in *E. coli***

In this work, CaCl<sub>2</sub> heat-shock transformation was used to introduce foreign DNA into *E. coli*. The general mechanisms of the Ca<sup>2+</sup> effect on the cells is not entirely known, but it is thought to facilitate binding of DNA to the surface of the cell. Calcium treatment has also been shown to disrupt the membrane, thereby increasing its permeability and hence facilitating DNA uptake (Chang et al., 2017; Liu et al., 2006).

To prepare chemically competent *E. coli* IM08B the following protocol was used. A 5 ml overnight culture of *E. coli* IM08B was set up in LB medium, incubated at 37 °C, shaking. After overnight incubation the culture was diluted 1/100 to a final volume of 100 ml in fresh LB medium in an Erlenmeyer flask and allowed to grow to an optical density (OD) of approximately 0.4. Cells were cooled on ice for approximately 20 minutes before harvesting the cells by centrifugation at 6000 rpm for 5 minutes at 4 °C. The supernatant was discarded. All subsequent steps were carried out at 4 °C. Cells were resuspended in ½ of the culture volume in 0.1 M ice cold CaCl<sub>2</sub> and kept on ice for 2 hours. Cells were harvested by centrifugation at 4000 rpm for 5 minutes and resuspended in approximately 5 ml 0.1 M CaCl<sub>2</sub> with 15% glycerol, depending on the pellet size. The competent cells were aliquoted in Eppendorf tubes and stored at -80 °C.

For transformation in *E. coli*, 50 µl chemically competent *E. coli* IM08B was thawed on ice and mixed with the correct plasmid or ligation reaction, usually 2 - 10 µl. The competent cells were

### 3 Methods

incubated with the DNA for 30 minutes on ice. Cells were heat shocked at 42 °C for 30 seconds and cooled on ice for 1-2 minutes. 250 µl SOC medium was added to the cells and cells were incubated at 37 °C, shaking, for approximately 1 hour. 50 µl and 200 µl were plated on LB agar plates with ampicillin (100 µg/ml) for selection of transformants. Transformants were verified by colony PCR (**Section 3.4.1**) and targeted gene sequencing (**Section 3.7**).

#### **3.8.2 Transformation in *S. aureus***

For Gram-positive bacterial species that are not known to be naturally competent, such as *S. aureus*, electroporation is the method of choice for introducing genetic material into the cell. During electroporation, an applied electric pulse produces an electric field across the cell membrane that alters the transmembrane potential of the cell. Due to the directional flow of current, the membrane becomes hyperpolarized on the side facing the anode of the electroporator and depolarized on the side facing the cathode. When the field strength is sufficient, the areas of the membrane directly facing the electrodes become electropermeabilized due to the transmembrane potential difference reaching a critical value. Negatively charged DNA is directed towards the cathode-facing portion of the cell membrane by electrophoresis from the applied electric field (Grosser & Richardson, 2016).

Preparation of *S. aureus* electrocompetent cells involves a series of washing steps in water and/or non-ionic solutions to remove all salts from the original culture media. High ion concentrations can result in arcing, or “shorting” of the electroporation cuvette. This produces an electric discharge that decreases cellular viability and typically indicates an unsuccessful electroporation (Grosser & Richardson, 2016). In this work, the following method was used to prepare electrocompetent cells for all strains of *S. aureus*. An overnight culture of the desired *S. aureus* strain was grown overnight in 5 ml BHI medium. The overnight culture was diluted 1/50 in fresh BHI and allowed to grow at 37 °C, shaking, to an OD of approximately 0.5. The culture was divided into two 50 ml centrifugation tubes and cooled for 10 minutes on ice. Cells were harvested by centrifugation at 4 °C and 4000 x g for 10 minutes. All subsequent steps were carried out at 4 °C or on ice. The supernatant was discarded, and cells were washed two times with ice cold dH<sub>2</sub>O. Cells were subsequently washed three times with ice cold 10% glycerol. The final pellets were combined and resuspended in approximately 2 ml 10% glycerol with 0.5 M sucrose, depending on the size of the pellet. Cells were aliquoted and stored at -80 °C.

In *S. aureus* a major hinder to genetic manipulations is the presence of restriction modification (RM) barriers, which prevent the uptake of foreign DNA. In the absence of host-specific methylation profiles, introduced DNA is recognized by the host as foreign and hence degraded. This complicates transformation in *S. aureus* in the laboratory setting. To bypass the host-encoded RM, plasmid artificial modification is used. The plasmid is then premethylated in an *E. coli* strain heterologously expressing methyltransferases of the target host (Monk et al., 2015). In this work, *E. coli* IM08B was used for correct methylation of plasmids before transformation into *S. aureus*. After plasmid isolation from *E. coli* IM08B, plasmids were directly electroporated into the desired electrocompetent *S. aureus* strains.

In this work, electroporation was conducted as follows. Electrocompetent cells were thawed on ice and 50  $\mu$ l of cells were mixed with ~500-1000 ng of plasmid DNA. Cells were transferred to a 1 mm electroporation cuvette and electroporation was carried out at 2.1V, 100  $\Omega$  and 25  $\mu$ F. After electroporation 950  $\mu$ l TSB with 0.5 M sucrose was added immediately and cells were allowed to recover at 37  $^{\circ}$ C, shaking, for approximately 2 hours. If a temperature sensitive plasmid was used, cells were incubated at 30  $^{\circ}$ C. Cells were pelleted by centrifugation and resuspended in 350  $\mu$ l of the medium. 50  $\mu$ l and 200  $\mu$ l were plated on TSA plates containing the appropriate antibiotic. Plates were incubated overnight, or until colonies appeared, at 37  $^{\circ}$ C or 30  $^{\circ}$ C. Transformants were verified by colony PCR (**Section 3.4.1**) or by targeted gene sequencing (**Section 3.7**).

#### **3.8.3 Blue white screening**

In this work, gene knockouts are constructed using an allelic exchange method in which the gene of interest is exchanged with an antibiotic resistance marker. Allelic exchange using a temperature sensitive double recombination system (further explained in **section 3.8.4**) is often not efficient because the frequency of double crossover events may be low (Reyrat et al., 1998). Consequently, allelic exchange mutants may represent only a fraction of the transformants and may therefore be difficult to isolate. To overcome this, a plasmid with a counter selectable marker was used. Transformants which have integrated the plasmid containing the counter selectable marker, either by single cross-over or incorrect recombination, retain a copy of the counter selectable marker in the chromosome (Reyrat et al., 1998).

In this work, blue white screening was used as a counter selectable marker system. This system is based on plasmids harboring a fragment of the *lacZ* gene, which creates a non-functional  $\beta$ -

galactosidase. Growth of bacteria harboring this plasmid on agar containing the chromogenic substrate 5-bromo-4-chloro-3-indolyl- $\beta$ -D-galactopyranoside (X-gal) results in blue colonies indicating the carriage of the counter selectable marker on the plasmid or in the chromosome (Chaffin & Rubens, 1998). Colonies that appear white lack the counter selectable marker. This system was used in this work to select for successful allelic exchange mutants in which a double cross over event had occurred.

#### **3.8.4 Construction of a NCTC8325-4 SAOUHSC\_00671 knockout mutant**

To construct a *SAOUHSC\_00671* knock out mutant, an allelic exchange plasmid was constructed using overlap extension PCR. The overlap extension PCR is a method based on the standard PCR (**Section 3.4**) but is used to splice two or more fragments together into one larger fragment. For DNA fragments to be spliced they need to have overlapping 3' ends. For each molecule, the primer at the end to be joined is designed to have a 5' overhang which is complementary to the 3' end of the adjacent fragment. For the construction of the *SAOUHSC\_00671* knock out mutant, the allelic exchange plasmid was designed in a way that the *SAOUHSC\_00671* gene was exchanged with a spectinomycin resistance cassette, allowing for selection of successful mutants. In the first step of the overlap extension PCR, the DNA fragments that were to be spliced were amplified using primers that introduced the complementary overhangs. As shown in **figure 3.2A**, the reverse primer for the upstream region of *SAOUHSC\_00671* (mm8) had a 5' overhang to the spectinomycin cassette, and the forward primer of the downstream region of *SAOUHSC\_00671* (mm9) had a 5' overhang to the other end of the spectinomycin cassette. In the second step of the overlap extension PCR (**Figure 3.2B**), the amplicons from the first step were combined in a PCR reaction with the outside primers. The overlapping regions of the DNA fragments functions as primers for the DNA polymerase and, in combination with the outside primers, a fragment composed of all three fragments were amplified. The overlap extension PCR was conducted using Phusion® HF Polymerase as described in **section 3.4** and the final PCR product was isolated using agarose gel electrophoresis and extraction of DNA from agarose gel (**Section 3.5**).

### 3 Methods

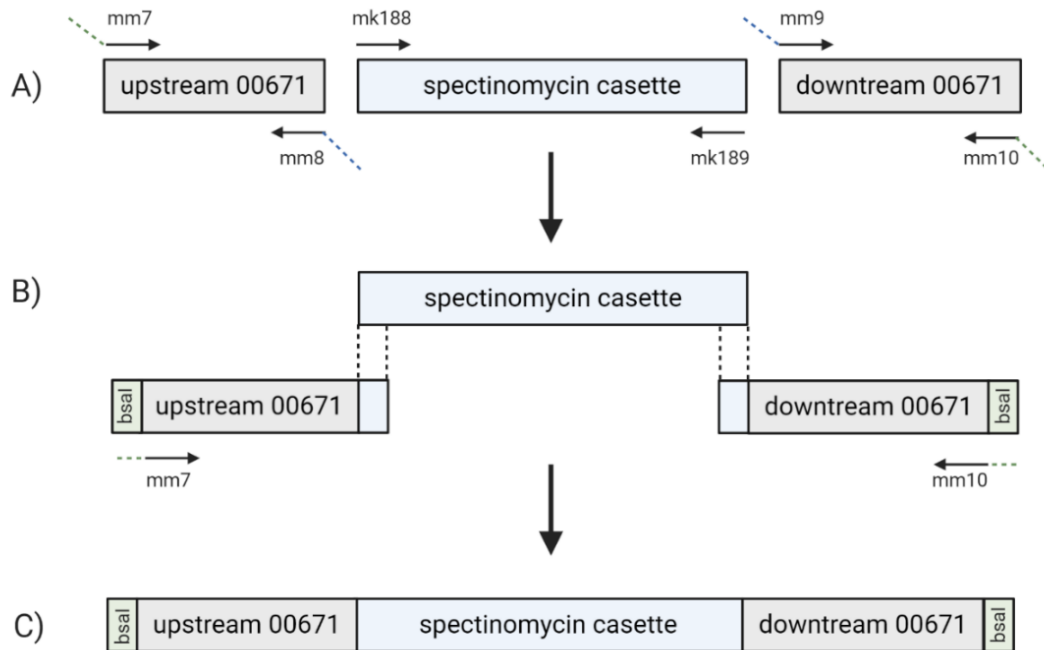


**Figure 3.2 Construction of a  $\Delta$ SA00671::*spc* allelic exchange plasmid for knockout in *S. aureus* NCTC7325-4.** Primers used are indicated by arrows pointing in a 5'-3' direction. The solid line indicates the annealing segment of the primer, while the dashed line indicates an overlapping tail or a tail which introduces a restriction site. **A)** Amplification of DNA fragments which are to be spliced. This includes fragments ~1000 bp upstream and downstream of the SAOUCS\_00671 gene, and a ~1.3 kb spectinomycin resistance cassette. Primer mm7 introduces a BsaI restriction site to the upstream fragment, and primer mm10 introduces the restriction site to the downstream fragment. **B)** All three fragments to be combined are added to a single PCR reaction containing the outside flanking primers mm7 and mm10 resulting in **C)** a DNA fragment consisting of all three initial fragments.

The outside primers (mm7 and mm10) introduced a BsaI restriction site to each end of the resulting spliced DNA fragment, allowing for restriction digestion and ligation into the pMAD-GG destination vector which harbors two BsaI recognition sites in the multiple cloning site (MCS) (see **section 3.6** for restriction digestion and ligation). The pMAD vector system used for knocking out genes in *S. aureus* is a temperature-sensitive double recombination system. Plasmids were transformed into *E. coli* followed by transformation into *S. aureus* as described in **section 3.8.1 and 3.8.2**. Following transformation into *S. aureus*, cells were grown at 30 °C, shaking, for 3.5 hours before plating on TSA plates with 5 µg/ml erythromycin and 40 µl X-gal (50 mg/ml). X-gal was added to plates for blue white screening of colonies (See **section 3.8.3** for blue white screening). Plates were incubated for 1-2 days at 30 °C. 1-4 blue colonies were selected, as these would harbor the allelic exchange plasmid, and re-streaked on TSA with erythromycin and X-gal and verified by colony PCR (**Section 3.4.1**). After overnight incubation at 30 °C, a blue colony was picked and grown in TSB for 2 hours at 30 °C. After 2 hours the temperature was increased to

### 3 Methods

43 °C, further incubating for 6 hours. After 6 hours, the culture was re-diluted 1/1000 and incubated overnight at 43 °C. Serial dilutions were plated on TSA with 100 µg/ml spectinomycin and X-gal and incubated at 43 °C for 1-2 days. At this high temperature, the pMAD-GG plasmid does not replicate and only clones where integration of the plasmid into the chromosome has occurred, maintain the antibiotic resistance. At this point, pale blue or blue colonies most likely is the result of a single crossover event, where the gene has not been deleted. White colonies, in which the counter selectable marker is absent, are likely a result of a double crossover event in which case the gene has been replaced with the spectinomycin cassette. Successful clones will at this point be spectinomycin resistant and erythromycin sensitive. White colonies were picked and re-streaked on TSA with spectinomycin and TSA with erythromycin and incubated overnight. Spectinomycin resistant, erythromycin sensitive colonies were selected for colony PCR using primers for the spectinomycin cassette and outside primers to ensure correct orientation of the inserts. Primers targeting the deleted genes were used to ensure that the gene had been deleted.

#### **3.8.5 Construction of a NCTC8325-4 SA00671 overexpression mutant**

To construct a *S. aureus* NCTC8325-4 strain overexpressing *SAOUHSC\_00671*, an overexpression plasmid was constructed using restriction digestion and ligation. The *SAOUHSC\_00671* gene, including the ribosomal binding site and start codon was amplified from *S. aureus* NCTC8325-4 using PCR (**Section 3.4**). Primers were designed to introduce a SalI recognition site on the 5' end of the gene and a NotI recognition site on the 3' end of the gene. The forward primer introducing the SalI restriction site also introduced a single base pair mutations in the *SAOUHSC\_00671* start codon, exchanging TTG to ATG. The amplicon was inserted into the plasmid pLOW using restriction digestion and ligation with restriction enzymes NotI and SalI, giving pLOW-00671 (see **section 3.6** for restriction digestion and ligation). In this work, a plasmid-based system for overexpression in *S. aureus* was used. The system uses a low-copy-number plasmid, pLOW, which contains an IPTG-inducible promoter, to allow IPTG-regulated gene expression (Liew et al., 2011). The ligated plasmid was transformed into *E. coli* followed by subsequent transformation into *S. aureus* NCTC8325-4. The plasmid was verified by colony PCR (**Section 3.4.1**) and targeted gene sequencing (**Section 3.7**).

### 3.8.6 Construction of a NCTC8325-4 $\Delta$ SAOUHSC\_00671 complementation strain

To obtain a *S. aureus* NCTC8325-4  $\Delta$ SAOUHSC\_00671 complementation strain, the pLOW-00671 plasmid (see **section 3.8.5**) was transformed into the NCTC8325-4  $\Delta$ SAOUHSC\_00671::*spc* strain MM149 by electroporation (**Section 3.8.2**).

### 3.8.7 Construction of a Newman $\Delta$ *ubiE*::*spc* allelic exchange plasmid

To construct a *S. aureus* Newman *ubiE* knockout mutant, an allelic exchange plasmid was constructed using golden gate assembly. The golden gate assembly takes advantage of the characteristics of type IIS restriction enzymes described in further detail in **section 3.6**. Since type IIS restriction enzymes cut outside their recognition site, the final assembly of fragments will no longer contain the recognition site. Consequently, no further digestion is possible after assembly, making it possible to carry out both the restriction digestion and the T4 ligation in a single reaction, the golden gate assembly (Engler et al., 2009; New England BioLabs, 2020a). In this work, the type IIS restriction enzyme BsaI was used for the construction of a  $\Delta$ *ubiE*::*spc* plasmid using the NEB Golden Gate Assembly Kit (New England BioLabs). A ~1000 bp region upstream of *ubiE*, a spectinomycin cassette, and a ~1000 bp downstream region of *ubiE* were amplified by PCR using primers that introduce a BsaI recognition site with the correct complementary overhangs to the adjacent DNA fragment. All three amplicons were combined in the golden gate assembly reaction, together with the destination plasmid pMAD-GG, as presented in **table 3.5**.

**Table 3.5** Components of the NEB Golden Gate Assembly reaction

Component	Negative control	Assembly reaction
Destination plasmid	75 ng	75 ng
Inserts <sup>1</sup>	-	2:1 molar ratio
T4 DNA ligase buffer (10x)	2 $\mu$ l	2 $\mu$ l
NEB Golden Gate Assembly Mix	1 $\mu$ l	1 $\mu$ l
dH <sub>2</sub> O	To a final volume of 20 $\mu$ l	To a final volume of 20 $\mu$ l

<sup>1</sup> amplicon inserts must possess 5' flanking bases and BsaI restriction sites at both ends of the amplicon and in the proper orientation

The assembly reaction was incubated at 37 °C for 1 hour before inactivation of the enzymes at 60 °C for 5 minutes. 2  $\mu$ l of the assembly reaction was transformed into *E. coli* IM08B and verified by colony PCR and sequencing as described in **section 3.4.1** and **3.7**. Plasmid was isolated from *E. coli* (**Section 3.2**) for the subsequent transformation into *S. aureus* (**Section 3.8.2**).

### 3.8.8 Construction of *S. aureus* CRISPRi strains

As described in **section 1.4**, the *S. aureus* CRISPRi system is a two-plasmid system where dCas9 is expressed behind an IPTG titratable promoter on one plasmid, and the sgRNA is expressed constitutively from a second plasmid. For the construction of *S. aureus* CRISPRi strains in this work, *S. aureus* strains already carried the plasmid encoding the dCas9. The sgRNA plasmids were constructed in the plasmid pVL2336 using oligos containing the sgRNA sequence (See **appendix A3** for sgRNA sequences). Plasmid pVL2336 is designed to allow introduction of gene-specific sgRNAs using Golden Gate cloning with enzyme BsmBI (See **section 3.6** for golden gate cloning). Oligo's were designed beforehand by Morten Kjos (NMBU) and Xue Liu (University of Lausanne, Switzerland). In brief, the sgRNA oligos consists of a 20-nt base pairing region and 4 bp overhang sequence, designed to overlap with the overhangs created by BsmBI (**Figure 3.1**). The 20-nt base pairing region is designed to target the non-template DNA strand close to the 5' end of the target gene, and adjacent to a PAM sequence. The final sgRNA plasmids express the sgRNAs (gene-specific 20 bp sequence, the Cas9 handle and a transcriptional terminator, **figure 1.4**), from a constitutive promoter.

To anneal the forward and reverse oligos reactions were set up as presented in **table 3.6**.

**Table 3.6** Components of the sgRNA oligo annealing reaction

Component	Total volume
Forward oligo (100 $\mu$ M)	2.5 $\mu$ l
Reverse oligo (100 $\mu$ M)	2.5 $\mu$ l
10x TEN-buffer	5 $\mu$ l
dH <sub>2</sub> O	To a final volume of 50 $\mu$ l

The reaction was incubated at 95 °C for 5 minutes before slowly cooling down to room temperature using a water bath. pVL2336 was digested using the type IIS restriction enzyme BsmBI and ligated with the desired sgRNA oligo using T4 DNA ligase as described in **section 3.6**. The resulting plasmid was transformed into *E. coli* and subsequently into *S. aureus* as described in **sections 3.8.1** and **3.8.2**. Correct transformants were selected for using ampicillin (100  $\mu$ g/ml) in *E. coli* and erythromycin (5  $\mu$ g/ml) and chloramphenicol (10  $\mu$ g/ml) in *S. aureus*.

Double-sgRNA plasmids were constructed using BglBrick cloning. In the pVL2336-sgRNA plasmid, the sgRNA sequence is flanked by two restriction sites for BglII and PstI at one end and

### 3 Methods

a restriction site for BamHI at the other end. To assemble two sgRNAs in one plasmid, for simplification sgRNA(1) and sgRNA(2), sgRNA(1) was cut out of the plasmid using BamHI and PstI. The plasmid containing sgRNA(2) was cut using BglII and PstI, opening the plasmid for the insertion of sgRNA(1) (**Figure 3.3**). The cut out sgRNA(1) was subsequently ligated into the sgRNA(2)-containing vector using T4 DNA ligase. The overhang sequences resulting from BamHI and BglII digestion are complementary, allowing for ligation, but the resulting ligation product sequence is not recognized by either two restriction enzymes. This results in a plasmid containing the sgRNA(2), followed by the sgRNA(1), which is still flanked by the BglBrick restriction sites, allowing for the subsequent insertion of multiple fragments using the same method.

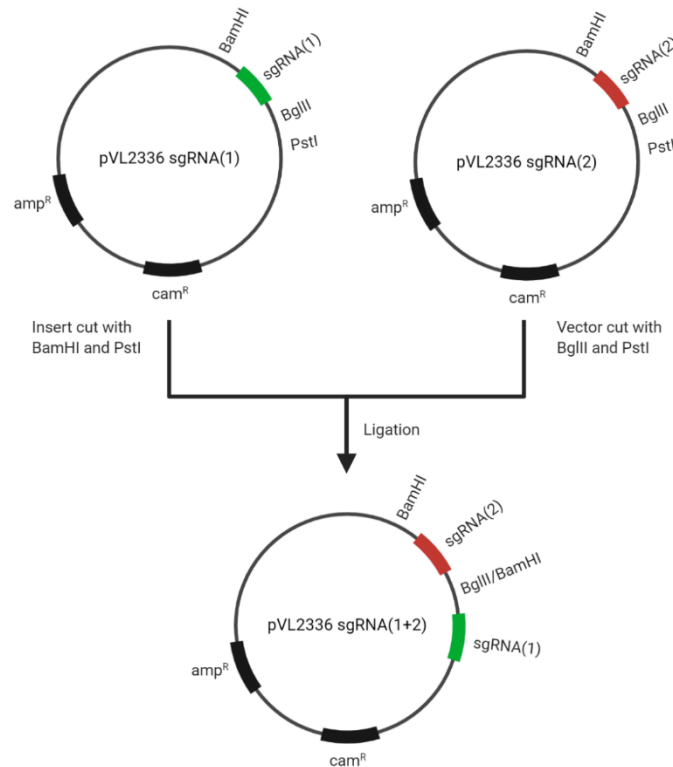


**Figure 3.3 Overview of the construction of double sgRNA plasmids by BglBrick cloning.** sgRNA(1) is cut out from the plasmid using restriction enzymes BamHI and PstI, while the plasmid harboring sgRNA(2) is opened by restriction digestion with BglII and PstI. The insert and vector are fused using the compatible BglII and BamHI restriction sites. The BglII and BamHI ligation results in a scar sequence which is not recognized by restriction enzymes. Additional sgRNAs can therefore be added using BglBrick cloning. Abbreviations: amp – ampicillin; cam - chloramphenicol

### 3.9 Growth curves

To determine the effect of gene depletions and gene deletions, in addition to overexpression of genes, growth curves of *S. aureus* strains were performed in microtiter plates, where optical density (OD) was monitored spectrophotometrically using the Synergy H1 Hybrid microtiter plate reader

### 3 Methods

(BioTek®). Overnight cultures of all strains were grown overnight in 5 ml TSB with the appropriate antibiotic and/or IPTG and diluted 1/100 in fresh TSB to a total volume of 300 µl in a 96-well microtiter plate. Strains were grown for 15 hours at 37 °C. OD<sub>600</sub> was measured at 10-minute intervals

#### **3.10 Biofilm assays**

##### **3.10.1 The crystal violet microtiter plate assay**

In this work, crystal violet (CV) staining was used to quantify biofilm formation of *S. aureus* in a 96-well microtiter plate assay based on the protocol used by Christensen et al. (1985). The theory of this approach is also described in **section 1.3**. Briefly, strains were grown at 37 °C whilst shaking overnight in 5 ml of suitable medium depending on the strain, supplemented with the appropriate antibiotics and/or IPTG. CRISPRi strains were grown with the addition of 300 µM IPTG to allow for depletion of the gene of interest. Following overnight incubation, the precultures were used to grow biofilm in flat-bottom 96-well plates (Sarstedt) by diluting the cultures 1/100 in fresh medium to a final volume of 100 µl in each well. Different media were tested, including TSB, TSB supplemented with MgCl<sub>2</sub> (TSBMg), TSB supplemented with 1% glucose and 1% NaCl (TSBGN) and BHI. In the final experiments, *S. aureus* NCTC8325-4 was grown in TSB, Newman in TSBMg and SH1000 in TSBGN containing antibiotics and 300 µM IPTG for induction of the CRISPRi system. Overexpression and complementation strains were grown in the presence of 50-1000 µM IPTG to induce expression from the plasmid. The microtiter plate was incubated statically for 24 hours at 37 °C to allow for biofilm formation. To quantify biofilm formation, CV staining was performed. This was done as follows. The medium of the wells, containing the planktonic cells, was removed by careful pipetting, and wells were washed once in saline (0.9% NaCl). Biofilm was dried for 5 minutes at room temperature. To stain the biofilm, 100 µl 0.02% (w/v) CV was added and incubated for 15 minutes at room temperature. The staining solution was subsequently discarded, and plates were washed twice with saline, or until no more dye was seen in the washing solution. For quantification the CV was dissolved in 200 µl 96% ethanol by incubating at room temperature for 10 minutes. The ethanol-solubilized CV was transferred to a fresh microtiter plate for quantification. Absorbance of the solution was measured at 600 nm in a microplate reader (BioTek®).

### 3.10.2 Macrocolony formation

*S. aureus* biofilm structure was studied in a macrocolony formation assay as described by Wermser and Lopez (2018) and in **section 1.3**. The presence of magnesium in the agar plate growth medium has been shown to promote robust and highly structured macrocolonies in *S. aureus* Newman, and strain Newman was therefore used for macrocolony studies in this work. To study macrocolony structure in *S. aureus* Newman, precultures were grown overnight in TSB, shaking at 37 °C. In the case of CRISPRi strains, 300 µM IPTG was added to the medium. Following overnight incubation 4 µl of the preculture was spotted onto TSBMg agar plates, also containing 300 µM IPTG in the case of CRISPRi strains and dried briefly. Plates were incubated at 37 °C for 5 days to allow for the formation of structured macrocolonies. Macrocolonies were imaged using a stereomicroscope (Axio Zoom. V16 coupled to a Zeiss AxioCam 503). Macrocolony structure was used in this work to study the depletion of a selected set of genes, some of which have previously been described in biofilm formation, using CRISPRi.

### 3.10.3 Screening a pooled CRISPRi library for genes involved in macrocolony formation

In this work, the macrocolony assay was also used to screen for novel genes involved in macrocolony formation and structuring which have not been previously shown to participate in biofilm formation. This was done using a CRISPRi pooled library in *S. aureus* Newman. Pooled CRISPRi libraries are made up of pooled mix of strains, each harboring a unique plasmid containing a specific sgRNA sequence. (Sanjana, 2017). The CRISPRi library used in this work was constructed by Maria Heggenhougen (NMBU) and Xue Liu (University of Lausanne, Switzerland). The library, which was originally designed based on the NCTC8325-4 genome, contains cells harboring 1928 unique sgRNAs which together target all transcriptional units of the NCTC8325-4 genome. Due to high sequence similarity between genomes, the NCTC8325-4 library can also be successfully transferred and used in Newman (personal communication, Dr. Morten Kjos).

For macrocolony formation using the CRISPRi pooled library, 5 µl of the library ( $6,7 \times 10^8$  CFU/ml) was inoculated in 5 ml TSB with erythromycin (5 µg/ml), chloramphenicol (10 µg/ml) and IPTG (300 µM) and grown to an OD<sub>600</sub> of approximately 0.8. A  $10^{-6}$  dilution was made of the preculture and 100 µl of the dilution was plated out on a total of 40 TSBMg agar plates containing antibiotics and IPTG. Plates were incubated for 5 days at 37 °C to allow for macrocolony formation.

### 3 Methods

After 5 days the plates were visually inspected for colonies with distinct macrocolony structures (i.e., wrinkles, folds, ridges, color). All colonies with structures different from the controls were selected and re-streaked on new TSB plates with antibiotics to obtain pure colonies. After incubation overnight at 37 °C, colonies were picked and inoculated in 5 ml TSB with antibiotics. Plasmids were purified from the overnight cultures as described in **section 3.2** and sent for targeted gene sequencing (**Section 3.7**) to identify which sgRNA-plasmid the different colonies harbored. Novel biofilm genes identified in the macrocolony pooled library screen were selected for further functional studies.

#### **3.10.4 Confocal laser scanning microscopy**

In this work, confocal laser scanning microscopy (CLSM) was used to study *S. aureus* NCTC8325-4 biofilm structure and thickness. Cells of the biofilm was visualized by staining with the FilmTracer™ LIVE/DEAD® Biofilm Viability Kit (Invitrogen). The staining kit utilizes the fluorescent nucleic acid stain SYTO9, which generally labels all bacteria in a population green, and the red fluorescent stain propidium iodine which only penetrates bacteria with damaged membranes, causing a reduction in the SYTO9 stain fluorescence when both dyes are present. To prepare for LIVE/DEAD CLSM, a preculture of *S. aureus* was grown overnight at 37 °C in 5 ml BHI with suitable antibiotics and/or IPTG. Following overnight incubation, the preculture was diluted 1/100 to a total volume of 300 µl in fresh medium in the wells of a chambered coverglass (ThermoFisher Scientific) and left to incubate at 37 °C for 24 hours to allow for biofilm formation. After biofilm formation, planktonic cells and medium was removed and the biofilm was washed gently with 300 µl saline (0.9% NaCl). The LIVE/DEAD working solution was prepared by combining 3 µl SYTO9 and 3 µl propidium iodine with saline to a total volume of 1 ml. Each biofilm-containing chamber was stained using 250 µl of the working solution and left to incubate at room temperature in the dark for 25 minutes. The stain was discarded, and the biofilm was washed gently using 300 µl saline. New 300 µl fresh saline was added to the chambers before imaging to avoid the biofilm from drying out. The biofilm was observed using the Zeiss LSM700 CLSM and images were acquired using the Zeiss ZenBlack software.

## 4 Results

### 4.1 Using CRISPR interference to study biofilm formation in *S. aureus*

#### 4.1.1 Construction of a *S. aureus* CRISPR interference strain collection for knockdown of proposed biofilm-related genes

Biofilm formation in *S. aureus* is a complex process involving multiple stages, all of which involves different gene expression- and regulation patterns (**Section 1.2**). The biofilm forming properties of *S. aureus* is linked to a wide range of chronic infections including osteomyelitis and endocarditis and *S. aureus* is notorious in forming biofilm on indwelling medical devices resulting in increased morbidity and mortality. *S. aureus* biofilm infections are difficult to treat, and physical removal of the source of infection in addition to antibiotic treatment are the common methods for treatment (Bhattacharya et al., 2015). The increasing levels of antibiotic resistance found among *S. aureus* clinical isolates contributes further to the difficulty in treatment of *S. aureus* infections, resulting in the need of new treatment strategies for *S. aureus* infections.

Understanding the genetic regulation of biofilm formation in *S. aureus* is essential to generate new treatment strategies for *S. aureus* biofilm associated infections. Although multiple genes have been identified to be involved in biofilm development, much of the complex biofilm lifestyle is still unknown. Identifying novel genes relevant for biofilm formation can provide new insights into the biofilm developmental process. One of the main approaches to study gene function has been chromosomal inactivation, also known as gene knockout or gene disruption. In *S. aureus* this is commonly achieved through gene inactivation by transposon mutagenesis (Chaudhuri et al., 2009) or deletions using a temperature sensitive plasmid. As gene knockout is a time-consuming method to study gene function in *S. aureus*, one aim of this work was to study whether knock down of gene expression by CRISPR interference (CRISPRi) can be used to screen for genes involved in *S. aureus* biofilm formation.

To study whether CRISPRi could be used to identify novel genes involved in *S. aureus* biofilm formation, a set of CRISPRi strains for knockdown of genes previously proposed to be involved in *S. aureus* biofilm was constructed. This CRISPRi collection was used in the microtiter plate assay (**Section 4.1.2**) and the macrocolony formation assay (**Section 4.1.3**) to check whether any of the targeted biofilm genes could be identified in these assays, and thus whether CRISPRi can be used

## 4 Results

to study *S. aureus* biofilm formation. The genes selected for CRISPRi knockdown of gene expression were selected based on genes proposed to be involved in biofilm formation based on different type of biofilm assays (Moormeier & Bayles, 2017; Otto, 2013; Periasamy et al., 2012; Swarupa et al., 2018; Wermser & Lopez, 2018) and is presented in **table 4.1** with a short description of their biological function. The genes selected for CRISPRi knockdown are mainly annotated to be involved in cell adhesion and biofilm formation (~37%) and central metabolism (~13%). Other biological functions represented by the targeted genes (e.g., cell wall organization, purine synthesis, polysaccharide synthesis, heat response and Mg<sup>2+</sup> transport) account for 50% of the genes. The composition of *S. aureus* biofilms often varies considerably between different strains and there is also a considerable genetic variations among strains of *S. aureus* (Cue et al., 2012; McCarthy & Lindsay, 2010). Three different strains of *S. aureus* were therefore included in this work to study biofilm formation using CRISPRi: SH1000, NCTC325-4 and Newman.

### **4.1.2 Using CRISPR interference and the crystal violet microtiter plate assay to study *S. aureus* biofilm formation**

One important aspect of the biofilm developmental process involves the attachment and formation of *S. aureus* biofilm on abiotic surfaces. A widely used method to study biofilm development on abiotic surfaces is the microtiter plate assay (see **section 1.3.1**). In this work, the microtiter plate assay with subsequent quantification of biofilm formation using crystal violet was investigated as a method to screen for novel biofilm-related genes using CRISPRi knockdown of gene expression in strains of *S. aureus*. As many different assay conditions have been reported for the microtiter plate assay (Chen et al., 2012), initial assays with our strains SH1000, Newman and NCTC8325-4 were conducted to determine optimal conditions for *S. aureus* biofilm formation.

Different growth media has been reported to induce biofilm formation in *S. aureus*, among them being TSB supplemented with 1% glucose and 1% NaCl (TSBGN) (Agarwal & Jain, 2013). In this work the difference between the often-used *S. aureus* growth medium BHI and TSBGN on biofilm formation in a microtiter plate assay was initially tested in *S. aureus* SH1000 using a CRISPRi control strain harboring a non-targeting sgRNA and the wild-type (WT) SH1000 strain. Precultures of strains were initially grown in BHI overnight before diluting cultures 1/10 in 96-well microtiter plates in either BHI or in TSBGN, supplemented with 300 µM IPTG used for induction of the CRISPRi system. Biofilm formation was quantified by crystal violet staining after 24 hours of

## 4 Results

incubation (**Figure 4.1A**). The same amount of biofilm was detected for the WT strain in both BHI and TSBGN, while higher levels of biofilm formation was detected for the CRISPRi control strain when grown in TSBGN. The reason for this difference is not known, but it was chosen to proceed using the TSBGN medium for *S. aureus* SH1000.

**Table 4.1** List of genes screened for relevance in *S. aureus* biofilm formation by CRISPRi knockdown of gene expression. Information on protein and biological function retrieved from [www.uniprot.org](http://www.uniprot.org), unless otherwise noted.

Accession number		Name	Protein	Biological function
NCTC8325-4 SH1000	Newman			
SAOUHSC_00019	NWMN_RS00085	<i>purA</i>	Adenylosuccinate synthetase	Purine synthesis
SAOUHSC_00114	NWMN_RS00535	<i>capA</i>	capsular polysaccharide biosynthesis protein	Lipopolysaccharide synthesis
SAOUHSC_00411	Not annotated	<i>psma1-4</i>	Phenol-soluble modulin alpha	Cytolysis
SAOUHSC_00486	NWMN_RS02705	<i>ftsH</i>	ATP-dependent zinc metalloprotease	Protein degradation
SAOUHSC_00544	NWMN_RS03030	<i>sdrC</i>	Serine-aspartate repeat-containing protein	Cell adhesion
SAOUHSC_00545	NWMN_RS03035	<i>sdrD</i>	Serine-aspartate repeat-containing protein	Cell adhesion
SAOUHSC_00620	NWMN_RS03360	<i>sarA</i>	Transcriptional regulator	Regulation of transcription
SAOUHSC_00711	NWMN_RS03800	<i>mpfA</i>	Magnesium protection factor A <sup>1</sup>	Proposed Mg <sup>2+</sup> export
SAOUHSC_00760	NWMN_RS04045	<i>gdpS</i>	GGDEF domain protein	Cell wall organization
SAOUHSC_00790	NWMN_RS04175	<i>clpP</i>	ATP-dependent Clp protease proteolytic subunit	Protein degradation
SAOUHSC_00799	NWMN_RS04215	<i>eno</i>	Enolase	Glycolysis
SAOUHSC_00812	NWMN_RS04280	<i>clfA</i>	Clumping factor A	Cell adhesion
SAOUHSC_00912	NWMN_RS04760	<i>clpB</i>	Chaperone protein	Heat response
SAOUHSC_00994	NWMN_RS05165	<i>atl</i>	Bifunctional autolysin	Peptidoglycan catabolism
SAOUHSC_01008	NWMN_RS05225	<i>purE-D</i>	Purine biosynthesis operon	Purine biosynthesis
SAOUHSC_01135	NWMN_RS06145	<i>psmβ1-2</i>	Phenol-soluble modulin beta	Pathogenesis
SAOUHSC_01182	NWMN_RS06355	<i>def2</i>	Peptide deformylase	Translation
SAOUHSC_01192	NWMN_RS06405	<i>fakA</i>	Glycerone kinase	Fatty acid synthesis
SAOUHSC_01910	NWMN_RS09430	<i>pckA</i>	Phosphoenolpyruvate carboxykinase	Gluconeogenesis
SAOUHSC_02265	NWMN_RS11225	<i>agrA</i>	Staphylococcal accessory gene regulator	Regulation of transcription
SAOUHSC_02647	NWMN_RS13050	<i>mqo</i>	Malate-quinone oxidoreductase	TCA cycle
SAOUHSC_02798	NWMN_RS13775	<i>sasG</i>	<i>S. aureus</i> surface protein G <sup>2</sup>	Cell adhesion
SAOUHSC_02802	NWMN_2397	<i>fnbB</i>	Fibronectin binding protein B	Cell adhesion
SAOUHSC_02803	NWMN_2399	<i>fnbA</i>	Fibronectin binding protein A	Cell adhesion
SAOUHSC_02822	NWMN_RS13880	<i>fbp</i>	Fructose-1,6-bisphosphatase	Gluconeogenesis
SAOUHSC_02963	NWMN_RS14535	<i>clfB</i>	Clumping factor B	Cell adhesion
SAOUHSC_03002	NWMN_RS14720	<i>icaA</i>	Poly-beta-1,6-N-acetyl-D-glucosamine synthase	PIA-biosynthesis
SAOUHSC_03003	NWMN_RS14725	<i>icaD</i>	Poly-beta-1,6-N-acetyl-D-glucosamine synthase	PIA-biosynthesis
SAOUHSC_03004	NWMN_RS14730	<i>icaB</i>	Poly-beta-1,6-N-acetyl-D-glucosamine N-deacetylase	PIA-biosynthesis
SAOUHSC_03005	NWMN_RS14735	<i>icaC</i>	Putative poly-beta-1,6-N-acetyl-D-glucosamine export protein	PIA-export

<sup>1</sup> Armitano et al. (2016)

<sup>2</sup> Corrigan et al. (2007)

## 4 Results

The *S. aureus* CRISPRi system is a two-plasmid system where the sgRNA is constitutively expressed from one plasmid, while the dCas9 is expressed behind an IPTG-titratable promoter on another plasmid. It is critical to determine the growth conditions which allows efficient knockdown of gene expression. Since the microtiter plate assay involves two different growth steps, one overnight incubation of the pre-culture and one 24-hour microtiter plate incubation for biofilm formation, different IPTG conditions were tested in the strain SH1000. Four different growth conditions were set up using a control strain harboring a non-targeting sgRNA and strains harboring sgRNAs targeting *icaA* and *atl* (**Figure 4.1B**). *icaA* is part of the *icaABCD* operon responsible for production of polysaccharide intercellular adhesion (PIA), and an *ica*-negative mutant in SH1000 has been shown to have a biofilm-negative phenotype (Fitzpatrick et al., 2005). *atl* encodes the major staphylococcal autolysin, which has been reported to be important for biofilm formation (Biswas et al., 2006; Heilmann et al., 1997). Precultures of all strains were grown overnight in TSB with and without 300  $\mu$ M IPTG supplemented to the growth medium. Subsequently, both precultures were grown both with and without IPTG supplemented to the growth medium for the biofilm formation. As expected, without addition of IPTG to the growth medium, no difference in biofilm formation was identified between the different strains. Also, when supplementing the medium with IPTG only in one of the growth steps, either growth of preculture or formation of biofilm, only small variations in biofilm formation was detected. When supplementing the medium with IPTG in both growth steps, a greater difference is detected between the CRISPRi knockdown strains compared to the control strain, and these conditions were therefore used in the following experiments.

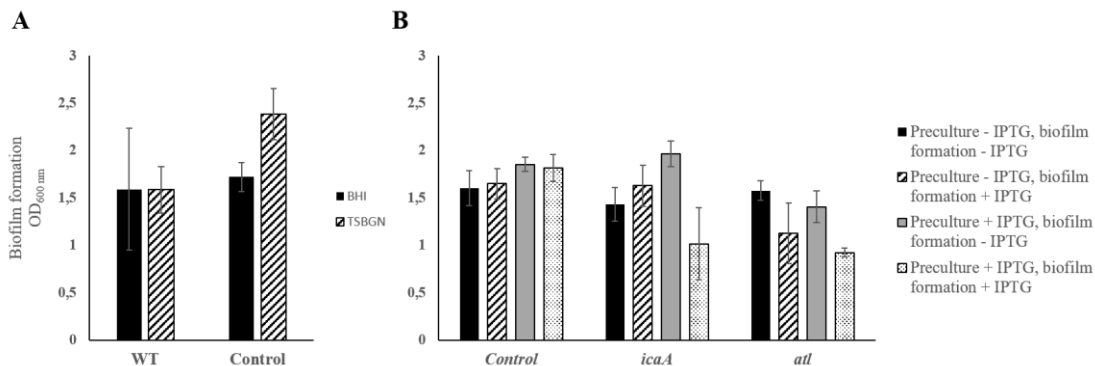


**Figure 4.1 Biofilm formation by *S. aureus* SH1000 CRISPRi knockdown strains under different growth conditions.** Biofilms were grown in 96-well microtiter plates for 24 hours. Biofilm formation was quantified by staining with 0.02% crystal violet. OD was measured at 600 nm. The control strain harbors a non-targeting sgRNA. **(A)** Growth of WT SH1000 and the CRISPRi control strain in BHI and TSB supplemented with 1% glucose and 1% NaCl (TSBGN). **(B)** Effect of induction with IPTG on biofilm formation by CRISPRi strains. Precultures were grown overnight with or without 300  $\mu$ M IPTG and diluted 1/100 in microtiter plates in fresh medium with or without 300  $\mu$ M IPTG. Error bars represent standard deviations based on three parallel measurements.

## 4 Results

In addition to strain SH1000, the strains Newman and NCTC8325-4 were studied in this work. Newman has been reported to form poor biofilm in plastic microtiter plates (Beenken et al., 2003; Mrak et al., 2012), but it was recently shown that macrocolony biofilm formation in *S. aureus* Newman is magnesium-dependent and that *S. aureus* Newman forms more robust biofilms when the medium is supplemented with magnesium (Wermser & Lopez, 2018). Biofilm formation by Newman CRISPRi strains in the microtiter plate assay was therefore tested using TSB supplemented with 100 mM MgCl<sub>2</sub> (TSBMg) in addition to TSBGN and TSB (**Figure 4.2A**, left panel). Biofilm formation by *S. aureus* Newman increases, as expected, when strains are grown in TSBMg compared to TSB and TSBGN. On the other hand, biofilm formation by the *S. aureus* NCTC8325-4 control strain was higher in either TSB or TSBGN as compared to TSBMg in the microtiter plate assay (**Figure 4.2C**, left panel). Furthermore, knockdown of *icaA* and *atl* was also performed in these strains. In Newman, little difference in biofilm formation can be detected when knocking down expression of these genes (**Figure 4.2A**, middle and right panels). For NCTC8325-4, the difference in detected biofilm formation is greater between the CRISPRi knockdown strains and the control strain when strains are grown in TSB as compared to TSBGN (**Figure 4.2C**, middle and right panels). Furthermore, when comparing biofilm formation of the three strains, SH1000, Newman and NCTC8325-4, Newman produces less biofilm in the microtiter plate than the other two strains, with the OD<sub>600</sub> of the control strain measured to be ~1 at the highest for Newman, and ~2.4 for SH1000 and NCTC8325-4.

Based on the results, the following conditions were used for the study of biofilm formation in the microtiter plate assay. All precultures of CRISPRi strains were grown overnight in TSB with 300 μM IPTG. Biofilm formation in the microtiter plate was also carried out incubating 24 hours with 300 μM IPTG supplemented to the growth medium. Biofilm formation in the microtiter plate assay by SH1000 was done in TSBGN while biofilm formation by NCTC8325-4 was carried out in TSB. As shown in **figure 4.2**, biofilm formation by Newman is less than both SH1000 and NCTC8325-4. As Newman proved to be a poorer biofilm former than the other strains, also shown by Cue et al. (2015), only SH1000 and NCTC8325-4 was used for further experiments with the crystal violet microtiter plate assay.

## 4 Results

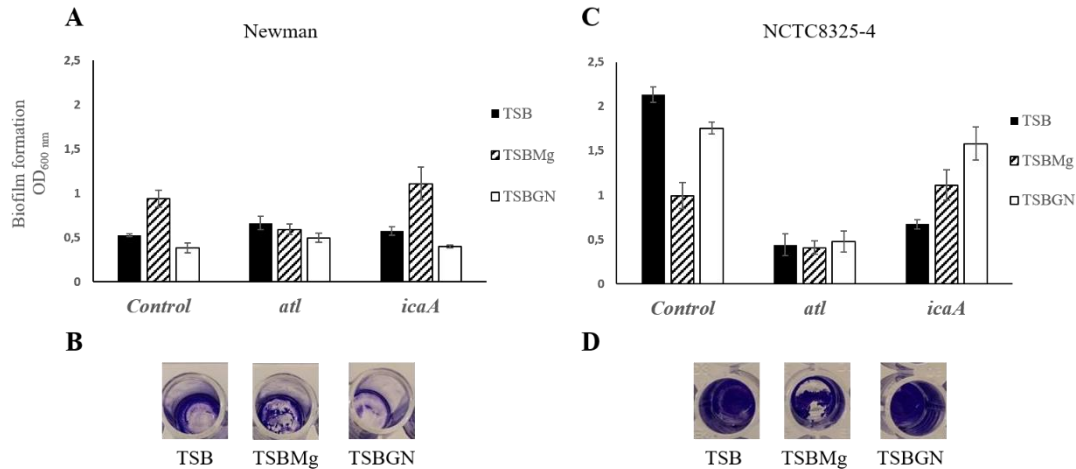


**Figure 4.2 Biofilm formation by *S. aureus* Newman and NCTC8325-4 CRISPRi knockdown strains.** Biofilms were grown in 96-well microtiter plates for 24 hours and biofilm formation was quantified by staining with 0.02% crystal violet. Biofilm formation was quantified for strains grown in TSB, TSB supplemented with 100 mM MgCl<sub>2</sub> (TSBMg) and TSB supplemented with 1% glucose and 1% NaCl (TSBGN). (A) Biofilm formation by *S. aureus* Newman CRISPRi knockdown strains. (B) Biofilm stained by crystal violet for the *S. aureus* Newman control strain grown in TSB, TSBMg and TSBGN. (C) Biofilm formation by *S. aureus* NCTC8325-4 CRISPRi knockdown strains. (D) Biofilm stained by crystal violet for the *S. aureus* NCTC8325-4 control strain grown in TSB, TSBMg and TSBGN. Error bars represent standard deviations based on three parallel measurements.

The initial results above with *icaA* and *atl* (Figure 4.1 and figure 4.2), suggest that CRISPRi could be used to identify genes involved in biofilm formation. To further investigate whether CRISPRi knockdown of gene expression could be used as a method to screen for novel genes involved in biofilm formation, a selection of 27 strains from the CRISPRi collection targeting genes previously proposed to be involved in biofilm formation was selected for initial screens. To do this, *S. aureus* SH1000 CRISPRi strains with sgRNA targeting the selected biofilm-associated genes for knockdown of expression was included in a series of microtiter plate assays followed by quantification of biofilm formation by staining with crystal violet. An upper and lower threshold for what was thought of as a significant increase or decrease was respectively set at 20% above and 20% below the OD measured for the control strain. It should be noted that the selected genes have been identified by different methods and in different studies, and it is thus not expected that all of them will be affecting biofilm formation in the polystyrene microtiter plate assay. Out of the 27 selected genes, 16 of the CRISPRi depletion strains were screened in two separate microtiter plate assays. Replicates are shown in grey and black stripes (Figure 4.3). The remaining 11 strains were screened only once (Figure 4.3B, white columns, figure 4.3C dotted columns).

## 4 Results

It is worth noting that when comparing the individual crystal violet microtiter plate assays, biofilm formation by the SH1000 control strain varies from assay to assay, with the measured OD<sub>600 nm</sub> ranging from ~1.4 to ~2.4 in three different assays. Furthermore, depletion of genes proposed to be involved in biofilm formation did, in multiple cases, give varying results from one crystal violet microtiter plate assay to another. The largest difference in biofilm formation between two assays was found to be after depletion of *psma1-4* which resulted in an increase in biofilm formation in one assay (**Figure 4.3A**) and a decrease in biofilm formation in the other (**Figure 4.3B**). Difference between assays were also observed for *ftsH*, *clfA* *clfB*, *capA*, *clpB*, *fnbA*, *sdrC* and *sdrD*, which had effect on the measured biofilm formation compared to the control only in one of the assays (**Figure 4.3A-C**).

From the genes that were tested only once, depletion of *pckA* resulted in an increase in biofilm formation and depletion of *icaB* and *icaD* resulted in a decrease in biofilm formation. As these genes were only screened once in the crystal violet microtiter plate assay and as results in biofilm formation can vary between separate assays, care should be taken, and conclusions should not be drawn based on the microtiter plate assay alone. A conclusion as to whether depletion of these genes have an effect on biofilm formation can therefore not be drawn without further screening. The reasons for the observed variation in the assay for the SH1000-strain will be discussed below.

Despite the relatively large variation in results from the SH1000 strain there were also some genes that gave consistent changes in biofilm formation capability in the two separate assays. Depletion of *agrA*, *psm $\beta$ 1-2* and *sasG* resulted in an increase in biofilm formation, and depletion of *atl* resulted in a decrease in biofilm formation in both assays, the latter as reported above. Both *agr*, *psm $\beta$ 1-2*, and *sasG* are associated with biofilm formation, with *agr* being known to repress the expression of cell surface proteins used in adherence and biofilm formation, and PSMs (*psm $\beta$ 1-2*) preventing hydrophobic interactions in adherence to polystyrene (Moormeier et al., 2014; Paharik & Horswill, 2016), corresponding to the depletion of these genes resulting in the increase in biofilm formation observed in this work. The reported role of SasG in *S. aureus* biofilm formation is variable. It is reported to inhibit adhesion to multiple ligands, like fibrinogen, while promoting adhesion to desquamated nasal epithelial cells (Corrigan et al., 2007). Finally, *atl* mutants have been shown to decrease adherence of *S. aureus* in the microtiter plate assay (Biswas et al., 2006), also corresponding to the findings in this work. These knockdown strains were also tested for

## 4 Results

growth defects, since major growth defects would affect the biofilm phenotype. The strains show similar growth rates to that of the control strain, which harbors a non-targeting sgRNA (**Figure 4.4**), and after 15 hours the cell density has reached the same as the control strain for all of the CRISPRi strains except the one depleted of *agrA*, having a slightly reduced growth after 15 hours of incubation.

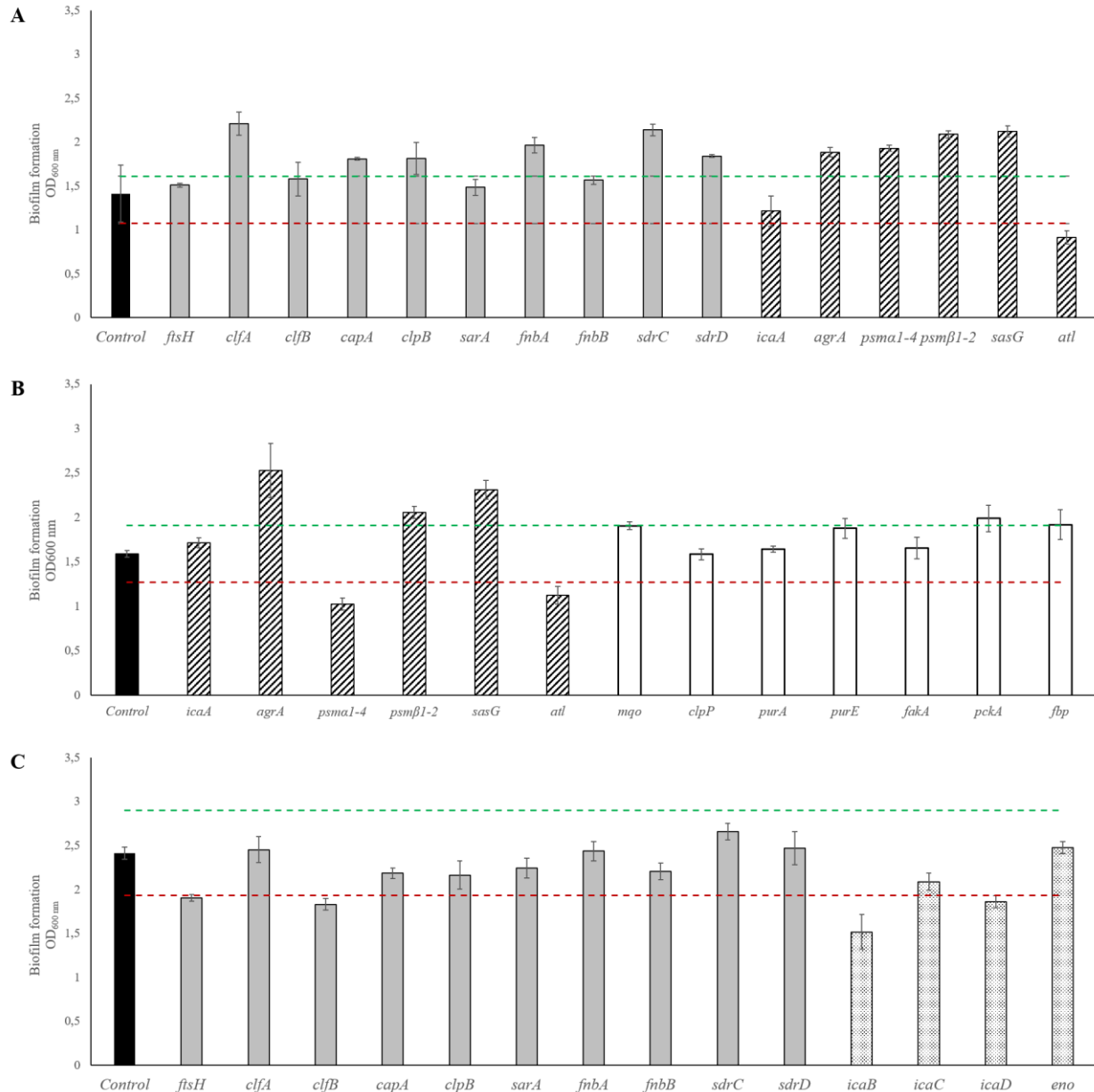


**Figure 4.3 Effect of CRISPRi knockdown of proposed biofilm-related genes on biofilm formation by *S. aureus* SH1000.** Precultures of *S. aureus* SH1000 CRISPRi knockdown strains were grown overnight in TSB supplemented with 300  $\mu$ M IPTG. Precultures were diluted 1/100 in fresh TSB w/ IPTG and biofilms were grown in 96-well microtiter plates for 24 hours and biofilm formation was quantified by staining with 0.02% crystal violet. Each strain was grown in triplicate. Biofilm formation was tested in three separate assays, with some strains being tested twice. Control strain harbors a non-targeting sgRNA. An upper (green dashed line) and lower (red dashed line) threshold was set at 20% above and 20% below the OD<sub>600 nm</sub> detected for the control strain. Error bars represent standard deviations based on three parallel measurements.

## 4 Results

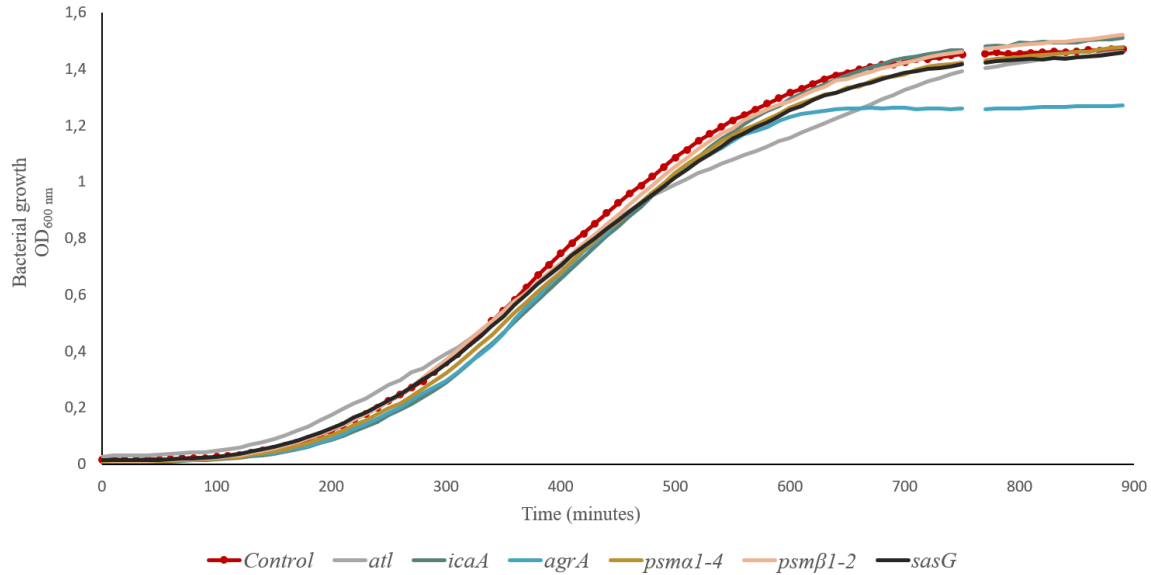


**Figure 4.4 Growth behavior of SH1000 CRISPRi knockdown strains showing an altered biofilm phenotype in the crystal violet microtiter plate assay.** Expression of genes were knocked down using CRISPRi. Precultures were grown overnight, and the CRISPRi system was induced with 300  $\mu$ M IPTG. Precultures were diluted 1/100 in fresh TSB w/IPTG and growth was measured at 10-minute intervals for ~15 hours. A CRISPRi strain harboring a non-targeting sgRNA was used as a control strain. Strains were grown in triplicate. After ~12 hours, a defect in the spectrophotometer resulted in a lack of measurement at this time point (gap in the curves).

The microtiter plate assay is a high throughput screening method as multiple conditions, and/or multiple strains can be screened at once. Taking all these points in consideration, the crystal violet microtiter plate assay can prove useful in screening CRISPRi depletion mutants for involvement in biofilm formation, however, it is also critical that multiple screens are performed to rule out assay variations. Further investigations are also needed in addition to the CRISPRi screen.

### 4.1.3 Using CRISPR interference to study *S. aureus* macrocolony formation

Macrocolony formation is considered as a model for biofilm formation (Ray et al., 2012; Wermser & Lopez, 2018) and the macrocolony formation assay has previously been used to identify novel genes involved in *S. aureus* USA300 macrocolony formation using a transposon library (Wermser & Lopez, 2018). One aim of this study was to determine whether *S. aureus* CRISPRi strains could be used in the macrocolony formation assays to identify novel genes involved in macrocolony formation. The macrocolony assay is based on macrocolony formation by *S. aureus* on agar plates, and supplementing the medium with magnesium has been found to increase the formation of robust and highly structured macrocolonies (Wermser & Lopez, 2018). In this work, macrocolony formation was initially tested in all three strains Newman, NCTC8325-4 and SH1000 using both

## 4 Results

TSB and TSB supplemented with 100  $\mu\text{M}$   $\text{MgCl}_2$  as growth medium in the agar plates (**Figure 4.5A**). For all three strains, structure and wrinkling of the macrocolonies increased when the medium was supplemented with magnesium. Color of the macrocolony varied between the three strains with NCTC8325-4 being white/grey, Newman being pale yellow and SH1000 being bright yellow/orange, probably due to varying levels of the pigment staphyloxanthin (Herbert et al., 2010). Strain Newman was selected for further studies, since this strain showed the most structured macrocolonies. Macrocolony structure progress during the time of incubation, and the number of days of incubation before structure is visible was investigated in the wild type strain *S. aureus* Newman by imaging every day for one week (**Figure 4.5B**). Small structure variations are visible after two days of incubation with small ring structures appearing in the center of the colony. After three days of incubation, folds and wrinkles start to appear, being more apparent after four and five days of incubation. After six days, the colony shape is more uneven, and after seven days of incubation the colony start to lose its folds and wrinkles and become even more uneven. Based on these results, subsequent macrocolony formation assays were carried out using strain Newman, incubating on TSBMg agar plates for 5 days before image acquisition.

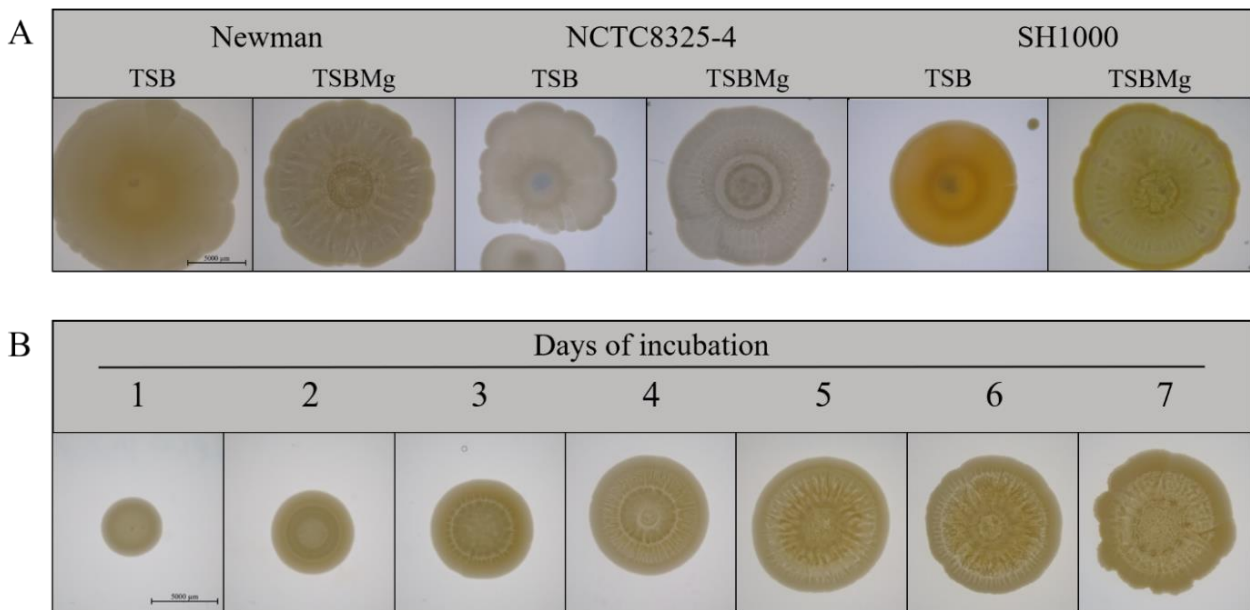


**Figure 4.5 *S. aureus* macrocolony biofilm formation.** (A) Effect of magnesium on macrocolony formation by *S. aureus* Newman, NCTC8325-4 and SH1000. Macrocolonies were grown on TSB or TSB supplemented with 100 mM  $\text{MgCl}_2$  (TSBMg). Precultures were grown spotted in 4  $\mu\text{l}$  on agar plates. Macrocolonies were imaged after 5 days. (B) Macrocolony formation by *S. aureus* Newman followed from 1 to 7 days. Scale bars 5 mm.

## 4 Results

To investigate whether CRISPRi knockdown of gene expression could be used as a method to screen for novel genes involved in macrocolony biofilm formation, a CRISPRi strain collection targeting a selection of 30 genes was used in an initial macrocolony test screen. The 30 selected genes (**Table 4.1**) have previously been proposed to be involved in biofilm formation and/or macrocolony formation and the aim was to investigate whether any of these genes could be identified in this work in a macrocolony screen using *S. aureus* Newman CRISPRi strains. A CRISPRi strain harboring a non-targeting sgRNA was used as a control strain.

As mentioned before, it should be noted that since the selected biofilm genes have been identified by different methods and in different studies, it was uncertain how many of them would affect macrocolony formation. However, eight of the selected genes have already been identified to be involved in macrocolony formation in a USA300 transposon library macrocolony screen (Wermser & Lopez, 2018). In their work,  $\Omega mpfA$ ,  $\Omega clpP$  and  $\Omega mgo$  showed little or no surface wrinkling,  $\Omega pckA$  and  $\Omega fbp$  mutants had thin macrocolonies with little or no surface wrinkling and  $\Omega purA$ ,  $\Omega purK$  and  $\Omega fakA$  showed pronounced surface wrinkling. In this work (**Figure 4.6**), depletion of *mpfA* and *clpP* showed no apparent change in surface wrinkling compared to the control strain (**Figure 4.6**, blue box) and depletion of *purA*, *pckA*, *fbp* and *fakA* all resulted in increased surface wrinkling (**Figure 4.6**, black box). Depletion of *mgo* resulted in a loss of structure with shorter wrinkles and folds while depletion of the *purEKCSQLFMNHD* operon resulted in an uneven colony morphology (**Figure 4.6**, red box). Depletion of some genes, not studied by Wermser and Lopez (2018), were found to result in an uneven morphology (*def2*) or loss of structure (*eno*, *gdpS*, *capA*). Macrocolonies of the remaining CRISPRi strains are presented in **appendix A3**.

When comparing the macrocolony screen by Wermser and Lopez (2018) with the macrocolony assay using CRISPRi knockdown of gene expression done in this work, many of the same genes were identified to have an altered macrocolony phenotype. Disruption of some genes resulted in different macrocolony structures in the USA300 screen than depletion of the same genes did in Newman. This can most likely be explained by strain differences, as macrocolonies differ between strains, also seen in **figure 4.5A**. Together, this shows that the macrocolony assay in combination with CRISPRi knockdown of gene expression can be used to screen and identify biofilm-associated genes involved in *S. aureus* macrocolony formation.

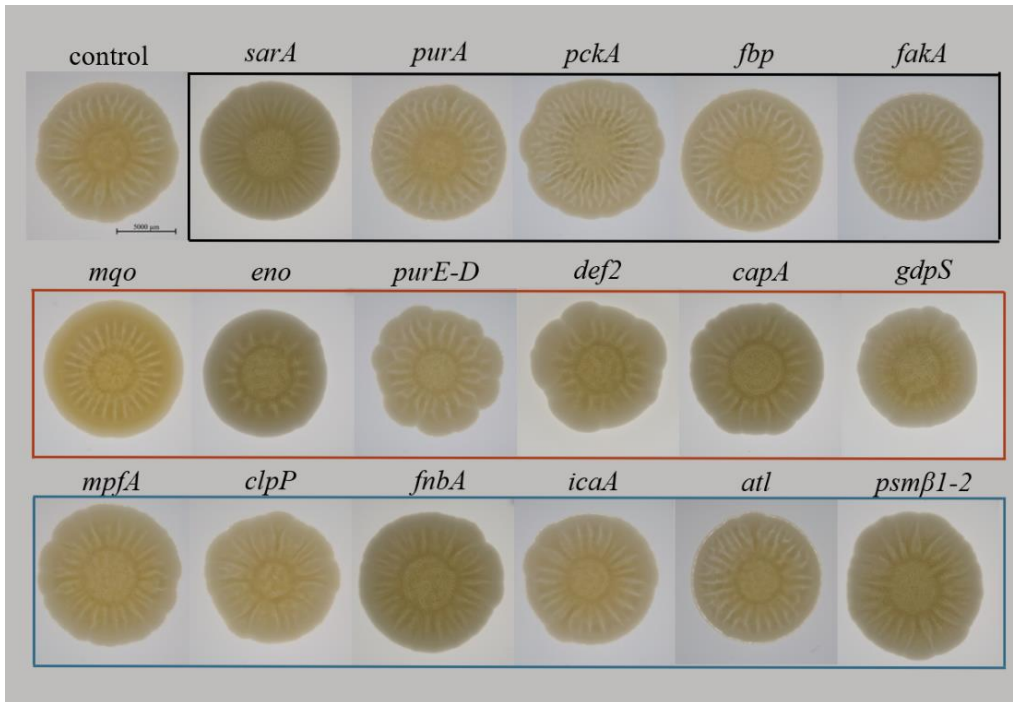


**Figure 4.6 Macrocolonies formed by *S. aureus* Newman after knockdown of gene expression of biofilm-associated genes.** Gene expression was knocked down by inducing the CRISPRi system with IPTG supplemented to the growth medium and agar plates. Macrocolonies were grown on TSB agar plates supplemented with 100 mM MgCl<sub>2</sub> and imaged after 5 days of incubation. Black box indicates structures with increased surface wrinkling, red box indicates macrocolonies with loss of structure or surface wrinkling, while blue box indicates macrocolonies similar to the control strain, which harbors a non-targeting sgRNA. Scalebar 5000 μM

## 4.2 Screening for WalRK regulated genes involved in biofilm formation

When investigating whether CRISPRi knockdown of gene expression could be used as a method to screen for novel genes involved in biofilm formation (**Section 4.1.2**), depletion of *atl* was found to cause a reduction in biofilm formation by *S. aureus* SH1000 as compared to the control strain. Major autolysin (Atl) of *S. aureus* is a peptidoglycan hydrolase involved in bacterial cell wall degradation and cell separation during cell division (Biswas et al., 2006). Atl is reported to promote attachment to polystyrene surfaces and play an important role in biofilm development (Porayath et al., 2018; Zoll et al., 2010). Expression of *atl* has been shown to be positively regulated by the response regulator WalR of the regulatory two-component system WalRK (Delauné et al., 2012; Dubrac et al., 2007). Since WalRK is known to regulate a set of genes putatively involved in cell wall remodeling, it was decided to screen the other WalRK regulated genes for involvement in *S. aureus* biofilm formation. As Atl functions in cell wall degradation, genes potentially related to cell wall degradation which have a consensus WalR binding site (Delauné et al., 2012; Dubrac et

## 4 Results

al., 2007) were screened for their effect on biofilm formation using CRISPRi knockdown of gene expression (**Table 4.2**). Additionally, a CRISPRi strain targeting the response regulator WalR for depletion was included in the screen.

**Table 4.2** List of genes potentially related to cell wall degradation with a consensus WalR binding site

Accession number	Name	Description of (predicted) function
SAOUHSC_00994	<i>atl</i> <sup>1</sup>	Bifunctional autolysin
SAOUHSC_00020	<i>walR</i> <sup>1</sup>	Response regulator
SAOUHSC_00248	<i>lytM</i> <sup>1</sup>	Glycyl-glycyl endopeptidase
SAOUHSC_00427	<i>sleI</i> <sup>2</sup>	N-Acetylmuramoyl-L-alanine amidase
SAOUHSC_00671	Uncharacterized <sup>1</sup>	CHAP domain-containing protein
SAOUHSC_00773	Uncharacterized <sup>1</sup>	CHAP domain-containing protein
SAOUHSC_02333	<i>sceD</i> <sup>1</sup>	
SAOUHSC_02571	<i>ssaA</i> <sup>1</sup>	CHAP domain-containing protein
SAOUHSC_02576	Uncharacterized <sup>1</sup>	CHAP domain-containing protein
SAOUHSC_02855	Uncharacterized <sup>2</sup>	CHAP domain-containing protein
SAOUHSC_02883	Uncharacterized <sup>1</sup>	CHAP domain-containing protein
SAOUHSC_02887	<i>isaA</i> <sup>1</sup>	

<sup>1</sup> Reference: Dubrac et al. (2007)

<sup>2</sup> Reference: Delauné et al. (2012)

Screening of the potential cell wall related, WalRK regulated genes was carried out in both *S. aureus* SH1000 and NCTC8325-4 using CRISPRi knockdown strains in a microtiter plate assay followed by quantification of biofilm formation by staining with crystal violet (**Figure 4.7**). As depletion of *atl* resulted in a decrease in biofilm formation, identification of other genes in which depletion caused a reduction in biofilm formation was screened for. A threshold for what was thought of as a significant reduction in detected biofilm formation was set at 20% below that measured for the control strain, which harbors a non-targeting sgRNA. Depletion of the potential WalRK regulated genes in SH1000 did not result in a reduction of biofilm below the set threshold, except for the already identified *atl*. In *S. aureus* NCTC8325-4 depletion of both *sleI* and *SAOUHSC\_00671*, in addition to the already identified *atl*, resulted in a decrease in biofilm formation below the set threshold. The reduction in biofilm formation resulting from *sleI* and *SAOUHSC\_00671* depletion was less than that of *atl*. SleI is suggested to be involved in the separation of daughter cells during cell division together with Atl (Kajimura et al., 2005), while the function of *SAOUHSC\_00671* remains unknown.

## 4 Results

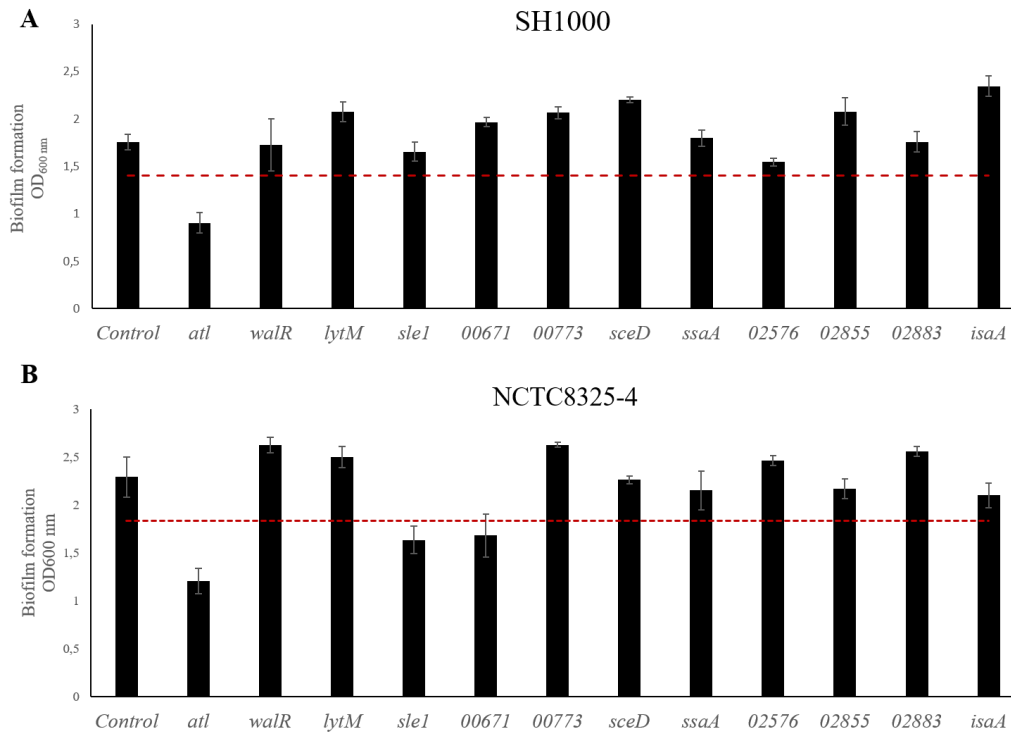


**Figure 4.7 Depletion of potential cell wall degrading enzymes regulated by WalRK on *S. aureus* biofilm formation.** Genes with a consensus WalR binding site which are known to- or proposed to be involved in *S. aureus* cell wall degradation were depleted using CRISPRi in (A) *S. aureus* SH1000 and (B) *S. aureus* NCTC8325-4. Biofilm was formed after 24 hours of incubation in 96-well microtiter plates and biofilm was quantified by staining with 0.02% crystal violet. OD was measured at 600 nm. A CRISPRi strain harboring a non-targeting sgRNA was included as a control, and a threshold line (red dashed line) for what was thought of as a significant reduction in biofilm formation was set to 20% below that measured of the control. Error bars represent standard deviations based on three parallel measurements.

### 4.3 SAOUHSC\_00671 is involved in *S. aureus* biofilm formation

When screening WalRK-regulated cell-wall degrading enzymes for involvement in *S. aureus* biofilm formation, depletion of SAOUHSC\_00671 and *sle1* was found to cause a reduction in biofilm formation in *S. aureus* NCTC8325-4, together with depletion of *atl*. Sle1, also known as Aaa (Hirschhausen et al., 2012), together with Atl, has both been implicated to be important in *S. aureus* biofilm development, with Atl mediating attachment to polystyrene, fibrinogen and vitronectin and Sle1 mediating attachment to fibrinogen, fibronectin and vitronectin (Biswas et al., 2006; Hirschhausen et al., 2012). As depletion SAOUHSC\_00671 also resulted in a reduction in biofilm formation, it was decided to look further into SAOUHSC\_00671 and *S. aureus* biofilm formation.

## 4 Results

Similarity searches with the amino acid sequence of *SAOUHSC\_00671* with predicted coding sequences present in public databases was conducted using the psiBLAST algorithm. This revealed the presence of open reading frames (ORFs) possessing similar amino acid sequences in multiple staphylococcal species, including *S. epidermidis*. During this search, similarity of the gene product of *SAOUHSC\_00671* to other proteins in the *S. aureus* NCTC8325-4 genome, including the staphylococcal secretory antigen A protein (SsaA, *SAOUHSC\_02571*) was identified. This similarity was also found by Osipovitch et al. (2015). In this work, the protein sequences were aligned using pBLAST, and the two proteins were found to share a 57% identity in the region between amino acid 148 and 265 for *SAOUHSC\_00671* and between amino acid 144 and 255 for SsaA. These sequences encompass a predicted C-terminal CHAP (cysteine/histidine-dependent amidohydrolase/peptidase) domain in both proteins (**Figure 4.8**). Likewise, the two proteins *SAOUHSC\_00671* and Sle1 had a 46% identity in the regions between amino acid 29 and 265 of *SAOUHSC\_00671* and between amino acid 93 and 334 of Sle1. These sequences cover the two predicted LysM domains and the predicted CHAP domain of the *SAOUHSC\_00671* gene product, and two of the predicted LysM domains and the predicted CHAP domain of Sle1 (**Figure 4.8**). In addition, all three proteins have predicted signal peptides for secretion through the general secretion pathway (Sec-pathway). The Sec-pathway is involved in both the secretion of unfolded proteins across the cytoplasmic membrane and the insertion of membrane proteins into the cytoplasmic membrane (Natale et al., 2008).

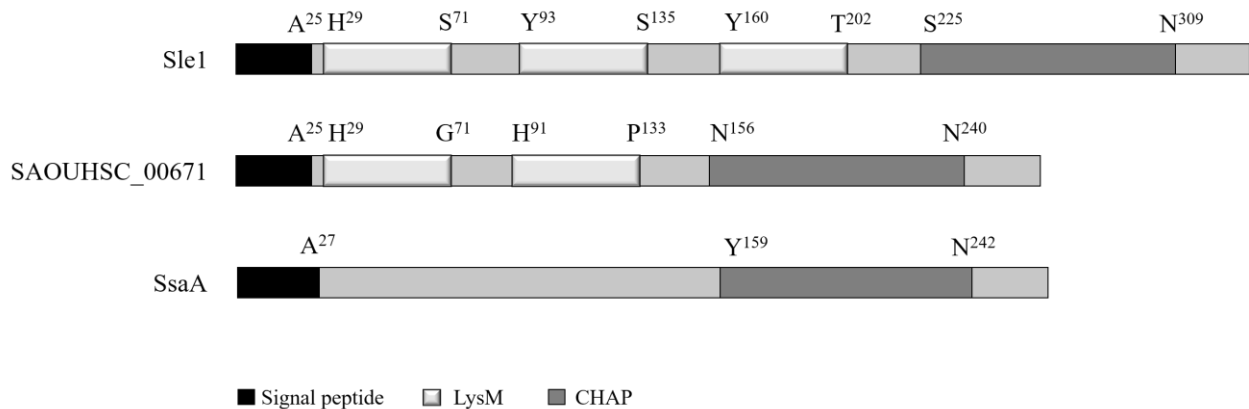


**Figure 4.8 Domain organization of Sle1, SAOUHSC\_00671 and SsaA.** LysM; lysin motif, CHAP; cysteine/histidine-dependent amidohydrolase/peptidase. Signal peptide was predicted using the SignalP 5.0 server and protein domains were predicted using the pfam database.

## 4 Results

The CHAP domain is found in a variety of different proteins, many of which are uncharacterized. It has been proposed that they mainly function in peptidoglycan hydrolysis, and the CHAP domains are associated with two different types of peptidoglycan cleavage activities: N-acetylmuramoyl-L-alanyl amidase as well as D-alanyl-glycyl endopeptidase activity (Delauné et al., 2011). The CHAP domain of Sle1 has been found to mediate bacteriolytic activity and mediate adherence to fibrinogen, fibronectin, and vitronectin (Hirschhausen et al., 2012), while the CHAP domain of SsaA plays a role in peptidoglycan crosslinking relaxation through crossbridge hydrolysis (Delauné et al., 2011). LysM domains are found to bind the peptidoglycan of the bacterial cell wall and are often found in cell wall hydrolases. The LysM domain of cell wall hydrolases aid in binding the enzyme to the peptidoglycan and proper positioning of the active site domain(s) toward their substrates (Visweswaran et al., 2014). The presence of a potential catalytic CHAP domain and LysM domains suggests a role of *SAOUHSC\_00671* in peptidoglycan hydrolysis that needs to be further investigated.

Kajimura et al. (2005) suggests that *S. aureus* uses the two peptidoglycan hydrolases Atl and Sle1 for cell separation after cell division. The sequence similarities of Sle1 and SAOUHCS\_00671 suggests that SAOUHCS\_00671 might have similar functions, and it was therefore tested whether depletion of Atl and Sle1 in combinations with SAOUHSC\_00671 would have an additional or synergistic effect on biofilm formation. To do this, the CRISPRi knockdown system was used again, this time by introducing a plasmid harboring two sgRNAs allowing for simultaneous depletion of two genes in *S. aureus* NCTC8325-4, which has been shown to work previously (Stamsås et al., 2018). Double depletion was done with the combinations *SAOUHSC\_00671* and *atl*, *SAOUHSC\_00671* and *sle1*, and *atl* and *sle1*. Biofilm formation after depletion was quantified in the microtiter plate assay by staining with crystal violet as before (**Figure 4.9**). A CRISPRi strain harboring a non-targeting sgRNA was used as a control strain, and a threshold for what was thought of as a significant reduction in biofilm formation was set at 20% below the OD measured for the control strain. As expected, depletion of all genes separately as well as the three double depletion strains resulted in a reduction in biofilm formation below the set threshold line. Somewhat surprisingly, depletion of *sle1* and *SAOUHSC\_00671* resulted in a greater decrease in biofilm formation than depletion of *atl*. However, the double depletion of *SAOUHSC\_00671* in combination with *atl* or *sle1* did not cause a further reduction in biofilm as compared to single

## 4 Results

depletion of *SAOUCHS\_00671*. Neither did double depletion of *atl* and *sle1* result in any additional decrease in biofilm formation compared to single depletion of *atl*.

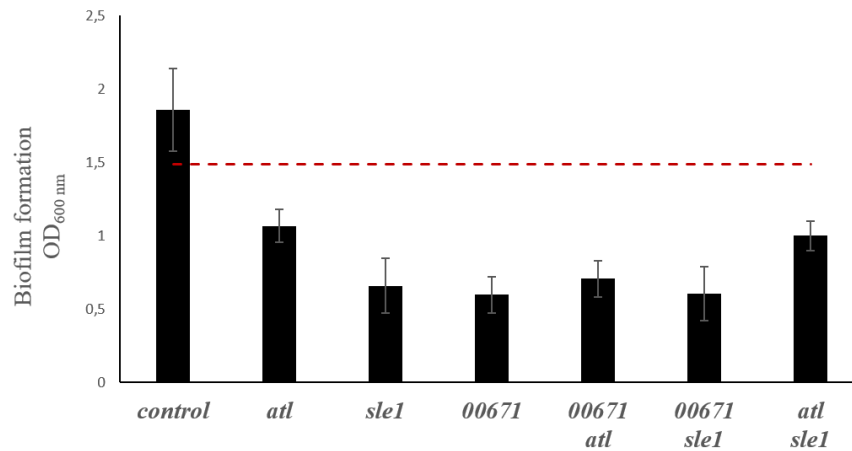


**Figure 4.9 Biofilm formation by *S. aureus* NCTC8325-4 after depletion of *atl*, *sle1* and *SAOUCHS\_00671*.** Biofilm was formed for 24 hours in 96-well microtiter plates and biofilm was quantified by staining with 0.02% crystal violet. OD was measured at 600 nm. Depletion of *atl*, *sle1*, *SAOUCHS\_00671*, *SAOUHSC\_00671* + *sle1*, *SAOUHSC\_00671* + *atl* and *atl* + *sle1* was done using CRISPRi. The control strain harbors a non-targeting sgRNA. Red dashed line: 20% below the OD measured for the control strain. Error bars represent standard deviations based on three parallel measurements.

Confocal laser scanning microscopy (CLSM) was used to study the effect of depleting *SAOUCHS\_00671* on biofilm distribution. The cells of the biofilm were visualized by LIVE/DEAD staining and the biofilm formed after depletion of *SAOUHSC\_00671* was compared to that of a control strain harboring a non-targeting sgRNA. The control strain forms a biofilm of more evenly distributed cells with few large unoccupied areas (black patches) than the *SAOUHSC\_00671* depletion strain (**Figure 4.10A**). The cells of the biofilm formed after *SAOUHSC\_00671* depletion appears to clump more together into aggregates. Additionally, more of the surface is unoccupied by cells, resulting in larger openings into the biofilm. More dead cells (>200 cells/field) are detected in the biofilm formed by the control strain than in the biofilm formed after depletion of *SAOUHSC\_00671* (~7 cells/field), however the significance of this observation still needs to be verified. The more uneven distribution of cells is also visible when looking on the biofilm from the side (**Figure 4.10B**) where one can see that the biofilm formed after depletion of *SAOUHSC\_00671* is also more uneven in thickness as compared to that formed by the control strain. The biofilm formed by the control strain has a thickness above 6  $\mu\text{m}$  at all points, while the thickness after depletion of *SAOUHSC\_00671* reaches down to approximately 4  $\mu\text{m}$  at certain places.

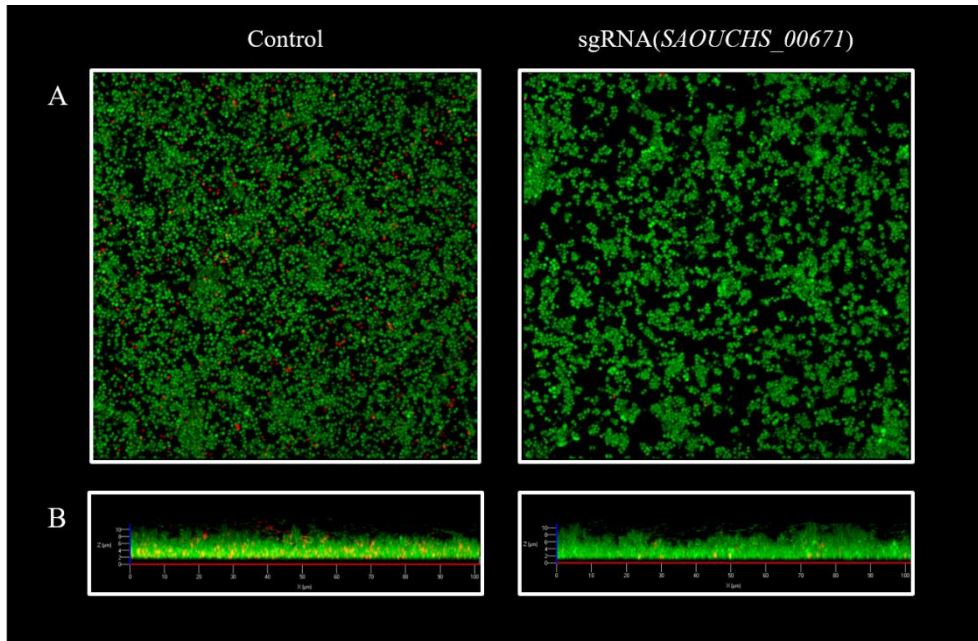


**Figure 4.10** Confocal laser scanning microscopy of *SAOUHSC\_00671* depleted *S. aureus* NCTC8325-4 biofilm. Knockdown of gene expression was carried out using *S. aureus* CRISPRi. Precultures were grown overnight with 300  $\mu$ M IPTG to induce depletion and biofilm was formed on chambered coverglass for 24 hours in the presence of 300  $\mu$ M IPTG. The control strain harbored a non-targeting sgRNA. Cells were stained using LIVE/DEAD staining. **(A)** top view of biofilm. **(B)** side view of biofilm.

To further analyze the function of *SAOUHSC\_00671*, a  $\Delta$ *SAOUHSC\_00671* mutant was constructed by allelic replacement of the *SAOUHSC\_00671* gene in the genome of NCTC8325-4 with a spectinomycin resistance cassette using the thermosensitive *S. aureus* – *E. coli* pMAD shuttle vector. Three individual  $\Delta$ *SAOUHSC\_00671*::*spc* mutants, named strain MM148, MM149 and MM150, were verified by colony PCR. To assess if the mutant phenotype was attributed to the deletion of *SAOUHSC\_00671*, a complementation of the *SAOUHSC\_00671* deletion was made with a plasmid, pLOW, harboring the *SAOUHSC\_00671* gene downstream of an IPTG inducible promoter, resulting in pLOW-00671. pLOW-00671 was transformed into MM149, giving the complementation strain MM154.

The biofilm phenotype of the  $\Delta$ *SAOUHSC\_00671* mutants was investigated in the microtiter plate assay with staining of the biofilm with crystal violet (**Figure 4.11**). Although all three deletion strains have been confirmed to lack the *SAOUHSC\_00671* gene, they for some reason showed different, but reproducible phenotypes in the microtiter plate assay as well as differences when it comes to growth behavior (**Figure 4.12**). Both MM148 and MM150 showed a slight increase in growth compared to WT, but only MM150 showed a reduction in biofilm formation as seen when depleting *SAOUHSC\_00671*. MM149 on the other hand, had a decreased growth rate, but displayed

## 4 Results

an increased trend with regard to biofilm formation. As *SAOUHSC\_00671* had been knocked out of all three strains, we were surprised to observe these differences and further studies are needed to identify if there have occurred any changes to the genome, possibly affecting growth and biofilm formation in these three individual mutants.

The complementation strain MM154 was constructed to assess whether the phenotype of WT NCTC8325-4 could be recovered by expressing *SAOUHSC\_00671* from a plasmid in the deletion strain. MM154 without induction of expression of *SAOUHSC\_00671* showed a reduction in biofilm formation compared to WT (**Figure 4.11**), and, the biofilm phenotype of the WT strain is recovered when inducing expression of *SAOUHSC\_00671* in MM154 with 500  $\mu$ M IPTG. MM154, with or without induction of IPTG show similar growth behavior (**Figure 4.12**)

As depletion of *SAOUHSC\_00671* causes a reduction in biofilm formation, it was also investigated whether overexpression of the gene would promote an increase in biofilm formation. The plasmid pLOW-00671 was introduced into *S. aureus* NCTC8325-4, producing the strain MM151. Induction with IPTG induces expression of *SAOUHSC\_00671* from the plasmid. The effect of overexpression on biofilm formation was studied in the microtiter plate assay, and biofilm formation was quantified by staining with crystal violet (**Figure 4.11**). As expected, no change in biofilm formation could be detected between WT NCTC8325-4 and MM151 when expression of *SAOUHSC\_00671* was not induced with IPTG. A slight increase in biofilm formation could be detected when inducing expression with IPTG (50  $\mu$ M). There was no increase in biofilm formation with further increasing concentrations of IPTG. No effect of overexpression of *SAOUHSC\_00671* on growth behavior could be detected (**Figure 4.12**).

Although these latter data from complementation and over-expression of *SAOUHSC\_00671* is fully in line with the CRISPRi results, the variation between the individual mutants demands further investigation and genome sequencing of all of these strains to further understand the role of *SAOUHSC\_00671* in biofilm formation.

## 4 Results

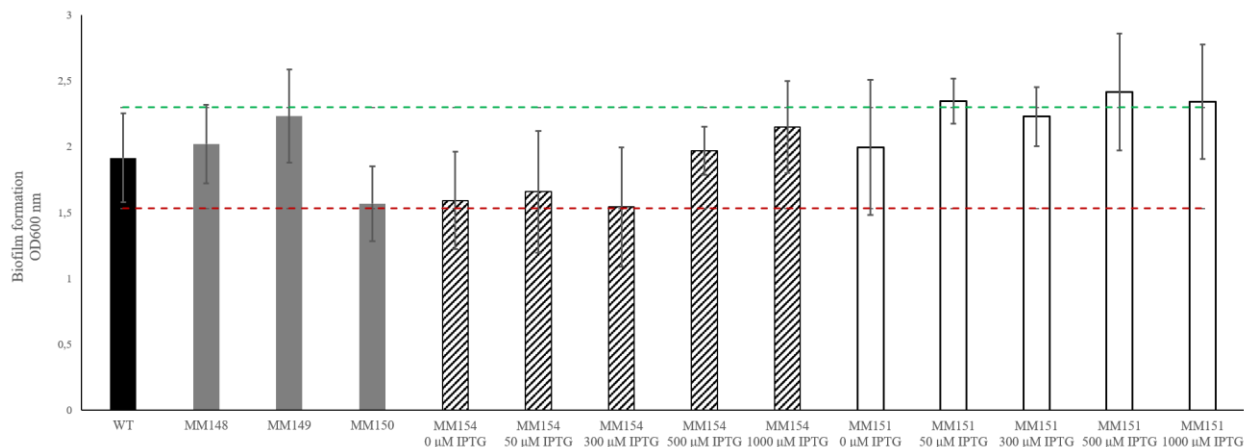


**Figure 4.11 Deletion and overexpression of *SAOUHSC\_00671* on biofilm formation by *S. aureus* NCTC8325-4.** Biofilms were grown in 96-well microtiter plates for 24 hours and biofilm formation was quantified by staining with 0.02% crystal violet. MM148, MM149 and MM150: deletion of *SAOUHSC\_00671* confirmed by colony PCR. MM154: Complementation strain where MM149 have been transformed with expression plasmid pLOW-00671. MM151: Overexpression strain where wild type (WT) NCTC8325-4 have been transformed with expression plasmid pLOW-00671. Induction of expression was carried out with IPTG concentrations ranging from 0 μM to 1000 μM

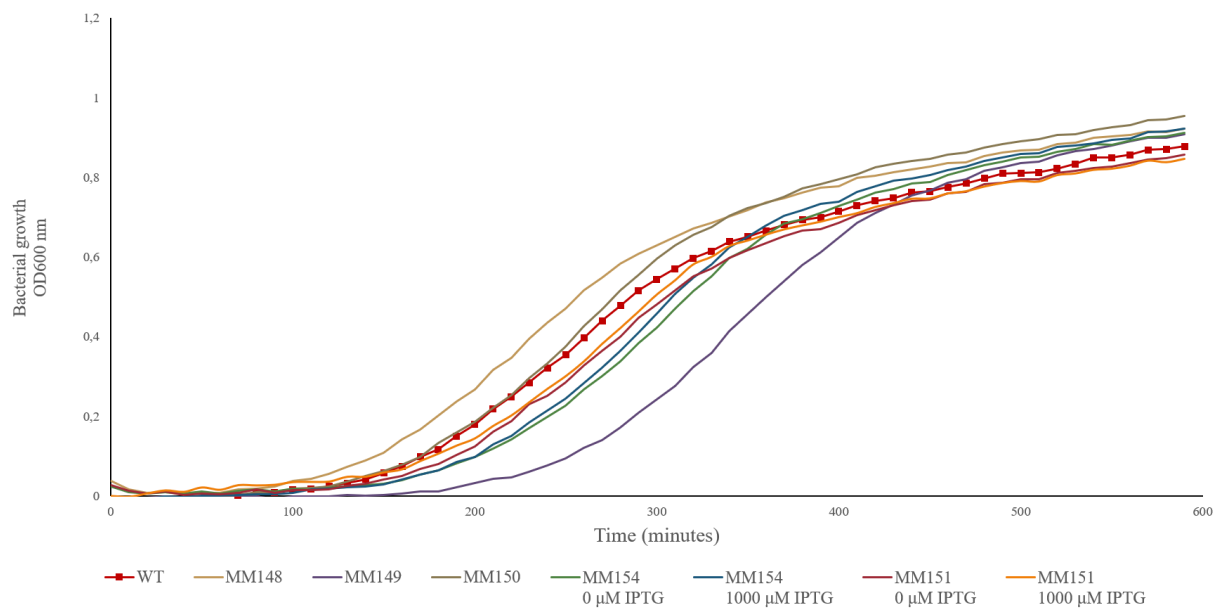


**Figure 4.12 Growth behavior of *S. aureus* NCTC8325-4 mutant strains.** Growth was measured at intervals for 10 hours at OD<sub>600nm</sub>. WT: wild type. MM148, MM149 and MM150: deletion of *SAOUHSC\_00671* confirmed by colony PCR. MM154: MM149 harboring a *SAOUHSC\_00671* expression plasmid. MM151: WT NCTC8325-4 harboring a *SAOUHSC\_00671* expression plasmid. Expression of *SAOUHSC\_00671* from plasmid was either uninduced or induced with 1000 μM IPTG.

#### 4.4 Identification of novel genes involved in *S. aureus* macrocolony formation using a CRISPRi interference pooled library

The macrocolony assay have previously been used to identify novel candidates involved in biofilm macrocolony formation in *S. aureus* USA300, where a set of mutants was systematically tested (Wermser & Lopez, 2018), and here we showed that CRISPRi for knockdown of gene expression could be used in combination with the macrocolony assay to study biofilm macrocolony genes in *S. aureus* strain Newman (Section 4.1.3). As an approach to screen for novel genes involved in *S. aureus* Newman macrocolony formation, it was decided to take advantage of a novel CRISPRi pooled library developed in another project (Maria V. Heggenhougen, Xue Liu, Morten Kjos). The CRISPRi pooled library, originally designed for NCTC8325-4, harbors 1928 unique sgRNAs targeting 2766 genomic features. The CRISPRi pooled library was grown to an OD<sub>600</sub> of ~0.8 with induction with 300 µM IPTG and then plated onto TSBMg agar plates with proper dilutions to give spacing between the colonies. In total, approximately 1500 colonies were incubated for 5 days to produce the macrocolonies. The colonies were then inspected visually, and 11 colonies that had a macrocolony structure different to that of the control were selected. The control strain harbors a non-targeting sgRNA. Pure cultures of the selected 11 colonies were made and the region encompassing the sgRNA on the plasmid was sequenced to identify which genes were depleted in each of these colonies (Table 4.1). The 11 pure cultures were again spotted on TSBMg plates and incubated for 5 days for imaging of macrocolony structure (Figure 4.13A). It was decided to use a similar classification of macrocolony structures into three categories as done by Wermser and Lopez (2018). Category 1 is made up of macrocolonies with little or no difference in surface wrinkling and structure compared to the control. Category 2 includes colonies where surface wrinkling is increased, compared to the control. Category 3 comprises macrocolonies where wrinkling is either completely lost or reduced, or where colony structure is altered.

Based on the above-defined characteristics, CRISPRi strains harboring sgRNAs for depletion of *tagO*, *icaB* and *NWMN\_RS03770* were classified into category 1, showing no large differences compared to the control strain upon repetition. The strain harboring a sgRNA targeting *pckA* were classified into category 2, while strains harboring sgRNAs targeting *sucA*, *fumC*, *ubiE*, *NWMN\_RS14065*, *hemE* and *znuC* were grouped into category 3. Of The 11 selected colonies, two harbored the same sgRNA, targeting *fumC* for depletion. The genes identified in the screen code for cytoplasmic proteins (50%), membrane proteins (20%) and extracellular proteins (10%) (Table

**4.3** and **figure 4.13B**). The subcellular localization is still unknown for some of the gene products. Among the candidates, the most prevalent biological functions were found to be biosynthesis of different compounds (30%), including PIA- and menaquinone biosynthesis, and different stages of the central metabolism (30%), including the tricarboxylic acid (TCA) cycle and gluconeogenesis (**Table 4.3** and **figure 4.13B**). Other functions found among the candidates were cell wall organization and DNA repair, classified as ‘others’ (20%).

**Table 4.3 Candidates identified in the CRISPRi pooled library screen.** 10 candidates were identified by visual inspection of 1500 colonies from a pooled *S. aureus* Newman CRISPRi library screen. Information on gene protein, biological function and subcellular localization was gathered from [www.uniprot.org](http://www.uniprot.org) and [www.aureowiki.med.uni-greifswald.de](http://www.aureowiki.med.uni-greifswald.de).

	Accession number	Name	Protein	Biological function	Localization	
Phenotypic category	1	NWMN_RS04050	<i>tagO</i>	Hypothetical protein	Cell wall	Membrane
		NWMN_RS14730	<i>icaB</i>	Poly-beta-1,6-N-acetyl-D-glucosamine N-deacetylase	PIA- biosynthesis	Extracellular
		NWMN_RS03770	-	Hypothetical protein	-	-
	2	NWMN_RS09430	<i>pckA</i>	Phosphoenolpyruvate carboxykinase (ATP)	Gluconeogenesis	Cytoplasm
	3	NWMN_RS07460	<i>sucA</i>	2-oxoglutarate dehydrogenase E1 component	TCA cycle	Cytoplasm
		NWMN_RS09820	<i>fumC</i>	Fumarate hydratase class II	TCA cycle	Cytoplasm
		NWMN_RS07770	<i>ubiE</i>	Putative menaquinone biosynthesis methyltransferase	Menaquinone - biosynthesis	-
		NWMN_RS14065	-	Methylated-DNA-protein-cysteine methyltransferase	DNA repair	Cytoplasm
		NWMN_RS09725	<i>hemE</i>	Uroporphyrinogen decarboxylase	protoporphyrin-IX - biosynthesis	Cytoplasm
		NWMN_RS08230	<i>znuC</i>	Putative ABC transporter	-	Membrane

Among the identified candidates, *pckA*, *fumC* and *sucA* are all involved in the central metabolic pathways, with *pckA* and *fumC* having already been identified to be involved in *S. aureus* USA300 macrocolony formation in a similar macrocolony assay (Wermser & Lopez, 2018), further proving CRISPRi and the macrocolony assay to be useful in identifying genes involved in macrocolony formation. Additionally, *icaB* is already known to be involved in *ica*-dependent biofilm formation in *S. aureus*. It was decided to look further into candidates of macrocolony category 3, where the structure and wrinkles of the macrocolony is either lost or reduced. UbiE and HemE belongs to one of the most represented functional group identified amongst the candidates, biosynthesis, while the biological function of *SAOUHSC\_02861* is still unknown. HemE is part of the heme-biosynthesis pathway, and other genes in this pathway has been identified previously (see discussion). ZnuC is

## 4 Results

the ATPase of the high-affinity ABC-type zinc transporter ZnuABC (Cassat & Skaar, 2012). The adhesion protein SasG displays zinc-dependent mechanical properties that are critical for its adhesive function during biofilm formation (Formosa-Dague et al., 2016), but how zinc-import is linked to macrocolony formation needs further investigation. The two candidate genes, *ubiE* and *NWMN\_RS03770* were chosen for further investigation.

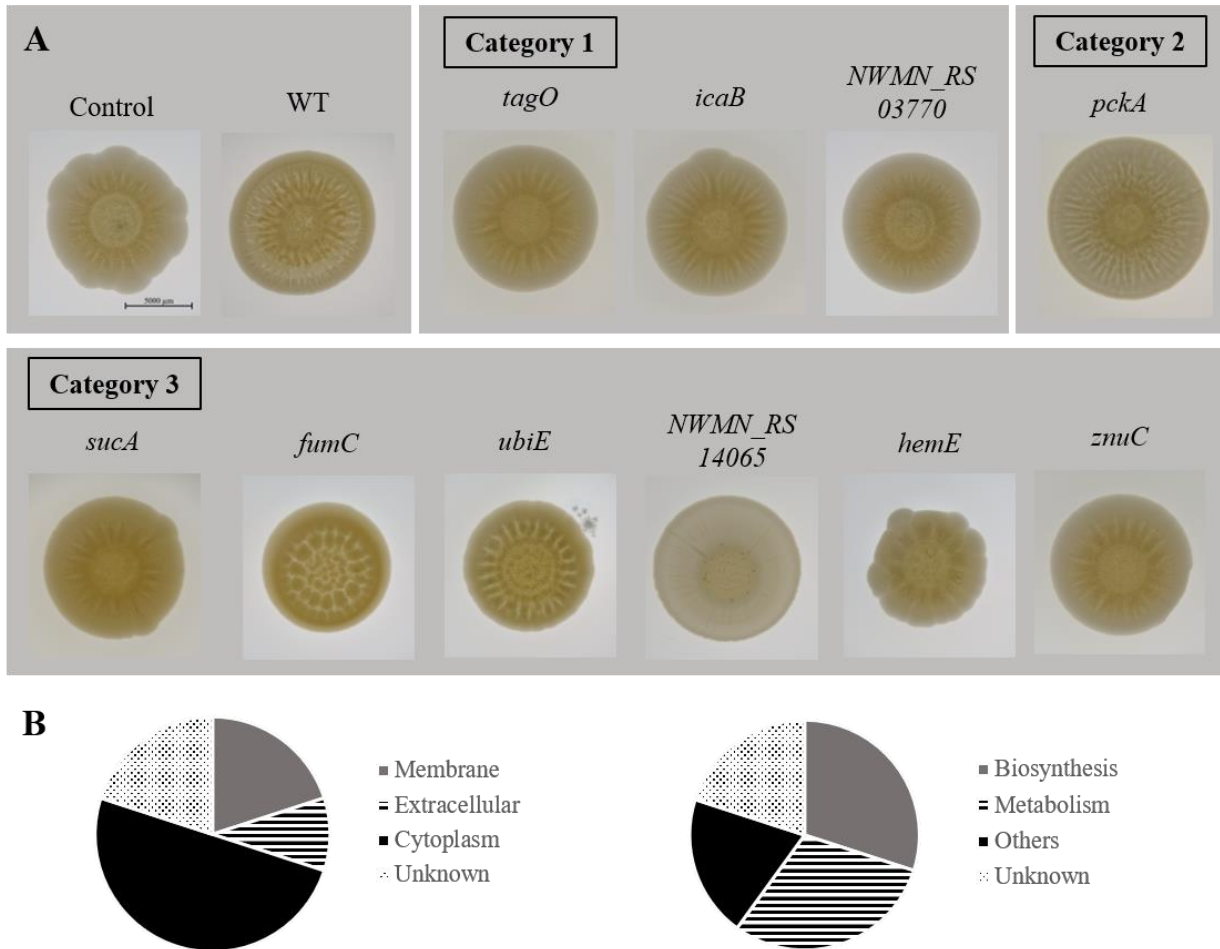


**Figure 4.13 Identification of novel genes involved in Newman macrocolony formation.** A CRISPRi pooled library targeting 2766 genomic features in *S. aureus* Newman for depletion was used to screen for novel genes involved in macrocolony formation. (A) Macrocolonies were imaged after 5 days of incubation on TSB agar supplemented with 100  $\mu$ M  $MgCl_2$ . Identified candidates of category 1 display little or no difference in macrocolony structure compared to the control harboring a non-targeting sgRNA. Category 2 candidates display either loss of macrocolony structure or change in macrocolony structure. Candidates of category 3 display increased surface wrinkling compared to the control. Scalebar 5 mm. (B) Distribution of subcellular localization and biological function among the proteins identified in the CRISPRi pooled library screen

#### 4.5 Impaired respiration alters *S. aureus* macrocolony formation

One of the colonies found to have an altered macrocolony structure, with shorter and thicker wrinkles harbored a sgRNA with a target site located within the *ubiE* gene. *ubiE* is located in a predicted operon containing the two genes *NWMN\_RS07775* and *hepT* (*NWMN\_RS07765*), located upstream and downstream of *ubiE*, respectively (**Figure 4.14**) ([www.microbesonline.org](http://www.microbesonline.org)). As the target site for the sgRNA is located at the beginning of *ubiE*, transcription of *hepT* is also blocked by dCas9, resulting in the identified macrocolony being depleted of both UbiE and HepT.

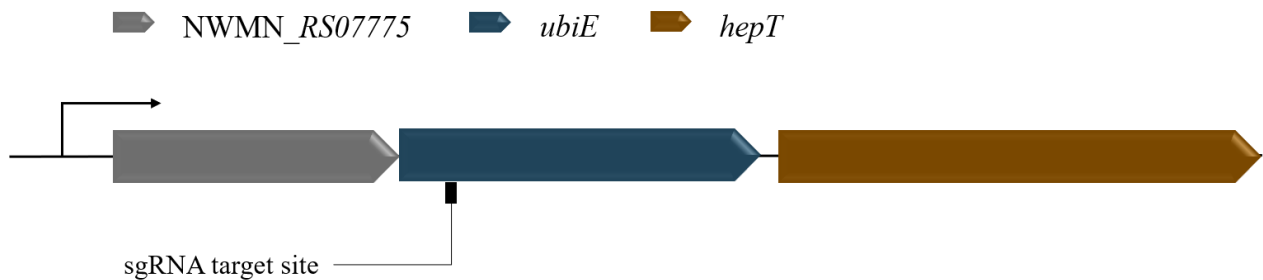


**Figure 4.14** Genetic organization of the operon containing the menaquinone biosynthesis genes *NWMN\_RS07775*, *ubiE* and *hepT*. The target site for knockdown of gene expression using CRISPRi is within the *ubiE* gene.

All three gene products of the operon are predicted to be involved in the synthesis of menaquinone (MK) from chorismate, in a multi-step pathway. MK plays an important role in electron transport in all Gram-positive bacteria, shuttling electrons between components of the electron transport chain. This provides the energy needed to maintain a proton gradient and potential energy used to convert ADP into ATP, and *S. aureus* strains lacking menaquinone are thus unable to respire (Boersch et al., 2018; Wakeman et al., 2012). The predicted pathway of MK biosynthesis is presented in **figure 4.15**. The participation of UbiE, *NWMN\_RS07775* and HepT are all proposed to be during the last steps of MK biosynthesis. Both *NWMN\_RS07775* and HepT show similarities to the heptaprenyl diphosphate synthase subunits, HepS and HepT of *B. subtilis* (Wakeman et al., 2012), with the two HepT proteins showing a 47% identity with 71% positive matches, and *NWMN\_RS07775* and HepS showing a 24% identity and 50% positive matches. HepS and HepT in *B. subtilis* are responsible for the production of the isoprenyl lipid chain which is used to replace the carboxyl of 1,4-dihydroxy-2-naphthoate (DHNA) in the conversion to demethylmenaquinone (DMK) (Meganathan & Kwon, 2009; Wakeman et al., 2012). *NWMN\_RS07775* and HepT are predicted to have similar functions in *S. aureus*. After DHNA is converted to DMK, DMK is subsequently methylated, yielding MK in the final step of the MK biosynthesis pathway. This step

## 4 Results

is predicted to be catalyzed by UbiE, which is an predicted S-adenosylmethionine:2-DMK methyltransferase (Wakeman et al., 2012).

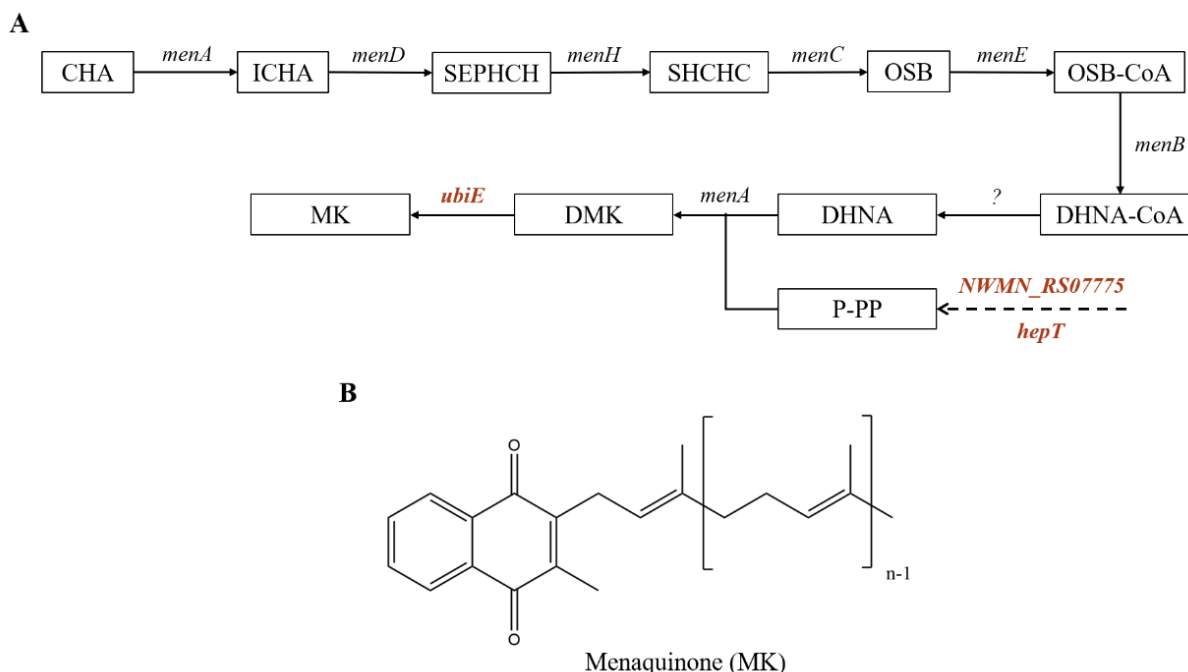


**Figure 4.15 Predicted pathway of menaquinone (MK) biosynthesis in *S. aureus*.** (A) The diagram shows the predicted menaquinone biosynthesis pathway with the enzymes required. Enzymes identified to alter *S. aureus* macrocolony formation are marked in red. The diagram is adapted from the KEGG database ([www.genome.ad.jp/kegg](http://www.genome.ad.jp/kegg)), Wakeman et al., (2012) and Meganathan & Kwon (2009). (B) Chemical structure of MK (Wakeman et al., 2012). Abbreviations: CHA, Chorismate; ICHA, Isochorismate; SEPHCH, 2-succinyl-5-enolpyruvyl-6-hydroxy-3-cyclohexene-1-carboxylate; SHCHC, 2-succinyl-6-hydroxy-2,4-cyclohexadiene-1-carboxylate; OSB, *o*-succinylbenzoate; OSB-CoA, *o*-succinylbenzoyl-CoA; DHNA-CoA, 1,4-dihydroxy-2-naphthoyl-CoA; DHNA, 1,4-dihydroxy-2-naphthoate; DMK, demethylmenaquinone, MK, menaquinone; P-PP, all-trans-polyprenyl-diphosphate. Dotted line denotes that there are intermediate reactions not shown in the diagram

MK is required for both aerobic and anaerobic electron transport, and the simultaneous knockdown of *ubiE* and *hepT* gene expression in the candidate colony is thus likely to impair respiration in *S. aureus*, inducing a switch from respiration to fermentation. To further investigate the role of menaquinone and UbiE in *S. aureus* Newman macrocolony formation, a  $\Delta ubiE$  mutant was constructed by replacing the *ubiE* gene with a spectinomycin resistant cassette. The macrocolony phenotype of the deletion mutant was tested in a macrocolony assay (**Figure 4.16**), resulting in a macrocolony with complete loss of surface wrinkling and a more pronounced yellow pigmentation.

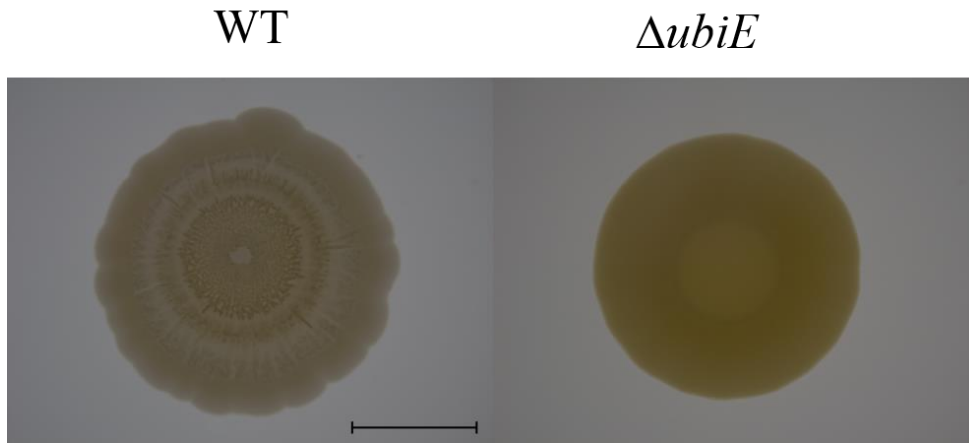


**Figure 4.16 Macrocolony biofilm defect in  $\Delta ubiE$ .**  $\Delta ubiE$  causes a complete lack of surface wrinkling of the macrocolony and a more pronounced yellow pigmentation. Macrocolonies were imaged after 5 days. Scale bar, 5 mm.

#### 4.6 Lack of the putative methyltransferase *NWMN\_RS14065* alters macrocolony formation

In the macrocolony pooled CRISPRi library screen, one colony had completely lost its macrocolony structure (**Figure 4.13**), with no wrinkles and a thin, transparent appearance. This colony was found to harbor a sgRNA targeting the gene *NWMN\_RS14065* for knockdown of gene expression. This gene is currently uncharacterized in *S. aureus*, although the gene product of *NWMN\_RS14065* is predicted to be a 6-O-methyl-DNA-protein-cysteine methyltransferase with one predicted ribonuclease-like domain, and one predicted DNA-binding domain (**Figure 4.17**). A similarity search using pBLAST shows that *NWMN\_RS14065* has a 45% identity with the Methylated-DNA-protein-cysteine methyltransferase (encoded by *adaB*) in *B. subtilis*, which is predicted to be involved in the repair of DNA in which it transfers the methyl group of O-6-methylguanine to a cysteine residue in the enzyme. This is thought to be a suicide reaction as the enzyme is irreversibly inactivated.

To further investigate the role of *NWMN\_RS14065* in macrocolony formation, a  $\Delta NWMN\_RS14065$  mutant was constructed by allelic replacement of the gene in the genome of strain Newman with a spectinomycin cassette using the thermosensitive *S. aureus* – *E. coli* pMAD shuttle vector (performed by Dr. Danae Morales Angeles, NMBU). The macrocolony formation assay was repeated with the  $\Delta NWMN\_RS14065::spc$  mutant, growing the macrocolony for 5 days on TSBMg agar plates (**Figure 4.17**). In contrast to the macrocolony resulting from depletion of

## 4 Results

*NWMN\_RS14065* which had completely lost its surface structure and wrinkling, the macrocolony of the deletion mutant showed surface wrinkling. Nevertheless, the deletion mutant showed macrocolony structuring different from that of the WT, with the WT showing more of a ring pattern, while the deletion mutant showed wrinkling reaching to the outer parts of the macrocolony.

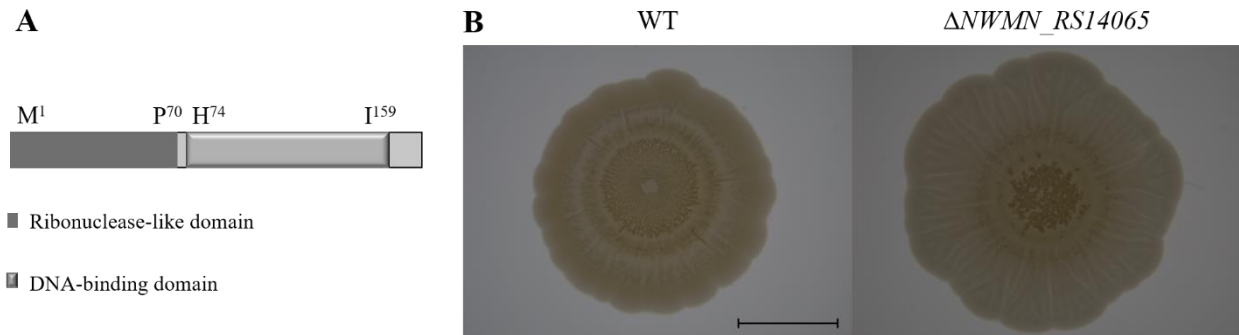


**Figure 4.17 Macrocolony biofilm defect in  $\Delta NWMN\_RS14065$ .** (A) Predicted 6-O-methylguanine DNA methyltransferase domains of the *NWMN\_RS14065* gene. (B)  $\Delta NWMN\_RS14065$  forms macrocolonies that are distinct from that of the WT. Macrocolonies were imaged after 5 days. Scale bar 5 mm.



## 5 Discussion

### 5.1 CRISPRi can be used to study biofilms of *S. aureus* model strains in two different assays

The biofilm mode of growth by *S. aureus* decreases the efficiency of both the immune defenses and of antimicrobials (Foster, 2005), making these infection difficult to combat. A greater understanding to the processes underlying *S. aureus* biofilm formation is therefore crucial in the development of new treatment strategies. To overcome the time-consuming methods established to study gene function in *S. aureus* and to facilitate the study of essential genes, a depletion system using CRISPRi knockdown of gene expression has been developed for *S. aureus* (Stamsås et al., 2018). One of the main goals of this work was to investigate whether the CRISPRi system could be used to study *S. aureus* biofilm formation and whether it could be used to identify novel genes involved in *S. aureus* biofilm formation. In this work, two different *in vitro* biofilm model systems were tested: the crystal violet microtiter plate assay and the macrocolony formation assay. To investigate if either of these two methods could be used in combination with CRISPRi knockdown of gene expression to study biofilm associated genes, a collection of CRISPRi strains in SH1000, NCTC8325-4 and Newman targeting genes previously associated with different types of biofilms were made and tested in both type of assays. It should be noted that the selected genes have been associated with biofilm assays from different strains using different experimental setups. It was therefore not expected that all of the CRISPRi strains should show effects in the two types of assays used here.

CRISPRi knockdown of gene expression is a straightforward method allowing for easy and rapid gene repression. The simplicity in changing the 20-nt targeting sequence of the sgRNA also makes it easy to target multiple different genes with ease. However, there are possible challenges when knocking down gene expression. Too high levels of dCas9 have been reported to result in abnormal cell morphology in *E. coli* (Cho et al., 2018), and levels of dCas9 expression thus needs to be taken into consideration. It is not known whether the CRISPRi system influences biofilm formation in any way. A difference was found in wild-type SH1000 biofilm formation and biofilm formation by a SH1000 CRISPRi strain harboring a non-targeting sgRNA (**Figure 4.1**), where the CRISPRi strain had an increased level of biofilm formation when grown in TSBGN. In the macrocolony assay, there were also some indications of differences between Newman wild-type and CRISPRi-

harboring control strains. We therefore chose to use the control strain (carrying the CRISPRi system with a non-targeting sgRNA) as reference in the different assays. Differences in the control strain between separate experiments of similar experimental setup further proves the need to investigate the impact of the CRISPRi system on cellular processes, and further validations with regard to off-target effects, including that of the non-targeting sgRNA.

The sgRNAs of the CRISPRi system was originally designed to target the genes of the NCTC8324-5 genome and might therefore not be as efficient in other strains. However, the targeting specificity of the sgRNAs in these CRISPRi biofilm strains (determined by the 20-nt long base-pairing region, **figure 1.4**) was verified for the strains SH1000 and Newman by in silico analysis. On the other hand, when working with the full CRISPRi library (containing 1928 sgRNAs) in the Newman strain, there may be off-target effects. These off-target effects are currently being investigated for different strains, including Newman (M. Heggenhougen & V. de Bakker, personal communication).

Despite the relatively large variations in the crystal violet microtiter plate assay using SH1000 CRISPRi strains (see discussion below), the depletion of the genes *agrA*, *psm $\beta$ 1-2*, *sasG* and *atl* gave consistent results (**Figure 4.3**). The increase in biofilm formation found when depleting *agrA* and *psm $\beta$ 1-2* and the decrease in biofilm formation found when depleting *atl* corresponds to what have been reported for these genes (Biswas et al., 2006; Moormeier & Bayles, 2017; Paharik & Horswill, 2016). Likewise, knockdown of gene expression using CRISPRi were also found to be useful to study biofilm-associated genes in the macrocolony formation assay. Depletion of the selection of biofilm-associated genes using CRISPRi in strain Newman resulted in visible variations between macrocolonies (**Figure 4.6**), with some strains showing increased surface wrinkling (*sarA*, *purA*, *pckA*, *fbp* and *fakA*) and some showing a loss of surface wrinkling and/or loss of shape (*mgo*, *eno*, *purE-D*, *def2*, *capA* and *gdpS*) (see detailed discussion below). Out of these 11 genes, eight of them were also identified in a transposon screen for genes involved in macrocolony formation by Wermser and Lopez (2018).

Together these results confirm that CRISPRi can be used to identify genes involved in *S. aureus* biofilm and macrocolony formation. However, the variability in results discussed below, substantiates the importance of conducting multiple separate crystal violet microtiter plate assays

to validate the biofilm phenotype and subsequent additional studies will also be necessary to validate the role of a given gene in *S. aureus* biofilm formation.

### **5.2 The crystal violet microtiter assay to study genes involved in biofilm by CRISPRi**

In the crystal violet assays, the ability of the strains to form biofilms on untreated polystyrene microtiter plates are studied. The crystal violet microtiter plate assay allows for changing multiple variables and screening large sets of strains simultaneously, thus providing a valuable method for screening large sets of strains and mutants in a short time.

Strain variations with regard to biofilm formation is well known and make it difficult to standardize the microtiter plate assay to apply to all *S. aureus* strains (Liu et al., 2020), which was evidenced by the different biofilm forming capabilities of strains SH1000, NCTC8325-4 and Newman, in which different growth conditions, such as addition of glucose and  $Mg^{2+}$  promoted biofilm formation in different strains (**Figure 4.1** and **figure 4.2**). For example, supplementation of glucose seems to promote biofilm formation by SH1000 more than it does NCTC8325-4 and Newman. The three strains NCTC8325-4, SH1000 and Newman vary from each other on a genetic level, and differences in regulation of biofilm-associated genes may explain some of the variation. While NCTC8325-4 and SH1000 both are derived from the sepsis isolate 8325, NCTC8325-4 harbor reduced activity of the alternative sigma factor  $\sigma^B$ , resulting from a 11 base pair deletion in *rsbU*. RsbU is a phosphatase regulating the dissociation of the complex of  $\sigma^B$  and anti-sigma factor RsbW (Bæk et al., 2013). In SH1000, the *rsbU* mutation is repaired, resulting in an active  $\sigma^B$  (Horsburgh et al., 2002).  $\sigma^B$  is a repressor of the *agr* quorum sensing system, which again is linked to the regulation of biofilm formation (Horsburgh et al., 2002; Paharik & Horswill, 2016). The effect of  $\sigma^B$  and *agr* on biofilms is quite intricate. Repression of the *agr* system results in increased expression of cell surface proteins used in adherence, in addition to decreasing the expression of PSMs and extracellular proteases, resulting in increased biofilm formation, while de-repression of the *agr* system (e.g., by a defect in  $\sigma^B$ ) has the opposite effect (Horsburgh et al., 2002; Paharik & Horswill, 2016). Notably, glucose is thought to inhibit the *agr* quorum sensing system through lowering the pH of the medium (Regassa et al., 1992). As the activity of the *agr* quorum sensing system differs between the strains on a genetic level, this might provide some explanation as to why differences are observed upon glucose supplementation.

Furthermore, supplementation of  $Mg^{2+}$  seems to promote biofilm formation by strain Newman, while not for NCTC8325-4 (**Figure 4.2**). It was also found to increase macrocolony structuring to a greater extent in Newman (**Figure 4.5A**). While the exact mechanism behind  $Mg^{2+}$  and biofilm formation is not known, it is proposed that extracellular  $Mg^{2+}$  is incorporated into the bacterial cell wall by binding teichoic acids, which increases cell wall rigidity. This is thought to provoke activation of  $\sigma^B$  expression which in turn represses the *agr* quorum sensing system, ultimately resulting in expression of biofilm associated genes (García-Betancur et al., 2017). Why extracellular  $Mg^{2+}$  results in higher biofilm formation in Newman, while not in NCTC8325-4 (TSBMG was not tested for SH1000) is uncertain but is probably due to genetic strain variations. For example, Newman carries a missense mutation in *saeS*, resulting in a complex pattern of virulence gene regulation that is quite different from that of strains with the wildtype *saeS* gene (Herbert et al., 2010). Newman also carries mutations in the biofilm-associated genes *fnbA* and *fnbB*, resulting in a loss of adhesion to ligands as fibrinogen and fibronectin (Grundmeier et al., 2004). All these genetic variations might impact biofilm formation, but to what extent different mechanisms is involved is a complex matter since biofilms are regulated by multiple systems.

From the selection of known biofilm-associated genes, it was shown that the depletion of *agrA*, *psm $\beta$ 1-2* and *atl* produced biofilm phenotypes consistent with what has previously been reported for knockout strains in the crystal violet assay (**Figure 4.3**). PSMs (*psm $\beta$ 1-2*) are thought to function as surfactants disrupting molecular interaction, and the *agr* quorum sensing system is known to repress the expression of cell surface proteins used in adherence and biofilm formation, while simultaneously promoting protease-mediated dispersal and expression of PSMs (Moormeier & Bayles, 2017; Paharik & Horswill, 2016). The autolysin *atl* is reported to promote attachment to polystyrene and to promote biofilm formation (Biswas et al., 2006) (see more discussion below). SasG, which in this work resulted in an increase in biofilm formation when depleted, have on the other hand been reported both to promote and inhibit biofilm formation in different studies. In one study, SasG was found to inhibit adhesion to ligands like fibrinogen, while promoting adhesion to desquamated nasal epithelial cells (Corrigan et al., 2007), while in another study it was found to play a role in the accumulation of biofilm, but not during primary attachment to tissue culture treated plates (Geoghegan et al., 2010). The fact that depletion of SasG in this work resulted in an increase in biofilm formation suggests that SasG plays multiple roles, depending on the

experimental background, and might inhibit adhesion in the experimental setup used in this study where biofilm formation was conducted on untreated polystyrene microtiter plates.

When studying biofilm formation in a microtiter plate assay, it is important to note that different genes are involved in the adhesion to different surfaces. This provides an explanation as to why depletion of multiple genes (**Figure 4.3**) did not result in any apparent changes in biofilm forming capabilities in the CRISPRi strains even though they are reported to be involved in biofilm formation. Some proteins, such as the major autolysin Atl, is known to participate in adherence to both polystyrene and other components such as fibrinogen and vitronectin (Biswas et al., 2006), while SasG promotes adhesion to desquamated nasal epithelial cells but inhibits adhesion to fibrinogen (Corrigan et al., 2007). Extending the crystal violet microtiter plate assay by coating the microtiter plate with varying ligands will possibly allow for the detection of other genes involved in biofilm formation. Likewise, some genes are involved in the primary attachment of biofilm formation, while others are involved in maturation or dispersal of the biofilm. The *agr* quorum system, for example, is found to be repressed during initial attachment, while being re-activated in biofilm communities to promote dispersal of cells (Lister & Horswill, 2014). The duration of incubation of cells in the microtiter plate might therefore also influence the results, as some genes are upregulated or downregulated in the early stages, and vice versa in the late stages of biofilm formation. It is worth noting that a threshold of 20% above and 20% below the OD measured for the control strain was chosen as what was thought of as a significant change in biofilm formation in the crystal violet microtiter plate assay. If the threshold was set differently, this would have resulted in an increased or decreased number of genes found in this work to be involved in biofilm formation, and thus influences the results.

The crystal violet microtiter plate assay showed relatively large variations when using the same strain in separate experiments. The crystal violet microtiter plate assay is dependent upon multiple steps of washing before and after staining, which can result in detachment and removal of some cells in the biofilm and will vary between experiments. Crystal violet staining is a widely used method for staining biofilm, but a standardized protocol is lacking, making it difficult to compare results between studies (Azeredo et al., 2017). It has also been shown to lack reproducibility in *P. aeruginosa* strains (Peeters et al., 2008). Another aspect to take into consideration when using the microtiter plate assay and staining with crystal violet is the possibility of an “edge effect” (Shukla

& Rao, 2017). Peripheral wells of the microtiter plate assay are more ventilated thus providing more O<sub>2</sub> for bacterial growth. *In vitro* experiments demonstrate that anaerobic conditions induce expression of biofilm associated genes (Balasubramanian et al., 2017), the aerobic or anaerobic conditions present when conducting biofilm assays will thus influence biofilm formation. Secondly, water evaporates quickly from peripheral wells, thereby driving the planktonic cells to stick to the walls, which in turn binds the crystal violet dye, giving a false reading as biofilm mass (Shukla & Rao, 2017). If the same strain is placed in different locations of the 96-well microtiter plate assay in separate experiments, this could adjust for some of the difference observed between separate experiments. However, in this work, the control strain was always located in the three wells in the upper left corner, and the variation between separate experiments is thus not explained alone by the edge effect. As biofilm formation is such a complexly regulated process, small variations in temperature, humidity, oxygen levels and other environmental conditions such as availability of nutrients like carbohydrates, iron and magnesium might result in variations in biofilm formation.

### **5.3 SAOUHSC\_00671 is a potential new biofilm associated protein regulated by the WalRK system**

During initial testing of the CRISPRi system with the crystal violet microtiter plate assay it was discovered that depletion of the autolysin Atl resulted in a consistent decrease in biofilm formation on a polystyrene surface. *atl* is under the regulatory control of the highly conserved WalRK (also known as YycG/YycF) two component system, which is essential for cell viability (Dubrac & Msadek, 2004). It was therefore decided to use the crystal violet microtiter plate assay to screen other WalRK-regulated genes for involvement in *S. aureus* biofilm formation. The genes regulated by the WalRK system encode proteins involved in cell wall metabolism, membrane-bound transport and pathogenicity. It has also been found that the WalRK system positively controls biofilm formation and autolysin synthesis (Dubrac et al., 2007). In this work, depletion of the WalRK regulated genes *sle1* and *SAOUHSC\_00671*, in addition to *atl*, was found to result in decreased biofilm formation in *S. aureus* NCTC8325-4 (**Figure 4.7B**). Atl is a cell wall hydrolase known to be involved in biofilm formation both through increasing adherence to polystyrene, fibrinogen and vitronectin (Hirschhausen et al., 2012), and through autolysis mediated release of extracellular DNA, a structural component of the extracellular matrix (Bose et al., 2012). Sle1, on the other hand, also a cell wall hydrolase, has not been found to be involved release of eDNA

## 5 Discussion

(Kajimura et al., 2005), but has been found to promote attachment to different surfaces, including fibrinogen, fibronectin, and vitronectin (Kajimura et al., 2005). As SAOUHSC\_00671 show sequence similarities to Sle1, with both proteins containing LysM domains and a CHAP domain, SAOUHSC\_00671 is most likely a cell wall hydrolase as well.

A deletion mutant ( $\Delta$ SAOUHSC\_00671::*spc*) was constructed to further study the involvement of SAOUHSC\_00671 in biofilm formation. Surprisingly, when repeating the crystal violet microtiter plate assay using three independent deletion mutants, they all showed different biofilm phenotypes (**Figure 4.11**). On the other hand, in an inducible complementation strain made in one of the  $\Delta$ SAOUHSC\_00671 deletion strains, the reduced biofilm observed without induction was recovered when expressing SAOUHSC\_00671 from a plasmid, as would be expected. Furthermore, overexpression of SAOUHSC\_00671 did result in an increase in biofilm formation, although not dramatic. Further investigation into these strains are necessary, and the deletion strains needs to be genome sequenced to understand these results and find out whether any additional mutations have occurred in the genome.

Although confirmations are needed, the results suggest that lack a of SAOUHSC\_00671 results in decreased attachment to a polystyrene surface. Like Sle1 (Hirschhausen et al., 2012; Kajimura et al., 2005), it is possible that SAOUHSC\_00671 also promotes biofilm formation through increased adherence, which need to be further investigated. Through analysis of domain truncation and exchange variants of SAOUHSC\_00671, Osipovitch et al. (2015) have demonstrated lytic activity of the putative CHAP domain. Although more research is needed to understand how the full-length protein work, this suggests that SAOUHSC\_00671 might have lytic activity. If SAOUHSC\_00671 is indeed a cell wall hydrolase, alterations of the cell surface in the absence of SAOUHSC\_00671 might affect physiochemical properties of the cell surface, which is important in the initial attachment during biofilm formation. No synergistic effects were found on biofilm formation when depleting both SAOUHSC\_00671 and Sle1 or SAOUHSC\_00671 and Atl (**Figure 4.9**). This suggests that adherence to polystyrene is somehow maintained in the presence of only one of the proteins, or that there are additional proteins present which promotes adhesion to polystyrene. The role of SAOUHSC\_00671 in attachment to other substances should also be investigated further and it is also important to determine whether it's role in biofilm formation is linked to surface

adhesion through changes in the cell wall (like *sle1* and *atl*) or through eDNA release through autolysis (like *atl*).

Both *atl* and *sle1* mutants have previously been shown to grow in clusters (Kajimura et al., 2005), which was also found by CLSM (**Figure 4.10**) when depleting cells of *SAOUHSC\_00671*. This may suggest the involvement of *SAOUHSC\_00671* in the separation of daughter cells during cell division. As confocal microscopy was only done once as an initial test, further microscopy using both CLSM and phase contrast microscopy are needed to confirm whether *SAOUHSC\_00671* is involved in daughter cell separation together with *Atl* and *Sle1*.

### **5.4 Macrocolony formation can be used as a simple biofilm model in screening for novel biofilm associated genes using a pooled CRISPRi library**

The macrocolony biofilm model is an established model to study aspects of biofilm formation, and in the *S. aureus* biofilm model, the supplementation of magnesium mimics magnesium-rich niches in the host. Strain Newman has been reported to form more robust and structured macrocolonies when grown in the presence of magnesium (Wermser & Lopez, 2018). In this work, magnesium was found to increase macrocolony structuring in the strains SH1000 and NCTC8325-4 as well as in Newman, but, as surface wrinkling was more pronounced in Newman (**Figure 4.5A**), this was the choice of strain when conducting macrocolony formation assays. Strain Newman has also been reported to be a poor biofilm producer under certain conditions (Beenken et al., 2003), and the macrocolony formation assay might therefore provide insight into new cellular processes involved in *S. aureus* biofilm formation, substantiated by the identification of novel pathways involved in USA300 macrocolony formation by Wermser and Lopez (2018). As a proof of concept for the use of CRISPRi in macrocolony assays, some of the genes identified previously in USA300 (Wermser & Lopez, 2018) were depleted in Newman, along with a larger selection of known biofilm-associated genes. As mentioned above, 11 genes from the selection were found to result in visible variations between macrocolonies (**Figure 4.6**), and eight of them were also identified in a transposon screen for genes involved in macrocolony formation.

Depletion of some genes resulted in increased surface wrinkling (*sarA*, *purA*, *pckA*, *fbp* and *fakA*) and some showing a loss of surface wrinkling and/or loss of shape (*mgo*, *eno*, *purE-D*, *def2*, *capA* and *gdpS*) (see detailed discussion below). Depletion of some genes selected from the transposon macrocolony screen by Wermser and Lopez (2018), did not give similar alterations in macrocolony

structures in this work. This is most likely explained by strain differences as the strain USA300 was used in the transposon macrocolony screen, while strain Newman was used in this work. As with the microtiter plate assay, the depletion of several genes from the selection did not result in any apparent change in macrocolony structure compared to the control. As the selected genes of the CRISPRi collection have been associated with biofilm formation in multiple different strains and in multiple different experimental setups, it is not expected that all genes will have an impact on macrocolony formation.

The categorization of phenotypic categories used in **figure 4.6** and **figure 4.13** was based on visual inspection of the macrocolony structures. This approach is prone to inaccuracy due to subjectivity of the person determining the categories. Automatic tools for quantifying macroscopic phenotypes will improve the macrocolony formation assay, reducing the subjectivity in categorization of the macrocolonies. Using an image analysis software like Iris, which have been shown to work for *Candida albicans* and *Escherichia coli* (Kritikos et al., 2017), could allow for systematic exploration of biofilm formation and macrocolony morphology. Further improvement of the macrocolony formation assay by using fluorescent dyes with DNA- or protein-binding properties to visualize the localization of components of the extracellular matrix or by using fluorescently tagged proteins should be investigated further.

Having confirmed that CRISPRi knockdown of gene expression could be used with the macrocolony assay, a pooled CRISPRi library of 1928 strains harboring unique sgRNAs were used in an unbiased screen in an attempt to identify new genes involved in macrocolony formation. Approximately 1500 colonies were inspected for changes in macrocolony structure, identifying 10 genes affecting macrocolony structure in Newman (**Figure 4.13**). Among these, *pckA* and *fumC* have already been identified previously to be involved in macrocolony formation (Wermser & Lopez, 2018), while *icaB* is known to be involved in *ica*-dependent biofilm formation (O'Gara, 2007), proving that the CRISPRi pooled library can be used to identify genes involved in biofilm formation using the macrocolony assay. The screen also identified several new candidates which needs to be further investigated with respect to their involvement in biofilm formation (see discussion below). Furthermore, one of the identified candidates were depleted of a putative essential gene (*tagO*). This gives hope as to whether CRISPRi can be used to identify essential

genes which are so far unknown to be involved in biofilm formation. Upscaling of the screen will allow for identification of multiple genes involved in *S. aureus* macrocolony formation.

### 5.5 Fully functional gluconeogenesis and TCA cycle are needed for proper macrocolony formation

Among the identified candidates from the pooled CRISPRi macrocolony screen, *fumC*, *pckA* and *sucA* are involved in carbohydrate metabolism. This suggests a link between macrocolony formation and the central metabolic pathways. Two of these genes, *fumC* and *pckA*, were also found to be involved in macrocolony formation by USA300 in a separate study by Wermser and Lopez (2018). In addition, Wermser and Lopez (2018) also identified several other genes involved in gluconeogenesis (*fbp*), the TCA cycle (*gltA*, *mgo*) and purine biosynthesis (*purA*, *purB*, *purC*, *purK*, *purL*), further suggesting a link between the central metabolic pathways and macrocolony formation.

PckA catalyzes the initial step of the **gluconeogenesis** pathway. Gluconeogenesis is the process of synthesizing glucose from TCA cycle intermediates or from glycolysis-derived pyruvate. PckA catalyzes the conversion of oxaloacetate to phosphoenolpyruvate (PEP), which is further converted during gluconeogenesis (Halsey et al., 2017; Wermser & Lopez, 2018). Wermser and Lopez (2018) hypothesize that a lack of PckA results in a fitness defect which likely contributes to the macrocolony defects they observed in a PckA-lacking USA300 mutant. In contrast to the PckA-lacking mutants studied by Wermser and Lopez (2018), which were thin and without 3D-structure, the PckA-depleted macrocolonies observed in this work had an increase in surface wrinkling compared to the control. As PckA-lacking mutants show contrasting macrocolony phenotypes in Newman and USA300, further investigation into the role of PckA and gluconeogenesis in biofilm formation is needed.

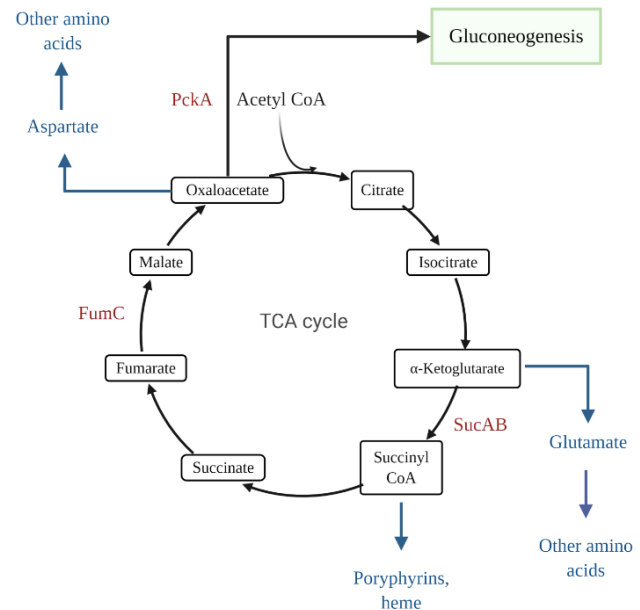


**Figure 5.1 Schematic of the TCA cycle intermediates and their roles in biosynthesis.** Enzymes found to be involved in macrocolony formation are shown in red. Biosynthetic pathways using TCA cycle intermediates are shown in blue. Schematic is adapted from Berg et al., 2002 and Halsey et al., 2017.

SucA and FumC are involved in carbohydrate metabolism via the **TCA cycle**. The TCA cycle is a central metabolic pathway that generates ATP and precursors for biosynthesis of macromolecules (**Figure 5.1**) (Berg et al., 2002). *sucA* encode one of the subunits of the  $\alpha$ -ketoglutarate dehydrogenase, which catalyzes the conversion of  $\alpha$ -ketoglutarate to succinyl-CoA. Succinyl-CoA is further used in the biosynthesis of porphyrins and heme, which are important for electron transport in the electron transport chain, and thus respiration (Berg et al., 2002). The potential role of respiration in biofilm formation will be discussed in **section 5.6**. Furthermore, FumC catalyzes the conversion of the TCA intermediate fumarate to malate, which is subsequently converted to oxaloacetate. Oxaloacetate is a precursor for the biosynthesis of aspartate, which is further used for the biosynthesis of other amino acids and purines (Berg et al., 2002). Wermser and Lopez (2018) presents a link between purine synthesis and macrocolony formation in USA300, while De Backer et al. (2018) have found that a lack of TCA-cycle enzymes results in a biofilm ECM with reduced levels of proteins, an important component of the ECM. The role of both SucA and FumC in biofilm formation might therefore be linked to several different processes, including synthesis of amino acids, purines and components of the electron transport chain, in addition to the protein composition of the ECM.

For future studies, it would be important to study if depletion or deletion of these genes involved in gluconeogenesis and the TCA cycle has an effect on growth behavior, as reduced growth would affect biofilm formation. De Backer et al. (2018) found that *fumC* did not show reduced growth, indicating that its effect on biofilm formation is not linked to growth.

### **5.6 A functional respiration is needed for proper macrocolony formation**

Of the macrocolony candidates identified in the pooled CRISPRi macrocolony screen (**Figure 4.13**), strains depleted of genes involved in respiration were found to have a loss of structure and/or surface wrinkling. The two genes *ubiE* and *hemE* encodes proteins involved in the synthesis of **menaquinone** and **heme**, respectively, both important for electron transport during respiratory metabolism in *S. aureus*. Wermser and Lopez (2018) also identified another enzyme part of heme biosynthesis, HemL, to be involved in macrocolony formation in *S. aureus* USA300. UbiE catalyzes the final step in the biosynthesis of the electron carrier MK (**Figure 4.15**) (Boersch et al., 2018). HemE is a part of the heme biosynthesis pathway, catalyzing the conversion of uroporphyrinogen III to coproporphyrinogen III which is further used in the biosynthesis of heme

B (protoheme IX), the precursor of heme A, heme C, heme D and heme O (Thöny-Meyer, 1997), which is then incorporated into the cytochromes of the electron transport chain. In the electron transport chain, oxidation of reduced MK is accomplished by cytochromes which are membrane proteins that contain heme, an iron-containing porphyrin. Without a functioning electron transport chain, the cells are unable to respire, and must therefore switch to a fermentative metabolism (Boersch et al., 2018; Wakeman et al., 2012). Models suggest that fermentative biofilms are induced by impaired respiration through two separate regulatory pathways (**Figure 5.2**). In one of the models, MK is necessary for stimulating the two-component regulatory system SrrAB, with the accumulation of reduced MK being shown to stimulate the SrrAB system, which directly or indirectly leads to increased transcription of *atl* and decreased transcription of genes (*tar*) encoding for wall teichoic acid biosynthesis. This in turn promotes the release of DNA and proteins, cell lysis and biofilm formation (Mashruwala et al., 2017b). The other model proposes that impaired cellular respiration stimulates the two-component regulatory system SaeRS via yet undefined signal molecule(s). Stimulation of the SaeRS system leads to increased expression of *atl*, resulting in increased autolysis and release of DNA and proteins, in addition to increased expression of *fnbA*, which is known to increase biofilm formation (Mashruwala et al., 2017a).

Depletion of both UbiE and HemE will likely result in impaired respiration both through the lack of MK produced by the UbiE-depleted cells, and through the accumulation of reduced MK in the HemE-depleted cells. Furthermore, supplementation of menaquinone has been found to increase biofilm formation by *S. aureus* in a microtiter plate assay (Kirby et al., 2014). Further investigations are thus needed to understand the stimulation of both the SrrAB and the SaeRS system, which are known to affect biofilm formation, and whether menaquinone has another role in biofilm formation. Humans do not possess a MK biosynthesis pathway, and MK is not utilized for electron transport in humans (Meganathan & Kwon, 2009). The MK pathway may therefore prove to be a potential drug target in the fight against *S. aureus* biofilm related infections.

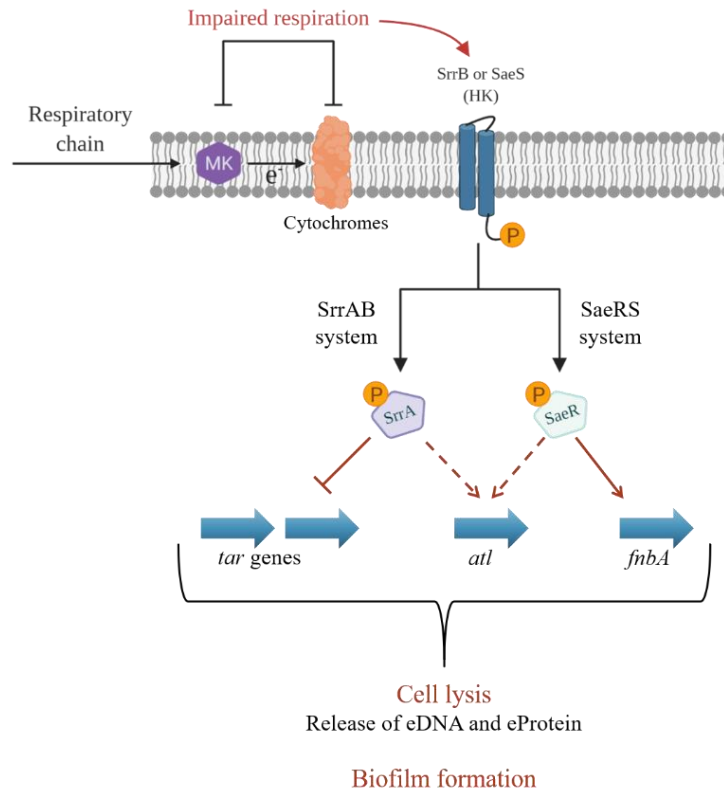


**Figure 5.2 Model for the influence of respiration upon the SrrAB- and SaeRS regulatory systems.** A decreased capacity to respire stimulates the SaeS histidine kinase and/or the SrrB histidine kinase, resulting in an increased concentration of phosphorylated SaeR or SrrA, respectively. This results, directly (solid lines) or indirectly (dashed lines) in increased expression of the cell wall hydrolase *Atl* and the fibrinogen binding protein *FnbA*, and decreased expression of genes (*tar*) encoding for wall teichoic acid (WTA) biosynthesis. The decrease in WTAs and the increase in *Atl*-mediated autolysis results in release of extracellular DNA (eDNA) and proteins (eProtein), ultimately resulting in increased biofilm formation. The model is adapted from Mashruwala et al., 2017a and Mashruwala et al., 2017b. MK, menaquinone; HK, histidine kinase

### 5.7 A putative methyltransferase seems to be important for macrocolony formation

In the pooled CRISPRi library macrocolony screen (**Figure 4.13**), depletion of *NWMN\_RS14065* showed a macrocolony structure distinct of all other depletion mutants, with the macrocolony being thin and transparent, with a complete loss of surface wrinkling and structure. *NWMN\_RS14065* encodes a putative 6-O-methyl-DNA-protein-cysteine methyltransferase which is involved in DNA repair. When repeating the macrocolony assay using a deletion mutant (**Figure 4.17**), the macrocolony, somewhat surprisingly, showed a surface wrinkling with what seems like an increase in wrinkles compared to the WT. The macrocolony structure still differed significantly from that of the WT. It is uncertain why deletion and depletion of the same gene resulted in different macrocolony structure and might be a result of some expression of *NWMN\_RS14065* being retained after depletion. There might also be assay variations, resulting in differences in separate

## 5 Discussion

experiments. Nevertheless, both depletion and deletion of *NWMN\_RS14065* resulted in a macrocolony biofilm defect which needs to be further investigated. From what we know, a link between DNA methylation and biofilm formation has not yet been established. Investigating the growth behavior of  $\Delta NWMN\_RS14065$  will give further insight into whether possible growth defects has an impact on the observed macrocolony defect, or if there are other pathways involved that are not yet identified.

## 6 Concluding remarks and future research

Through the experiments performed in this work it was shown that CRISPRi knockdown of gene expression could be used to identify novel genes involved in biofilm- and/or macrocolony formation using two different biofilm model systems. The crystal violet microtiter plate assay showed to be somewhat unstable, and further experiments using different strains experimental conditions could give insight into factors influencing the assay. Improvements might also be possible by trying different methods for washing and staining with crystal violet, in a way which has less impact on the formed biofilm. In any assay, it would be beneficial to test different environmental conditions.

Using CRISPRi and the two biofilm model systems, we were able to identify several genes which have not been directly described in biofilm formation yet. The novel candidate SAOUHSC\_00671 is putatively involved in cell wall hydrolysis, a function previously described to be involved in *S. aureus* biofilm formation through the proteins Atl and Sle1. Further classification of SAOUHSC\_00671 and its role in biofilm formation is an important step towards understanding the underlying processes of biofilm formation. Impaired respiration was found to result in macrocolony defects with strains depleted of UbiE and HemE, involved in menaquinone and heme biosynthesis, respectively. Respiration has in other studies been suggested to influence biofilm formation through the two regulatory systems SrrAB and SaeRS. Further investigations as to whether UbiE- or HemE- lacking cells are defective in macrocolony formation due to their effect on either of these two regulatory systems will give further insight into the role of respiration and biofilm formation. The menaquinone pathway is an interesting therapeutic target as the pathway does not exist in humans. Depletion of a putative methyltransferase, NWMN\_RS14065, indicated to be involved in DNA repair also resulted in macrocolony formation defects. There has not yet been described a link between DNA repair and biofilm formation. The growth behavior of NWMN\_RS14065-lacking cells have not yet been tested, which will indicate whether it influences biofilm formation through its possible effect on growth rate, or through other, not yet identified mechanisms.

Both the crystal violet microtiter plate assay and the macrocolony formation assay proved to be useful simple methods of screening for biofilm-associated genes, and upscaling the assays by screening the entire CRISPRi library of 1928 strains could result in the identification of additional novel genes involved in biofilm formation.

6 Concluding remarks

## References

- Agarwal, A. & Jain, A. (2013). Glucose & sodium chloride induced biofilm production & ica operon in clinical isolates of staphylococci. *Indian J Med Res*, 138 (2): 262-266.
- Archer, N. K., Mazaitis, M. J., Costerton, J. W., Leid, J. G., Powers, M. E. & Shirtliff, M. E. (2011). *Staphylococcus aureus* biofilms: properties, regulation, and roles in human disease. *Virulence*, 2 (5): 445-59. doi: 10.4161/viru.2.5.17724.
- Armitano, J., Redder, P., Guimarães, V. A. & Linder, P. (2016). An Essential Factor for High Mg(2+) Tolerance of *Staphylococcus aureus*. *Front Microbiol*, 7: 1888-1888. doi: 10.3389/fmicb.2016.01888.
- Armstrong-Esther, C. A. (1976). Carriage patterns of *Staphylococcus aureus* in a healthy non-hospital population of adults and children. *Ann Hum Biol*, 3 (3): 221-227. doi: 10.1080/03014467600001381.
- Arnaud, M., Chastanet, A. & Débarbouillé, M. (2004). New vector for efficient allelic replacement in naturally nontransformable, low-GC-content, gram-positive bacteria. *Appl Environ Microbiol*, 70 (11): 6887-91. doi: 10.1128/aem.70.11.6887-6891.2004.
- Azeredo, J., Azevedo, N. F., Briandet, R., Cerca, N., Coenye, T., Costa, A. R., Desvaux, M., Di Bonaventura, G., Hébraud, M., Jaglic, Z., et al. (2017). Critical review on biofilm methods. *Crit Rev Microbiol*, 43 (3): 313-351. doi: 10.1080/1040841X.2016.1208146.
- Bagnoli, F., Rappuoli, R. & Grandi, G. (2018). *Staphylococcus aureus: Microbiology, Pathology, Immunology, Therapy and Prophylaxis*: Springer International Publishing.
- Balasubramanian, D., Harper, L., Shopsin, B. & Torres, V. J. (2017). *Staphylococcus aureus* pathogenesis in diverse host environments. *Pathog Dis*, 75 (1): ftx005. doi: 10.1093/femspd/ftx005.
- Beenken, K. E., Blevins, J. S. & Smeltzer, M. S. (2003). Mutation of sarA in *Staphylococcus aureus* Limits Biofilm Formation. *Infect Immun*, 71 (7): 4206. doi: 10.1128/IAI.71.7.4206-4211.2003.
- Beenken, K. E., Dunman, P. M., McAleese, F., Macapagal, D., Murphy, E., Projan, S. J., Blevins, J. S. & Smeltzer, M. S. (2004). Global gene expression in *Staphylococcus aureus* biofilms. *J Bacteriol*, 186 (14): 4665-4684. doi: 10.1128/JB.186.14.4665-4684.2004.
- Beenken, K. E., Mrak, L. N., Griffin, L. M., Zielinska, A. K., Shaw, L. N., Rice, K. C., Horswill, A. R., Bayles, K. W. & Smeltzer, M. S. (2010). Epistatic relationships between sarA and agr in *Staphylococcus aureus* biofilm formation. *PloS One*, 5 (5): e10790-e10790. doi: 10.1371/journal.pone.0010790.
- Bera, A., Biswas, R., Herbert, S., Kulauzovic, E., Weidenmaier, C., Peschel, A. & Götz, F. (2007). Influence of wall teichoic acid on lysozyme resistance in *Staphylococcus aureus*. *J Bacteriol*, 189 (1): 280-283. doi: 10.1128/JB.01221-06.
- Berg, J., Tymoczko, J. & Stryer, L. (2002). *Biochemistry, 5th edition*. New York: W H Freeman.
- Bhattacharya, M., Wozniak, D. J., Stoodley, P. & Hall-Stoodley, L. (2015). Prevention and treatment of *Staphylococcus aureus* biofilms. *Expert Rev Anti Infect Ther*, 13 (12): 1499-1516. doi: 10.1586/14787210.2015.1100533.
- Bien, J., Sokolova, O. & Bozko, P. (2011). Characterization of Virulence Factors of *Staphylococcus aureus*: Novel Function of Known Virulence Factors That Are Implicated in Activation of Airway Epithelial Proinflammatory Response. *J Pathog*, 2011: 601905-601905. doi: 10.4061/2011/601905.

## References

- Biswas, R., Voggu, L., Simon, U. K., Hentschel, P., Thumm, G. & Götz, F. (2006). Activity of the major staphylococcal autolysin Atl. *FEMS Microbiol Lett*, 259 (2): 260-268. doi: 10.1111/j.1574-6968.2006.00281.x.
- Bode, L. G., Kluytmans, J. A., Wertheim, H. F., Bogaers, D., Vandenbroucke-Grauls, C. M., Roosendaal, R., Troelstra, A., Box, A. T., Voss, A., van der Tweel, I., et al. (2010). Preventing surgical-site infections in nasal carriers of *Staphylococcus aureus*. *N Engl J Med*, 362 (1): 9-17. doi: 10.1056/NEJMoa0808939.
- Boersch, M., Rudrawar, S., Grant, G. & Zunk, M. (2018). Menaquinone biosynthesis inhibition: a review of advancements toward a new antibiotic mechanism. *RSC Advances*, 8 (10): 5099-5105. doi: 10.1039/C7RA12950E.
- Boles, B. R. & Horswill, A. R. (2011). Staphylococcal biofilm disassembly. *Trends Microbiol*, 19 (9): 449-55. doi: 10.1016/j.tim.2011.06.004.
- Bose, J. L., Lehman, M. K., Fey, P. D. & Bayles, K. W. (2012). Contribution of the *Staphylococcus aureus* Atl AM and GL Murein Hydrolase Activities in Cell Division, Autolysis, and Biofilm Formation. *PLoS One*, 7 (7): e42244. doi: 10.1371/journal.pone.0042244.
- Branda, S. S., González-Pastor, J. E., Ben-Yehuda, S., Losick, R. & Kolter, R. (2001). Fruiting body formation by *Bacillus subtilis*. *Proc Natl Acad Sci USA*, 98 (20): 11621-11626. doi: 10.1073/pnas.191384198.
- Bæk, K. T., Frees, D., Renzoni, A., Barras, C., Rodriguez, N., Manzano, C. & Kelley, W. L. (2013). Genetic Variation in the *Staphylococcus aureus* 8325 Strain Lineage Revealed by Whole-Genome Sequencing. *PLoS One*, 8 (9): e77122. doi: 10.1371/journal.pone.0077122.
- Cassat, J. E. & Skaar, E. P. (2012). Metal ion acquisition in *Staphylococcus aureus*: overcoming nutritional immunity. *Semin Immunopathol.*, 34 (2): 215-235. doi: 10.1007/s00281-011-0294-4.
- Ceri, H., Olson, M. E., Stremick, C., Read, R. R., Morck, D. & Buret, A. (1999). The Calgary Biofilm Device: new technology for rapid determination of antibiotic susceptibilities of bacterial biofilms. *J Clin Microbiol.*, 37 (6): 1771-6.
- Chaffin, D. O. & Rubens, C. E. (1998). Blue/white screening of recombinant plasmids in Gram-positive bacteria by interruption of alkaline phosphatase gene (*phoZ*) expression. *Gene*, 219 (1): 91-99. doi: [https://doi.org/10.1016/S0378-1119\(98\)00396-5](https://doi.org/10.1016/S0378-1119(98)00396-5).
- Chambers, H. F. & Deleo, F. R. (2009). Waves of resistance: *Staphylococcus aureus* in the antibiotic era. *Nat Rev Microbiol.*, 7 (9): 629-641. doi: 10.1038/nrmicro2200.
- Chang, A. Y., Chau, V., Landas, J. A. & Pang, Y. (2017). Preparation of calcium competent *Escherichia coli* and heat-shock transformation. *JEMI Methods*, 1: 22-25.
- Charpentier, E., Anton, A. I., Barry, P., Alfonso, B., Fang, Y. & Novick, R. P. (2004). Novel cassette-based shuttle vector system for gram-positive bacteria. *Appl Environ Microbiol*, 70 (10): 6076-85. doi: 10.1128/aem.70.10.6076-6085.2004.
- Chaudhuri, R. R., Allen, A. G., Owen, P. J., Shalom, G., Stone, K., Harrison, M., Burgis, T. A., Lockyer, M., Garcia-Lara, J., Foster, S. J., et al. (2009). Comprehensive identification of essential *Staphylococcus aureus* genes using Transposon-Mediated Differential Hybridisation (TMDH). *BMC genomics*, 10: 291-291. doi: 10.1186/1471-2164-10-291.
- Chen, P., Abercrombie, J. J., Jeffrey, N. R. & Leung, K. P. (2012). An improved medium for growing *Staphylococcus aureus* biofilm. *J Microbiol Meth*, 90 (2): 115-118. doi: <https://doi.org/10.1016/j.mimet.2012.04.009>.
- Cheung, G. Y. C., Joo, H.-S., Chatterjee, S. S. & Otto, M. (2014). Phenol-soluble modulins--critical determinants of staphylococcal virulence. *FEMS Microbiol Rev*, 38 (4): 698-719. doi: 10.1111/1574-6976.12057.

## References

- Cho, S., Choe, D., Lee, E., Kim, S. C., Palsson, B. & Cho, B. K. (2018). High-Level dCas9 Expression Induces Abnormal Cell Morphology in *Escherichia coli*. *ACS Synth Biol*, 7 (4): 1085-1094. doi: 10.1021/acssynbio.7b00462.
- Christensen, G. D., Simpson, W. A., Younger, J. J., Baddour, L. M., Barrett, F. F., Melton, D. M. & Beachey, E. H. (1985). Adherence of coagulase-negative staphylococci to plastic tissue culture plates: a quantitative model for the adherence of staphylococci to medical devices. *J Clin Microbiol*, 22 (6): 996-1006.
- Chylinski, K., Makarova, K. S., Charpentier, E. & Koonin, E. V. (2014). Classification and evolution of type II CRISPR-Cas systems. *Nucleic Acids Res*, 42 (10): 6091-6105. doi: 10.1093/nar/gku241.
- Coenye, T. & Nelis, H. J. (2010). In vitro and in vivo model systems to study microbial biofilm formation. *J Microbiol Methods*, 83 (2): 89-105. doi: 10.1016/j.mimet.2010.08.018.
- Corrigan, R. M., Rigby, D., Handley, P. & Foster, T. J. (2007). The role of *Staphylococcus aureus* surface protein SasG in adherence and biofilm formation. *Microbiology*, 153 (Pt 8): 2435-2446. doi: 10.1099/mic.0.2007/006676-0.
- Cue, D., Lei, M. G. & Lee, C. Y. (2012). Genetic regulation of the intercellular adhesion locus in staphylococci. *Front Cell Infect Microbiol*, 2: 38-38. doi: 10.3389/fcimb.2012.00038.
- Cue, D., Junecko, J. M., Lei, M. G., Blevins, J. S., Smeltzer, M. S. & Lee, C. Y. (2015). SaeRS-dependent inhibition of biofilm formation in *Staphylococcus aureus* Newman. *PLoS One*, 10 (4): e0123027-e0123027. doi: 10.1371/journal.pone.0123027.
- Cui, L., Vigouroux, A., Rousset, F., Varet, H., Khanna, V. & Bikard, D. (2018). A CRISPRi screen in *E. coli* reveals sequence-specific toxicity of dCas9. *Nat Comm*, 9 (1): 1912. doi: 10.1038/s41467-018-04209-5.
- De Backer, S., Sabirova, J., De Pauw, I., De Greve, H., Hernalsteens, J.-P., Goossens, H. & Malhotra-Kumar, S. (2018). Enzymes Catalyzing the TCA- and Urea Cycle Influence the Matrix Composition of Biofilms Formed by Methicillin-Resistant *Staphylococcus aureus* USA300. *Microorganisms*, 6 (4): 113. doi: 10.3390/microorganisms6040113.
- de la Fuente-Núñez, C., Reffuveille, F., Fernández, L. & Hancock, R. E. W. (2013). Bacterial biofilm development as a multicellular adaptation: antibiotic resistance and new therapeutic strategies. *Curr Opin Microbiol*, 16 (5): 580-589. doi: <https://doi.org/10.1016/j.mib.2013.06.013>.
- Delauné, A., Poupel, O., Mallet, A., Coic, Y.-M., Msadek, T. & Dubrac, S. (2011). Peptidoglycan crosslinking relaxation plays an important role in *Staphylococcus aureus* WalKR-dependent cell viability. *PLoS one*, 6 (2): e17054-e17054. doi: 10.1371/journal.pone.0017054.
- Delauné, A., Dubrac, S., Blanchet, C., Poupel, O., Mäder, U., Hiron, A., Leduc, A., Fitting, C., Nicolas, P., Cavaillon, J.-M., et al. (2012). The WalKR system controls major staphylococcal virulence genes and is involved in triggering the host inflammatory response. *Infect Immun*, 80 (10): 3438-3453. doi: 10.1128/IAI.00195-12.
- Dietrich, L. E. P., Okegbe, C., Price-Whelan, A., Sakhtah, H., Hunter, R. C. & Newman, D. K. (2013). Bacterial Community Morphogenesis Is Intimately Linked to the Intracellular Redox State. *J Bacteriol*, 195 (7): 1371. doi: 10.1128/JB.02273-12.
- Donlan, R. M. & Costerton, J. W. (2002). Biofilms: survival mechanisms of clinically relevant microorganisms. *Clin Microbiol Rev*, 15 (2): 167-193. doi: 10.1128/cmr.15.2.167-193.2002.

## References

- Dubrac, S. & Msadek, T. (2004). Identification of genes controlled by the essential YycG/YycF two-component system of *Staphylococcus aureus*. *J Bacteriol*, 186 (4): 1175-1181. doi: 10.1128/jb.186.4.1175-1181.2004.
- Dubrac, S., Boneca, I. G., Poupel, O. & Msadek, T. (2007). New insights into the WalK/WalR (YycG/YycF) essential signal transduction pathway reveal a major role in controlling cell wall metabolism and biofilm formation in *Staphylococcus aureus*. *J Bacteriol*, 189 (22): 8257-8269. doi: 10.1128/JB.00645-07.
- Dunman, P. M., Murphy, E., Haney, S., Palacios, D., Tucker-Kellogg, G., Wu, S., Brown, E. L., Zagursky, R. J., Shlaes, D. & Projan, S. J. (2001). Transcription profiling-based identification of *Staphylococcus aureus* genes regulated by the agr and/or sarA loci. *J Bacteriol*, 183 (24): 7341-7353. doi: 10.1128/JB.183.24.7341-7353.2001.
- Duthie, E. & Lorenz, L. L. (1952). Staphylococcal coagulase: mode of action and antigenicity. *Microbiology*, 6 (1-2): 95-107.
- ECDC. (2013). *Point prevalence survey of healthcare associated infections and antimicrobial use in European acute care hospitals*. Stockholm: European Centre for Disease Control and Prevention.
- Engler, C., Gruetzner, R., Kandzia, R. & Marillonnet, S. (2009). Golden Gate Shuffling: A One-Pot DNA Shuffling Method Based on Type IIs Restriction Enzymes. *PLoS One*, 4 (5): e5553. doi: 10.1371/journal.pone.0005553.
- Entenza, J.-M., Moreillon, P., Senn, M. M., Kormanec, J., Dunman, P. M., Berger-Bächi, B., Projan, S. & Bischoff, M. (2005). Role of sigmaB in the expression of *Staphylococcus aureus* cell wall adhesins ClfA and FnbA and contribution to infectivity in a rat model of experimental endocarditis. *Infect Immun*, 73 (2): 990-998. doi: 10.1128/IAI.73.2.990-998.2005.
- Feng, Y., Chen, C.-J., Su, L.-H., Hu, S., Yu, J. & Chiu, C.-H. (2008). Evolution and pathogenesis of *Staphylococcus aureus*: lessons learned from genotyping and comparative genomics. *FEMS Microbiol Rev*, 32 (1): 23-37. doi: 10.1111/j.1574-6976.2007.00086.x.
- Fischetti, V. A., Novick, R. P., Ferretti, J. J., Portnoy, D. A., Braunstein, M. & Rood, J. I. (2019). *Gram-Positive Pathogens*: Wiley.
- Fitzpatrick, F., Humphreys, H. & O'Gara, J. P. (2005). Evidence for icaADBC-independent biofilm development mechanism in methicillin-resistant *Staphylococcus aureus* clinical isolates. *J Clin Microbiol*, 43 (4): 1973-1976. doi: 10.1128/JCM.43.4.1973-1976.2005.
- Flemming, H.-C. & Wingender, J. (2010). The biofilm matrix. *Nat Rev Microbiol*, 8 (9): 623-633. doi: 10.1038/nrmicro2415.
- Fletcher, M. (1977). The effects of culture concentration and age, time, and temperature on bacterial attachment to polystyrene. *Can J Microbiol*, 23 (1): 1-6. doi: 10.1139/m77-001.
- Formosa-Dague, C., Speziale, P., Foster, T. J., Geoghegan, J. A. & Dufrêne, Y. F. (2016). Zinc-dependent mechanical properties of *Staphylococcus aureus* biofilm-forming surface protein SasG. *Proc Natl Acad Sci USA*, 113 (2): 410-415. doi: 10.1073/pnas.1519265113.
- Foster, T. J. (2005). Immune evasion by staphylococci. *Nat Rev Microbiol*, 3 (12): 948-958. doi: 10.1038/nrmicro1289.
- Foster, T. J., Geoghegan, J. A., Ganesh, V. K. & Höök, M. (2014). Adhesion, invasion and evasion: the many functions of the surface proteins of *Staphylococcus aureus*. *Nat Rev Microbiol*, 12 (1): 49-62. doi: 10.1038/nrmicro3161.
- Foster, T. J. (2017). Antibiotic resistance in *Staphylococcus aureus*. Current status and future prospects. *FEMS Microbiol Rev*, 41 (3): 430-449. doi: 10.1093/femsre/fux007.

## References

- Foulston, L., Elsholz, A. K., DeFrancesco, A. S. & Losick, R. (2014). The extracellular matrix of *Staphylococcus aureus* biofilms comprises cytoplasmic proteins that associate with the cell surface in response to decreasing pH. *mBio*, 5 (5): e01667-14. doi: 10.1128/mBio.01667-14.
- García-Betancur, J.-C., Goñi-Moreno, A., Horger, T., Schott, M., Sharan, M., Eikmeier, J., Wohlmuth, B., Zernecke, A., Ohlsen, K., Kuttler, C., et al. (2017). Cell differentiation defines acute and chronic infection cell types in *Staphylococcus aureus*. *eLife*, 6: e28023. doi: 10.7554/eLife.28023.
- Geoghegan, J. A., Corrigan, R. M., Gruszka, D. T., Speziale, P., Gara, J. P., Potts, J. R. & Foster, T. J. (2010). Role of Surface Protein SasG in Biofilm Formation by *Staphylococcus aureus*. *J Bacteriol*, 192 (21): 5663. doi: 10.1128/JB.00628-10.
- Gross, M., Cramton, S. E., Götz, F. & Peschel, A. (2001). Key role of teichoic acid net charge in *Staphylococcus aureus* colonization of artificial surfaces. *Infect Immun*, 69 (5): 3423-3426. doi: 10.1128/IAI.69.5.3423-3426.2001.
- Grosser, M. R. & Richardson, A. R. (2016). Method for Preparation and Electroporation of *S. aureus* and *S. epidermidis*. In Bose, J. L. (ed.) *The Genetic Manipulation of Staphylococci: Methods and Protocols*, pp. 51-57. New York, NY: Springer New York.
- Grundmeier, M., Hussain, M., Becker, P., Heilmann, C., Peters, G. & Sinha, B. (2004). Truncation of fibronectin-binding proteins in *Staphylococcus aureus* strain Newman leads to deficient adherence and host cell invasion due to loss of the cell wall anchor function. *Infect Immun*, 72 (12): 7155-7163. doi: 10.1128/IAI.72.12.7155-7163.2004.
- Guzzo, M., Castro, L. K., Reisch, C. R., Guo, M. S. & Laub, M. T. (2020). A CRISPR Interference System for Efficient and Rapid Gene Knockdown in *Caulobacter crescentus*. *mBio*, 11 (1): e02415-19. doi: 10.1128/mBio.02415-19.
- Götz, F. & Mayer, S. (2013). Both Terminal Oxidases Contribute to Fitness and Virulence during Organ-Specific *Staphylococcus aureus* Colonization. *mBio*, 4 (6): e00976-13. doi: 10.1128/mBio.00976-13.
- Haag, A. F., Fitzgerald, J. R. & Penadés, J. R. (2019). *Staphylococcus aureus* in Animals. *Microbiol Spectr*, 7 (3). doi: doi:10.1128/microbiolspec.GPP3-0060-2019.
- Halsey, C. R., Lei, S., Wax, J. K., Lehman, M. K., Nuxoll, A. S., Steinke, L., Sadykov, M., Powers, R. & Fey, P. D. (2017). Amino Acid Catabolism in *Staphylococcus aureus* and the Function of Carbon Catabolite Repression. *mBio*, 8 (1): e01434-16. doi: 10.1128/mBio.01434-16.
- Hammer, N. D., Reniere, M. L., Cassat, J. E., Zhang, Y., Hirsch, A. O., Indriati Hood, M. & Skaar, E. P. (2013). Two Heme-Dependent Terminal Oxidases Power *Staphylococcus aureus* Organ-Specific Colonization of the Vertebrate Host. *mBio*, 4 (4): e00241-13. doi: 10.1128/mBio.00241-13.
- Heilmann, C., Hussain, M., Peters, G. & Götz, F. (1997). Evidence for autolysin-mediated primary attachment of *Staphylococcus epidermidis* to a polystyrene surface. *Mol Microbiol*, 24 (5): 1013-1024. doi: 10.1046/j.1365-2958.1997.4101774.x.
- Helle, L., Kull, M., Mayer, S., Marincola, G., Zelder, M. E., Goerke, C., Wolz, C. & Bertram, R. (2011). Vectors for improved Tet repressor-dependent gradual gene induction or silencing in *Staphylococcus aureus*. *Microbiology*, 157 (Pt 12): 3314-3323. doi: 10.1099/mic.0.052548-0.
- Herbert, S., Ziebandt, A.-K., Ohlsen, K., Schäfer, T., Hecker, M., Albrecht, D., Novick, R. & Götz, F. (2010). Repair of Global Regulators in *Staphylococcus aureus* 8325 and Comparative Analysis with Other Clinical Isolates. *Infect Immun*, 78 (6): 2877. doi: 10.1128/IAI.00088-10.

## References

- Hirschhausen, N., Schlesier, T., Peters, G. & Heilmann, C. (2012). Characterization of the Modular Design of the Autolysin/Adhesin Aaa from *Staphylococcus aureus*. *PLoS One*, 7 (6): e40353. doi: 10.1371/journal.pone.0040353.
- Holtfreter, S. & Bröker, B. (2004). Staphylococcal superantigens: Do they play a role in sepsis? *Arch Immunol Ther Exp*, 53: 13-27.
- Horsburgh, M. J., Aish, J. L., White, I. J., Shaw, L., Lithgow, J. K. & Foster, S. J. (2002). sigmaB modulates virulence determinant expression and stress resistance: characterization of a functional rsbU strain derived from *Staphylococcus aureus* 8325-4. *J Bacteriol*, 184 (19): 5457-5467. doi: 10.1128/jb.184.19.5457-5467.2002.
- Houston, P., Rowe, S. E., Pozzi, C., Waters, E. M. & O'Gara, J. P. (2011). Essential role for the major autolysin in the fibronectin-binding protein-mediated *Staphylococcus aureus* biofilm phenotype. *Infect Immun*, 79 (3): 1153-65. doi: 10.1128/iai.00364-10.
- Huff, E. & Silverman, C. S. (1968). Lysis of *Staphylococcus aureus* cell walls by a soluble staphylococcal enzyme. *J Bacteriol*, 95 (1): 99-106.
- Ito, T., Okuma, K., Ma, X. X., Yuzawa, H. & Hiramatsu, K. (2003). Insights on antibiotic resistance of *Staphylococcus aureus* from its whole genome: genomic island SCC. *Drug Resist Updat*, 6 (1): 41-52. doi: [https://doi.org/10.1016/S1368-7646\(03\)00003-7](https://doi.org/10.1016/S1368-7646(03)00003-7).
- Jefferson, K. K., Cramton, S. E., Götz, F. & Pier, G. B. (2003). Identification of a 5-nucleotide sequence that controls expression of the *ica* locus in *Staphylococcus aureus* and characterization of the DNA-binding properties of IcaR. *Mol Microbiol*, 48 (4): 889-99. doi: 10.1046/j.1365-2958.2003.03482.x.
- Jevons, M. P. (1961). "Celbenin" - resistant Staphylococci. *Br Med J*, 1 (5219): 124-125.
- Jiang, F. & Doudna, J. A. (2017). CRISPR–Cas9 Structures and Mechanisms. *Annu Rev Biophys*, 46 (1): 505-529. doi: 10.1146/annurev-biophys-062215-010822.
- Kajimura, J., Fujiwara, T., Yamada, S., Suzawa, Y., Nishida, T., Oyamada, Y., Hayashi, I., Yamagishi, J. i., Komatsuzawa, H. & Sugai, M. (2005). Identification and molecular characterization of an N-acetylmuramyl-l-alanine amidase Sle1 involved in cell separation of *Staphylococcus aureus*. *Mol Microbiol*, 58 (4): 1087-1101. doi: 10.1111/j.1365-2958.2005.04881.x.
- Kaplan, J. B., Izano, E. A., Gopal, P., Karwacki, M. T., Kim, S., Bose, J. L., Bayles, K. W. & Horswill, A. R. (2012). Low levels of  $\beta$ -lactam antibiotics induce extracellular DNA release and biofilm formation in *Staphylococcus aureus*. *mBio*, 3 (4): e00198. doi: 10.1128/mBio.00198-12.
- Kavanaugh, J. S. & Horswill, A. R. (2016). Impact of Environmental Cues on Staphylococcal Quorum Sensing and Biofilm Development. *J Biol Chem*, 291 (24): 12556-12564. doi: 10.1074/jbc.R116.722710.
- Khan, H. A., Ahmad, A. & Mehboob, R. (2015). Nosocomial infections and their control strategies. *Asian Pac J Trop Biomed*, 5 (7): 509-514. doi: <https://doi.org/10.1016/j.apjtb.2015.05.001>.
- Kim, H. & Kim, J.-S. (2014). A guide to genome engineering with programmable nucleases. *Nat Rev Genet*, 15 (5): 321-334. doi: 10.1038/nrg3686.
- Kirby, D. T., Savage, J. M. & Plotkin, B. J. (2014). Menaquinone (Vitamin K2) enhancement of *Staphylococcus aureus* biofilm formation. *J Biosci Med*, 2014.
- Kjos, M. (2019). Transcriptional Knockdown in Pneumococci Using CRISPR Interference. In Iovino, F. (ed.) *Streptococcus pneumoniae: Methods and Protocols*, pp. 89-98. New York, NY: Springer New York.
- Kluytmans, J. A. J. W., Mouton, J. W., VandenBergh, M. F. Q., Manders, M.-J. A. A. J., Maat, A. P. W. M., Wagenvoort, J. H. T., Michel, M. F. & Verbrugh, H. A. (1996). Reduction of

## References

- Surgical-Site Infections in Cardiothoracic Surgery by Elimination of Nasal Carriage of *Staphylococcus aureus*. *Infect Control Hosp Epidemiol*, 17 (12): 780-785. doi: 10.1017/S0195941700003465.
- Koch, G., Yepes, A., Förstner, K. U., Wermser, C., Stengel, S. T., Modamio, J., Ohlsen, K., Foster, K. R. & Lopez, D. (2014). Evolution of resistance to a last-resort antibiotic in *Staphylococcus aureus* via bacterial competition. *Cell*, 158 (5): 1060-1071. doi: 10.1016/j.cell.2014.06.046.
- Koenig, R. L., Ray, J. L., Maleki, S. J., Smeltzer, M. S. & Hurlburt, B. K. (2004). *Staphylococcus aureus* AgrA binding to the RNAlII-agr regulatory region. *J Bacteriol*, 186 (22): 7549-7555. doi: 10.1128/JB.186.22.7549-7555.2004.
- Kritikos, G., Banzhaf, M., Herrera-Dominguez, L., Koumoutsi, A., Wartel, M., Zietek, M. & Typas, A. (2017). A tool named Iris for versatile high-throughput phenotyping in microorganisms. *Nat Microbiol*, 2: 17014-17014. doi: 10.1038/nmicrobiol.2017.14.
- Lauderdale, K. J., Boles, B. R., Cheung, A. L. & Horswill, A. R. (2009). Interconnections between Sigma B, agr, and proteolytic activity in *Staphylococcus aureus* biofilm maturation. *Infect Immun*, 77 (4): 1623-1635. doi: 10.1128/IAI.01036-08.
- Le, K. Y. & Otto, M. (2015). Quorum-sensing regulation in staphylococci-an overview. *Front Microbiol*, 6: 1174-1174. doi: 10.3389/fmicb.2015.01174.
- Le, K. Y., Villaruz, A. E., Zheng, Y., He, L., Fisher, E. L., Nguyen, T. H., Ho, T. V., Yeh, A. J., Joo, H.-S., Cheung, G. Y. C., et al. (2019). Role of Phenol-Soluble Modulins in *Staphylococcus epidermidis* Biofilm Formation and Infection of Indwelling Medical Devices. *J Mol Biol*, 431 (16): 3015-3027. doi: <https://doi.org/10.1016/j.jmb.2019.03.030>.
- Lee, P. Y., Costumbrado, J., Hsu, C.-Y. & Kim, Y. H. (2012). Agarose gel electrophoresis for the separation of DNA fragments. *J Vis Exp* (62): 3923. doi: 10.3791/3923.
- Liew, A. T. F., Theis, T., Jensen, S. O., Garcia-Lara, J., Foster, S. J., Firth, N., Lewis, P. J. & Harry, E. J. (2011). A simple plasmid-based system that allows rapid generation of tightly controlled gene expression in *Staphylococcus aureus*. *Microbiology*, 157 (Pt 3): 666-676. doi: 10.1099/mic.0.045146-0.
- Lindsay, J. A. (2014). *Staphylococcus aureus* genomics and the impact of horizontal gene transfer. *Int J Med Microbiol*, 304 (2): 103-109. doi: <https://doi.org/10.1016/j.ijmm.2013.11.010>.
- Lister, J. L. & Horswill, A. R. (2014). *Staphylococcus aureus* biofilms: recent developments in biofilm dispersal. *Front Cell Infect Microbiol*, 4: 178-178. doi: 10.3389/fcimb.2014.00178.
- Liu, G. Y. (2009). Molecular Pathogenesis of *Staphylococcus aureus* Infection. *Pediatr Res*, 65 (7): 71-77. doi: 10.1203/PDR.0b013e31819dc44d.
- Liu, I., Liu, M. & Shergill, K. (2006). The effect of spheroplast formation on the transformation efficiency in *Escherichia coli* DH5 $\alpha$ . *J Exp Microbiol Immunol*, 9: 81-85.
- Liu, X., Gallay, C., Kjos, M., Domenech, A., Slager, J., van Kessel, S. P., Knoops, K., Sorg, R. A., Zhang, J. R. & Veening, J. W. (2017). High-throughput CRISPRi phenotyping identifies new essential genes in *Streptococcus pneumoniae*. *Mol Syst Biol*, 13 (5): 931. doi: 10.15252/msb.20167449.
- Liu, Y., Zhang, J. & Ji, Y. (2020). Environmental factors modulate biofilm formation by *Staphylococcus aureus*. *Sci Prog*, 103 (1): 36850419898659. doi: 10.1177/0036850419898659.
- Lo, Y. M. D. & Chan, K. C. A. (2006). Introduction to the Polymerase Chain Reaction. In Lo, Y. M. D., Chiu, R. W. K. & Chan, K. C. A. (eds) *Clinical Applications of PCR*, pp. 1-10. Totowa, NJ: Humana Press.

## References

- Lowy, F. D. (1998). *Staphylococcus aureus* Infections. *N Engl J Med*, 339 (8): 520-532. doi: 10.1056/NEJM199808203390806.
- Mann, E. E., Rice, K. C., Boles, B. R., Endres, J. L., Ranjit, D., Chandramohan, L., Tsang, L. H., Smeltzer, M. S., Horswill, A. R. & Bayles, K. W. (2009). Modulation of eDNA release and degradation affects *Staphylococcus aureus* biofilm maturation. *PLoS One*, 4 (6): e5822-e5822. doi: 10.1371/journal.pone.0005822.
- Martí, M., Trotonda, M. P., Tormo-Más, M. Á., Vergara-Irigaray, M., Cheung, A. L., Lasa, I. & Penadés, J. R. (2010). Extracellular proteases inhibit protein-dependent biofilm formation in *Staphylococcus aureus*. *Microbes Infect*, 12 (1): 55-64. doi: <https://doi.org/10.1016/j.micinf.2009.10.005>.
- Mashruwala, A. A., Gries, C. M., Scherr, T. D., Kielian, T. & Boyd, J. M. (2017a). SaeRS Is Responsive to Cellular Respiratory Status and Regulates Fermentative Biofilm Formation in *Staphylococcus aureus*. *Infect Immun*, 85 (8): e00157-17. doi: 10.1128/IAI.00157-17.
- Mashruwala, A. A., Guchte, A. v. d. & Boyd, J. M. (2017b). Impaired respiration elicits SrrAB-dependent programmed cell lysis and biofilm formation in *Staphylococcus aureus*. *eLife*, 6: e23845. doi: 10.7554/eLife.23845.
- McCarthy, A. J. & Lindsay, J. A. (2010). Genetic variation in *Staphylococcus aureus* surface and immune evasion genes is lineage associated: implications for vaccine design and host-pathogen interactions. *BMC Microbiol*, 10: 173-173. doi: 10.1186/1471-2180-10-173.
- McNamara, P. J. & Proctor, R. A. (2000). *Staphylococcus aureus* small colony variants, electron transport and persistent infections. *Int J Antimicrob Agents*, 14 (2): 117-122. doi: [https://doi.org/10.1016/S0924-8579\(99\)00170-3](https://doi.org/10.1016/S0924-8579(99)00170-3).
- Meganathan, R. & Kwon, O. (2009). Biosynthesis of Menaquinone (Vitamin K2) and Ubiquinone (Coenzyme Q). *EcoSal Plus*, 3 (2): 10.1128/ecosalplus.3.6.3.3. doi: 10.1128/ecosalplus.3.6.3.3.
- Merritt, J. H., Kadouri, D. E. & O'Toole, G. A. (2005). Growing and analyzing static biofilms. *Curr Prot Microbiol*, Chapter 1: Unit-1B.1. doi: 10.1002/9780471729259.mc01b01s00.
- Mike, L. A., Dutter, B. F., Stauff, D. L., Moore, J. L., Vitko, N. P., Aranmolate, O., Kehl-Fie, T. E., Sullivan, S., Reid, P. R., DuBois, J. L., et al. (2013). Activation of heme biosynthesis by a small molecule that is toxic to fermenting *Staphylococcus aureus*. *Proc Natl Acad Sci USA*, 110 (20): 8206. doi: 10.1073/pnas.1303674110.
- Mir, A., Edraki, A., Lee, J. & Sontheimer, E. J. (2018). Type II-C CRISPR-Cas9 Biology, Mechanism, and Application. *ACS Chem Biol*, 13 (2): 357-365. doi: 10.1021/acscchembio.7b00855.
- Monk, I. R. & Foster, T. J. (2012). Genetic manipulation of Staphylococci-breaking through the barrier. *Fron Cell Infect Microbiol*, 2: 49-49. doi: 10.3389/fcimb.2012.00049.
- Monk, I. R., Tree, J. J., Howden, B. P., Stinear, T. P. & Foster, T. J. (2015). Complete Bypass of Restriction Systems for Major *Staphylococcus aureus*. *mBio*, 6 (3): e00308-15. doi: 10.1128/mBio.00308-15.
- Moormeier, D. E., Bose, J. L., Horswill, A. R. & Bayles, K. W. (2014). Temporal and Stochastic Control of *Staphylococcus aureus* Biofilm Development. *mBio*, 5 (5): e01341-14. doi: 10.1128/mBio.01341-14.
- Moormeier, D. E. & Bayles, K. W. (2017). *Staphylococcus aureus* biofilm: a complex developmental organism. *Mol Microbiol*, 104 (3): 365-376. doi: 10.1111/mmi.13634.
- Mrak, L. N., Zielinska, A. K., Beenken, K. E., Mrak, I. N., Atwood, D. N., Griffin, L. M., Lee, C. Y. & Smeltzer, M. S. (2012). saeRS and sarA act synergistically to repress protease

## References

- production and promote biofilm formation in *Staphylococcus aureus*. *PloS One*, 7 (6): e38453-e38453. doi: 10.1371/journal.pone.0038453.
- Naber, C. K. (2009). *Staphylococcus aureus* Bacteremia: Epidemiology, Pathophysiology, and Management Strategies. *Clin Infect Dis*, 48 (Supplement\_4): S231-S237. doi: 10.1086/598189.
- Natale, P., Brüser, T. & Driessen, A. J. M. (2008). Sec- and Tat-mediated protein secretion across the bacterial cytoplasmic membrane—Distinct translocases and mechanisms. *Biochim Biophys Acta*, 1778 (9): 1735-1756. doi: <https://doi.org/10.1016/j.bbamem.2007.07.015>.
- New England BioLabs. (2020a). *Everything You Ever Wanted to Know About Type II Restriction Enzymes*. Available at: <https://international.neb.com/tools-and-resources/feature-articles/everything-you-ever-wanted-to-know-about-type-ii-restriction-enzymes> (accessed: April 15, 2020).
- New England BioLabs. (2020b). *PCR Protocol for Phusion® High-Fidelity DNA Polymerase (M0530)*. Available at: <https://international.neb.com/protocols/0001/01/01/pcr-protocol-m0530> (accessed: April 4, 2020).
- Novick, R. (1967). Properties of a cryptic high-frequency transducing phage in *Staphylococcus aureus*. *Virology*, 33 (1): 155-166. doi: [https://doi.org/10.1016/0042-6822\(67\)90105-5](https://doi.org/10.1016/0042-6822(67)90105-5).
- Novick, R. P. (2003). Autoinduction and signal transduction in the regulation of *staphylococcal virulence*. *Mol Microbiol*, 48 (6): 1429-1449. doi: 10.1046/j.1365-2958.2003.03526.x.
- O'Gara, J. P. (2007). *ica* and beyond: biofilm mechanisms and regulation in *Staphylococcus epidermidis* and *Staphylococcus aureus*. *FEMS Microbiol Lett*, 270 (2): 179-188. doi: 10.1111/j.1574-6968.2007.00688.x.
- O'Toole, G. A. & Kolter, R. (1998). Initiation of biofilm formation in *Pseudomonas fluorescens* WCS365 proceeds via multiple, convergent signalling pathways: a genetic analysis. *Mol Microbiol*, 28 (3): 449-461. doi: 10.1046/j.1365-2958.1998.00797.x.
- Ogston, A. (1881). Report upon Micro-Organisms in Surgical Diseases. *Br Med J*, 1 (1054): 369.b2-369.b375. doi: 10.1136/bmj.1.1054.369.
- Ogston, A. (1882). Micrococcus Poisoning. *J Anat Physiol*, 16 (Pt 4): 526-567.
- Osipovitch, D. C., Therrien, S. & Griswold, K. E. (2015). Discovery of novel *S. aureus* autolysins and molecular engineering to enhance bacteriolytic activity. *Appl Microbiol Biotechnol*, 99 (15): 6315-6326. doi: 10.1007/s00253-015-6443-2.
- Otto, M. (2008). Staphylococcal biofilms. *Curr Top Microbiol Immun*, 322: 207-228. doi: 10.1007/978-3-540-75418-3\_10.
- Otto, M. (2013). Staphylococcal Infections: Mechanisms of Biofilm Maturation and Detachment as Critical Determinants of Pathogenicity. *Annu Rev Med*, 64 (1): 175-188. doi: 10.1146/annurev-med-042711-140023.
- Otto, M. (2014). *Staphylococcus aureus* toxins. *Curr Opin Microbiol*, 17: 32-37. doi: 10.1016/j.mib.2013.11.004.
- Paharik, A. E. & Horswill, A. R. (2016). The Staphylococcal Biofilm: Adhesins, Regulation, and Host Response. *Microbiol Spectr*, 4 (2): 10.1128/microbiolspec.VMBF-0022-2015. doi: 10.1128/microbiolspec.VMBF-0022-2015.
- Pantosti, A., Sanchini, A. & Monaco, M. (2007). Mechanisms of antibiotic resistance in *Staphylococcus aureus*. *Future Microbiol*, 2 (3): 323-34. doi: 10.2217/17460913.2.3.323.
- Peacock, S. J. & Paterson, G. K. (2015). Mechanisms of Methicillin Resistance in *Staphylococcus aureus*. *Annu Rev Biochem*, 84: 577-601. doi: 10.1146/annurev-biochem-060614-034516.

## References

- Peeters, E., Nelis, H. J. & Coenye, T. (2008). Comparison of multiple methods for quantification of microbial biofilms grown in microtiter plates. *J Microbiol Methods*, 72 (2): 157-165. doi: <https://doi.org/10.1016/j.mimet.2007.11.010>.
- Periasamy, S., Joo, H. S., Duong, A. C., Bach, T. H., Tan, V. Y., Chatterjee, S. S., Cheung, G. Y. & Otto, M. (2012). How *Staphylococcus aureus* biofilms develop their characteristic structure. *Proc Natl Acad Sci USA*, 109 (4): 1281-6. doi: 10.1073/pnas.1115006109.
- Peschel, A. & Otto, M. (2013). Phenol-soluble modulins and staphylococcal infection. *Nat Rev Microbiol*, 11 (10): 667-673. doi: 10.1038/nrmicro3110.
- Peters, J. M., Colavin, A., Shi, H., Czarny, T. L., Larson, M. H., Wong, S., Hawkins, J. S., Lu, C. H. S., Koo, B.-M., Marta, E., et al. (2016). A Comprehensive, CRISPR-based Functional Analysis of Essential Genes in Bacteria. *Cell*, 165 (6): 1493-1506. doi: 10.1016/j.cell.2016.05.003.
- Peton, V. & Le Loir, Y. (2014). *Staphylococcus aureus* in veterinary medicine. *Infect Genet Evol*, 21: 602-615. doi: <https://doi.org/10.1016/j.meegid.2013.08.011>.
- Porayath, C., Suresh, M. K., Biswas, R., Nair, B. G., Mishra, N. & Pal, S. (2018). Autolysin mediated adherence of *Staphylococcus aureus* with Fibronectin, Gelatin and Heparin. *Int J Biol Macromol*, 110: 179-184. doi: 10.1016/j.ijbiomac.2018.01.047.
- Prax, M., Lee, C. Y. & Bertram, R. (2013). An update on the molecular genetics toolbox for staphylococci. *Microbiology*, 159 (Pt 3): 421-435. doi: 10.1099/mic.0.061705-0.
- Qi, Lei S., Larson, Matthew H., Gilbert, Luke A., Doudna, Jennifer A., Weissman, Jonathan S., Arkin, Adam P. & Lim, Wendell A. (2013). Repurposing CRISPR as an RNA-Guided Platform for Sequence-Specific Control of Gene Expression. *Cell*, 152 (5): 1173-1183. doi: 10.1016/j.cell.2013.02.022.
- Queck, S. Y., Jameson-Lee, M., Villaruz, A. E., Bach, T.-H. L., Khan, B. A., Sturdevant, D. E., Ricklefs, S. M., Li, M. & Otto, M. (2008). RNAlII-independent target gene control by the agr quorum-sensing system: insight into the evolution of virulence regulation in *Staphylococcus aureus*. *Mol Cell*, 32 (1): 150-158. doi: 10.1016/j.molcel.2008.08.005.
- Ramesh, R., Munshi, A. & Panda, S. K. (1992). Polymerase chain reaction. *Natl Med J India*, 5 (3): 115-9.
- Rani, S. A., Pitts, B., Beyenal, H., Veluchamy, R. A., Lewandowski, Z., Davison, W. M., Buckingham-Meyer, K. & Stewart, P. S. (2007). Spatial patterns of DNA replication, protein synthesis, and oxygen concentration within bacterial biofilms reveal diverse physiological states. *J Bacteriol*, 189 (11): 4223-4233. doi: 10.1128/JB.00107-07.
- Ray, V. A., Morris, A. R. & Visick, K. L. (2012). A semi-quantitative approach to assess biofilm formation using wrinkled colony development. *J Vis Exp* (64): e4035-e4035. doi: 10.3791/4035.
- Rechtin, T. M., Gillaspay, A. F., Schumacher, M. A., Brennan, R. G., Smeltzer, M. S. & Hurlburt, B. K. (1999). Characterization of the SarA virulence gene regulator of *Staphylococcus aureus*. *Mol Microbiol*, 33 (2): 307-16. doi: 10.1046/j.1365-2958.1999.01474.x.
- Regassa, L. B., Novick, R. P. & Betley, M. J. (1992). Glucose and nonmaintained pH decrease expression of the accessory gene regulator (agr) in *Staphylococcus aureus*. *Infect Immun*, 60 (8): 3381-8.
- Reyrat, J. M., Pelicic, V., Gicquel, B. & Rappuoli, R. (1998). Counterselectable markers: untapped tools for bacterial genetics and pathogenesis. *Infect Immun*, 66 (9): 4011-4017.
- Rice, K. C., Mann, E. E., Endres, J. L., Weiss, E. C., Cassat, J. E., Smeltzer, M. S. & Bayles, K. W. (2007). The cidA murein hydrolase regulator contributes to DNA release and biofilm

## References

- development in *Staphylococcus aureus*. *Proceedings of the National Academy of Sciences of the United States of America*, 104 (19): 8113-8118. doi: 10.1073/pnas.0610226104.
- Rudra, P. & Boyd, J. M. (2020). Metabolic control of virulence factor production in *Staphylococcus aureus*. *Curr Opin Microbiol*, 55: 81-87. doi: <https://doi.org/10.1016/j.mib.2020.03.004>.
- Sanjana, N. E. (2017). Genome-scale CRISPR pooled screens. *Anal Biochem*, 532: 95-99. doi: <https://doi.org/10.1016/j.ab.2016.05.014>.
- Sato'o, Y., Hisatsune, J., Yu, L., Sakuma, T., Yamamoto, T. & Sugai, M. (2018). Tailor-made gene silencing of *Staphylococcus aureus* clinical isolates by CRISPR interference. *PLoS One*, 13 (1): e0185987-e0185987. doi: 10.1371/journal.pone.0185987.
- Scherr, T. D., Hanke, M. L., Huang, O., James, D. B. A., Horswill, A. R., Bayles, K. W., Fey, P. D., Torres, V. J. & Kielian, T. (2015). *Staphylococcus aureus* Biofilms Induce Macrophage Dysfunction Through Leukocidin AB and Alpha-Toxin. *mBio*, 6 (4): e01021-15. doi: 10.1128/mBio.01021-15.
- Schlafer, S. & Meyer, R. L. (2017). Confocal microscopy imaging of the biofilm matrix. *J Microbiol Methods*, 138: 50-59. doi: <https://doi.org/10.1016/j.mimet.2016.03.002>.
- Schwartz, K., Syed, A. K., Stephenson, R. E., Rickard, A. H. & Boles, B. R. (2012). Functional Amyloids Composed of Phenol Soluble Modulins Stabilize *Staphylococcus aureus* Biofilms. *PLoS Pathog*, 8 (6): e1002744. doi: 10.1371/journal.ppat.1002744.
- Serra, D. O. & Hengge, R. (2014). Stress responses go three dimensional - the spatial order of physiological differentiation in bacterial macrocolony biofilms. *Environ Microbiol*, 16 (6): 1455-1471. doi: 10.1111/1462-2920.12483.
- Serra, D. O., Klauck, G. & Hengge, R. (2015). Vertical stratification of matrix production is essential for physical integrity and architecture of macrocolony biofilms of *Escherichia coli*. *Environ Microbiol*, 17 (12): 5073-5088. doi: 10.1111/1462-2920.12991.
- Shukla, S. K. & Rao, T. S. (2017). An Improved Crystal Violet Assay for Biofilm Quantification in 96-Well Microtitre Plate. *bioRxiv*: 100214. doi: 10.1101/100214.
- Sigma-Aldrich. (2020). *REDTaq ReadyMix PCR Reaction Mix with MgCl2*. Available at: [https://bioresurs.uu.se/wp-content/uploads/2016/09/bilagan2013\\_3\\_d1s80tekniskbulletin.pdf](https://bioresurs.uu.se/wp-content/uploads/2016/09/bilagan2013_3_d1s80tekniskbulletin.pdf) (accessed: April 14, 2020).
- Singh, R., Ray, P., Das, A. & Sharma, M. (2010). Penetration of antibiotics through *Staphylococcus aureus* and *Staphylococcus epidermidis* biofilms. *J Antimicrob Chemother*, 65 (9): 1955-1958. doi: 10.1093/jac/dkq257.
- Stamsås, G. A., Myrbråten, I. S., Straume, D., Salehian, Z., Veening, J. W., Håvarstein, L. S. & Kjos, M. (2018). CozEa and CozEb play overlapping and essential roles in controlling cell division in *Staphylococcus aureus*. *Mol Microbiol*, 109 (5): 615-632. doi: 10.1111/mmi.13999.
- Styers, D., Sheehan, D. J., Hogan, P. & Sahm, D. F. (2006). Laboratory-based surveillance of current antimicrobial resistance patterns and trends among *Staphylococcus aureus*: 2005 status in the United States. *Anna Clin Microbiol Antimicrob*, 5: 2-2. doi: 10.1186/1476-0711-5-2.
- Svenningsen, S. L. (2018). Small RNA-Based Regulation of Bacterial Quorum Sensing and Biofilm Formation. *Microbiol Spectr*, 6 (4). doi: doi:10.1128/microbiolspec.RWR-0017-2018.
- Swarupa, V., Chaudhury, A. & Sarma, P. V. G. K. (2018). Iron enhances the peptidyl deformylase activity and biofilm formation in *Staphylococcus aureus*. *3 Biotech*, 8 (1): 32-32. doi: 10.1007/s13205-017-1050-9.

## References

- Thurlow, L. R., Hanke, M. L., Fritz, T., Angle, A., Aldrich, A., Williams, S. H., Engebretsen, I. L., Bayles, K. W., Horswill, A. R. & Kielian, T. (2011). *Staphylococcus aureus* Biofilms Prevent Macrophage Phagocytosis and Attenuate Inflammation In Vivo. *J Immunol*, 186 (11): 6585. doi: 10.4049/jimmunol.1002794.
- Tong, S. Y., Davis, J. S., Eichenberger, E., Holland, T. L. & Fowler, V. G., Jr. (2015). *Staphylococcus aureus* infections: epidemiology, pathophysiology, clinical manifestations, and management. *Clin Microbiol Rev*, 28 (3): 603-61. doi: 10.1128/cmr.00134-14.
- Visweswaran, G. R. R., Leenhouts, K., van Roosmalen, M., Kok, J. & Buist, G. (2014). Exploiting the peptidoglycan-binding motif, LysM, for medical and industrial applications. *Appl Microbiol Biotechnol*, 98 (10): 4331-4345. doi: 10.1007/s00253-014-5633-7.
- von Eiff, C., Becker, K., Machka, K., Stammer, H. & Peters, G. (2001). Nasal Carriage as a Source of *Staphylococcus aureus* Bacteremia. *N Engl J Med*, 344 (1): 11-16. doi: 10.1056/NEJM200101043440102.
- Wakeman, C. A., Hammer, N. D., Stauff, D. L., Attia, A. S., Anzaldi, L. L., Dikalov, S. I., Calcutt, M. W. & Skaar, E. P. (2012). Menaquinone biosynthesis potentiates haem toxicity in *Staphylococcus aureus*. *Mol Microbiol*, 86 (6): 1376-1392. doi: 10.1111/mmi.12063.
- Waters, E. M., Rowe, S. E., O'Gara, J. P. & Conlon, B. P. (2016). Convergence of *Staphylococcus aureus* Persister and Biofilm Research: Can Biofilms Be Defined as Communities of Adherent Persister Cells? *PLoS Pathog*, 12 (12): e1006012-e1006012. doi: 10.1371/journal.ppat.1006012.
- Wermser, C. & Lopez, D. (2018). Identification of *Staphylococcus aureus* genes involved in the formation of structured macrocolonies. *Microbiology*, 164 (5): 801-815. doi: 10.1099/mic.0.000660.
- Wertheim, H. F. L., Melles, D. C., Vos, M. C., van Leeuwen, W., van Belkum, A., Verbrugh, H. A. & Nouwen, J. L. (2005). The role of nasal carriage in *Staphylococcus aureus* infections. *Lancet Infect Dis*, 5 (12): 751-762. doi: [https://doi.org/10.1016/S1473-3099\(05\)70295-4](https://doi.org/10.1016/S1473-3099(05)70295-4).
- Whitchurch, C. B., Tolker-Nielsen, T., Ragas, P. C. & Mattick, J. S. (2002). Extracellular DNA required for bacterial biofilm formation. *Science*, 295 (5559): 1487. doi: 10.1126/science.295.5559.1487.
- Williams, R. E. (1963). Healthy carriage of *Staphylococcus aureus*: its prevalence and importance. *Bacteriol Rev*, 27 (1): 56-71.
- Zhang, F., Wen, Y. & Guo, X. (2014). CRISPR/Cas9 for genome editing: progress, implications and challenges. *Hum Mol Genet*, 23 (R1): R40-R46. doi: 10.1093/hmg/ddu125.
- Zhao, C., Shu, X. & Sun, B. (2017). Construction of a Gene Knockdown System Based on Catalytically Inactive ("Dead") Cas9 (dCas9) in *Staphylococcus aureus*. *Appl Environ Microbiol*, 83 (12): e00291-17. doi: 10.1128/AEM.00291-17.
- Zoll, S., Pätzold, B., Schlag, M., Götz, F., Kalbacher, H. & Stehle, T. (2010). Structural basis of cell wall cleavage by a staphylococcal autolysin. *PLoS Pathog*, 6 (3): e1000807-e1000807. doi: 10.1371/journal.ppat.1000807.

## Appendix

### A1 List of *E. coli* strains used or constructed in this work

Strain	Genotype and characteristics <sup>1</sup>	Source or reference
IM08B	DH10B, $\Delta dcm$ , $P_{\text{help}}\text{-}hsdMS$ , $P_{N25}\text{-}hsdS$ (strain expressing the <i>S. aureus</i> CC8 specific methylation genes)	Monk et al., 2015
MM2	IM08B, but pVL2336-sgRNA(ctaA), amp <sup>R</sup>	This work
MM3	IM08B, but pVL2336-sgRNA(mqo), amp <sup>R</sup>	This work
MM4	IM08B, but pVL2336-sgRNA(purA), amp <sup>R</sup>	This work
MM5	IM08B, but pVL2336-sgRNA(purK), amp <sup>R</sup>	This work
MM12	IM08B, but pVL2336-sgRNA(1118-fakA), amp <sup>R</sup>	This work
MM13	IM08B, but pVL2336-sgRNA(pckA), amp <sup>R</sup>	This work
MM14	IM08B, but pVL2336-sgRNA(fbp), amp <sup>R</sup>	This work
MM15	IM08B, but pVL2336-sgRNA(00030), amp <sup>R</sup>	This work
MM16	IM08B, but pVL2336-sgRNA(gdpS), amp <sup>R</sup>	This work
MM17	IM08B, but pVL2336-sgRNA(stp1), amp <sup>R</sup>	This work
MM18	IM08B, but pVL2336-sgRNA(clpP), amp <sup>R</sup>	This work
MM19	IM08B, but pVL2336-sgRNA(icaA), amp <sup>R</sup>	Lab collection
MM20	IM08B, but pVL2336-sgRNA(icaB), amp <sup>R</sup>	Lab collection
MM21	IM08B, but pVL2336-sgRNA(icaC), amp <sup>R</sup>	Lab collection
MM22	IM08B, but pVL-2336-sgRNA(icaD), amp <sup>R</sup>	Lab collection
MM23	IM08B, but pVL2336-sgRNA(ftsH), amp <sup>R</sup>	Lab collection
MM24	IM08B, but pVL2336-sgRNA(clfA), amp <sup>R</sup>	Lab collection
MM25	IM08B, but pVL2336-sgRNA(clfB), amp <sup>R</sup>	Lab collection
MM26	IM08B, but pVL2336-sgRNA(eno), amp <sup>R</sup>	Lab collection
MM27	IM08B, but pVL2336-sgRNA(capA), amp <sup>R</sup>	Lab collection
MM28	IM08B, but pVL2336-sgRNA(00502), amp <sup>R</sup>	Lab collection
MM29	IM08B, but pVL2336-sgRNA(clpB), amp <sup>R</sup>	Lab collection
MM30	IM08B, but pVL2336-sgRNA(sarA), amp <sup>R</sup>	Lab collection
MM31	IM08B, but, pVL2336-sgRNA(fnbA), amp <sup>R</sup>	Lab collection
MM32	IM08B, but, pVL2336-sgRNA(fnbB), amp <sup>R</sup>	Lab collection
MM33	IM08B, but, pVL2336-sgRNA(sdrC), amp <sup>R</sup>	Lab collection
MM34	IM08B, but, pVL2336-sgRNA(sdrD), amp <sup>R</sup>	Lab collection
MM35	IM08B, but, pVL2336-sgRNA(agrA), amp <sup>R</sup>	Lab collection
MM36	IM08B, but, pVL2336-sgRNA(psm $\alpha$ 1-4), amp <sup>R</sup>	Lab collection
MM37	IM08B, but, pVL2336-sgRNA(psm $\beta$ 1-2), amp <sup>R</sup>	Lab collection
MM39	IM08B, but, pVL2336-sgRNA(atl), amp <sup>R</sup>	Lab collection
MM40	IM08B, but, pVL2336-sgRNA(sasG), amp <sup>R</sup>	Lab collection
MM70	IM08B, but, pVL2336-sgRNA(mpfA), amp <sup>R</sup>	This work
MM123	IM08B, but, pVL2336-sgRNA(00671+atl), amp <sup>R</sup>	This work
MM124	IM08B, but, pVL2336-sgRNA(00671+sle1), amp <sup>R</sup>	This work
MM125	IM08B, but, pVL2336-sgRNA(atl + sle1), amp <sup>R</sup>	This work
MM145	IM08B, but pMAD-GG- $\Delta$ 00671, amp <sup>R</sup>	This work
MM147	IM08B, but pMAD-GG- $\Delta$ 01487, amp <sup>R</sup>	This work
MM152	IM08B, but pLOW-00671, amp <sup>R</sup>	This work

<sup>1</sup> amp; ampicillin

**A2 List of *S. aureus* strains used or constructed in this work**

<b>Strain</b>	<b>Genotype and characteristics<sup>1</sup></b>	<b>Reference</b>
<i>S. aureus</i> SH1000		
S9	SH1000, but pLOW-dCas9, Ery <sup>R</sup>	Lab collection
IM246	S9, but pCG248-sgRNA (00225), ery <sup>R</sup> , cam <sup>R</sup>	Lab collection
IM247	S9, but pCG248-sgRNA(00344), ery <sup>R</sup> , cam <sup>R</sup>	Lab collection
IM248	S9, but pCG248-sgRNA(00444), ery <sup>R</sup> , cam <sup>R</sup>	Lab collection
IM249	S9, but pCG248-sgRNA(00762), ery <sup>R</sup> , cam <sup>R</sup>	Lab collection
IM250	S9, but pCG248-sgRNA(00892), ery <sup>R</sup> , cam <sup>R</sup>	Lab collection
IM253	S9, but pCG248-sgRNA(01477), ery <sup>R</sup> , cam <sup>R</sup>	Lab collection
IM255	S9, but pCG248-sgRNA(01622), ery <sup>R</sup> , cam <sup>R</sup>	Lab collection
IM256	S9, but pCG248-sgRNA(01702), ery <sup>R</sup> , cam <sup>R</sup>	Lab collection
IM257	S9, but pCG248-sgRNA(01722), ery <sup>R</sup> , cam <sup>R</sup>	Lab collection
IM258	S9, but pCG248-sgRNA(01757), ery <sup>R</sup> , cam <sup>R</sup>	Lab collection
IM260	S9, but pCG248-sgRNA(01782), ery <sup>R</sup> , cam <sup>R</sup>	Lab collection
IM262	S9, but pCG248-sgRNA(02280), ery <sup>R</sup> , cam <sup>R</sup>	Lab collection
IM293	S9, but pCG248-sgRNA(walR), ery <sup>R</sup> , cam <sup>R</sup>	Lab collection
MH185	S9, but pVL2336-sgRNA(lytM), ery <sup>R</sup> , cam <sup>R</sup>	Lab collection
MH186	S9, but pVL2336-sgRNA(sle1), ery <sup>R</sup> , cam <sup>R</sup>	Lab collection
MH187	S9, but pVL2336-sgRNA(00671), ery <sup>R</sup> , cam <sup>R</sup>	Lab collection
MH188	S9, but pVL2336-sgRNA(00773), ery <sup>R</sup> , cam <sup>R</sup>	Lab collection
MH189	S9, but pVL2336-sgRNA(sceD), ery <sup>R</sup> , cam <sup>R</sup>	Lab collection
MH190	S9, but pVL2336-sgRNA(ssaA), ery <sup>R</sup> , cam <sup>R</sup>	Lab collection
MH191	S9, but pVL2336-sgRNA(02576), ery <sup>R</sup> , cam <sup>R</sup>	Lab collection
MH192	S9, but pVL2336-sgRNA(02855), ery <sup>R</sup> , cam <sup>R</sup>	Lab collection
MH193	S9, but pVL2336-sgRNA(02883), ery <sup>R</sup> , cam <sup>R</sup>	Lab collection
MH194	S9, but pVL2336-sgRNA(isaA), ery <sup>R</sup> , cam <sup>R</sup>	Lab collection
MM6	S9, but pVL2336-sgRNA(mqo), ery <sup>R</sup> , cam <sup>R</sup>	This work
MM7	S9, but pVL2336-sgRNA(purK), ery <sup>R</sup> , cam <sup>R</sup>	This work
MM8	S9, but pVL2336-sgRNA(purA), ery <sup>R</sup> , cam <sup>R</sup>	This work
MM10	S9, but pVL2336-sgRNA(luc), ery <sup>R</sup> , cam <sup>R</sup>	Lab collection
MM11	S9, but pVL2336-sgRNA(01908), ery <sup>R</sup> , cam <sup>R</sup>	Lab collection
MM41	S9, but pVL2336-sgRNA(icaA), ery <sup>R</sup> , cam <sup>R</sup>	Lab collection
MM42	S9, but pVL2336-sgRNA(icaB), ery <sup>R</sup> , cam <sup>R</sup>	Lab collection
MM43	S9, but pVL2336-sgRNA(icaC), ery <sup>R</sup> , cam <sup>R</sup>	Lab collection
MM44	S9, but pVL-2336-sgRNA(icaD), ery <sup>R</sup> , cam <sup>R</sup>	Lab collection
MM45	S9, but pVL2336-sgRNA(ftsH), ery <sup>R</sup> , cam <sup>R</sup>	Lab collection
MM46	S9, but pVL2336-sgRNA(clfA), ery <sup>R</sup> , cam <sup>R</sup>	Lab collection
MM47	S9, but pVL2336-sgRNA(clfB), ery <sup>R</sup> , cam <sup>R</sup>	Lab collection
MM48	S9, but pVL2336-sgRNA(Eno), ery <sup>R</sup> , cam <sup>R</sup>	Lab collection
MM49	S9, but pVL2336-sgRNA(capA), ery <sup>R</sup> , cam <sup>R</sup>	Lab collection
MM50	S9, but pVL2336-sgRNA(ctsR), ery <sup>R</sup> , cam <sup>R</sup>	Lab collection
MM51	S9, but pVL2336-sgRNA(clpB), ery <sup>R</sup> , cam <sup>R</sup>	Lab collection
MM52	S9, but pVL2336-sgRNA(sarA), ery <sup>R</sup> , cam <sup>R</sup>	Lab collection
MM53	S9, but pVL2336-sgRNA(fnbA), ery <sup>R</sup> , cam <sup>R</sup>	Lab collection
MM54	S9, but pVL2336-sgRNA(fnbB), ery <sup>R</sup> , cam <sup>R</sup>	Lab collection
MM55	S9, but pVL2336-sgRNA(sdrC), ery <sup>R</sup> , cam <sup>R</sup>	Lab collection
MM56	S9, but pVL2336-sgRNA(sdrD), ery <sup>R</sup> , cam <sup>R</sup>	Lab collection
MM57	S9, but pVL2336-sgRNA(agrA), ery <sup>R</sup> , cam <sup>R</sup>	Lab collection
MM58	S9, but pVL2336-sgRNA(psm $\alpha$ 1-4), ery <sup>R</sup> , cam <sup>R</sup>	Lab collection

Appendix

MM59	S9, but pVL2336-sgRNA(psmβ1-2), ery <sup>R</sup> , cam <sup>R</sup>	Lab collection
MM60	S9, but pVL2336-sgRNA(sasG), ery <sup>R</sup> , cam <sup>R</sup>	Lab collection
MM62	S9, but pVL2336-sgRNA(Atl), ery <sup>R</sup> , cam <sup>R</sup>	Lab collection
MM63	S9, but pVL2336-sgRNA(1118-fakA), ery <sup>R</sup> , cam <sup>R</sup>	This work
MM64	S9, but pVL2336-sgRNA(stp1), ery <sup>R</sup> , cam <sup>R</sup>	This work
MM65	S9, but pVL2336-sgRNA(gdpS), ery <sup>R</sup> , cam <sup>R</sup>	This work
MM66	S9, but pVL2336-sgRNA(00030), ery <sup>R</sup> , cam <sup>R</sup>	This work
MM67	S9, but pVL2336-sgRNA(fbp), ery <sup>R</sup> , cam <sup>R</sup>	This work
MM68	S9, but pVL2336-sgRNA(pckA), ery <sup>R</sup> , cam <sup>R</sup>	This work
MM69	S9, but pVL2336-sgRNA(clpP), ery <sup>R</sup> , cam <sup>R</sup>	This work
MM71	S9, but pVL2336-sgRNA(mpfA), ery <sup>R</sup> , cam <sup>R</sup>	This work
<hr/>		
<i>S. aureus</i> NCTC8325-4		
MH225	NCTC8325-4, but pLOW_dCas9_extra_lacO, ery <sup>R</sup>	Lab collection
MM73	MH225, but pVL2336-sgRNA(atl), ery <sup>R</sup> , cam <sup>R</sup>	This work
MM74	MH225, but pVL2336-sgRNA(icaA), ery <sup>R</sup> , cam <sup>R</sup>	This work
MM75	MH225, but pVL2336-sgRNA(luc), ery <sup>R</sup> , cam <sup>R</sup>	This work
MM111	MH225, but pVL2336-sgRNA(walR), ery <sup>R</sup> , cam <sup>R</sup>	Lab collection
MM112	MH225, but pVL2336-sgRNA(lytM), ery <sup>R</sup> , cam <sup>R</sup>	Lab collection
MM113	MH225, but pVL2336-sgRNA(sle1), ery <sup>R</sup> , cam <sup>R</sup>	Lab collection
MM114	MH225, but pVL2336-sgRNA(00671), ery <sup>R</sup> , cam <sup>R</sup>	Lab collection
MM115	MH225, but pVL2336-sgRNA(00773), ery <sup>R</sup> , cam <sup>R</sup>	Lab collection
MM116	MH225, but pVL2336-sgRNA(sceD), ery <sup>R</sup> , cam <sup>R</sup>	Lab collection
MM117	MH225, but pVL2336-sgRNA(ssaA), ery <sup>R</sup> , cam <sup>R</sup>	Lab collection
MM118	MH225, but pVL2336-sgRNA(02576), ery <sup>R</sup> , cam <sup>R</sup>	Lab collection
MM119	MH225, but pVL2336-sgRNA(02855), ery <sup>R</sup> , cam <sup>R</sup>	Lab collection
MM120	MH225, but pVL2336-sgRNA(02883), ery <sup>R</sup> , cam <sup>R</sup>	Lab collection
MM121	MH225, but pVL2336-sgRNA(02887), ery <sup>R</sup> , cam <sup>R</sup>	Lab collection
MM129	MH225, but pVL2336-sgRNA(00671+atl), ery <sup>R</sup> , cam <sup>R</sup>	This work
MM130	MH225, but pVL2336-sgRNA(00671+sle1), ery <sup>R</sup> , cam <sup>R</sup>	This work
MM131	MH225, but pVL2336-sgRNA(atl+sle1), ery <sup>R</sup> , cam <sup>R</sup>	This work
MM149	NCTC8325-4, Δ00671::Spc	This work
MM151	NCTC8325-4, but pLOW-00671	This work
MM154	MM149, but pLOW-00671	This work
<hr/>		
<i>S. aureus</i> Newman		
MH226	Newman, but pLOW_dCas9_extra_lacO, ery <sup>R</sup>	Lab collection
MM76	MH226, but pCG248-sgRNA(luc), ery <sup>R</sup> , cam <sup>R</sup>	This work
MM77	MH226, but pVL2336-sgRNA(Atl), ery <sup>R</sup> , cam <sup>R</sup>	This work
MM78	MH226, but pVL2336-sgRNA(icaA), ery <sup>R</sup> , cam <sup>R</sup>	This work
MM79	MH226, but pVL2336-sgRNA(pckA), ery <sup>R</sup> , cam <sup>R</sup>	This work
MM80	MH226, but pVL2336-sgRNA(mpfA), ery <sup>R</sup> , cam <sup>R</sup>	This work
MM81	MH226, but pVL2336-sgRNA(clpP), ery <sup>R</sup> , cam <sup>R</sup>	This work
MM82	MH226, but pVL2336-sgRNA(1118-fakA), ery <sup>R</sup> , cam <sup>R</sup>	This work
MM83	MH226, but pVL2336-sgRNA(agrA), ery <sup>R</sup> , cam <sup>R</sup>	This work
MM84	MH226, but pVL2336-sgRNA(01908), ery <sup>R</sup> , cam <sup>R</sup>	This work
MM85	MH226, but pVL2336-sgRNA(purK), ery <sup>R</sup> , cam <sup>R</sup>	This work
MM86	MH226, but pVL2336-sgRNA(mqo), ery <sup>R</sup> , cam <sup>R</sup>	This work
MM87	MH226, but pVL2336-sgRNA(purA), ery <sup>R</sup> , cam <sup>R</sup>	This work
MM88	MH226, but pVL2336-sgRNA(Fbp), ery <sup>R</sup> , cam <sup>R</sup>	This work
MM90	MH226, but pVL2336-sgRNA(00030), ery <sup>R</sup> , cam <sup>R</sup>	This work
MM91	MH226, but pVL2336-sgRNA(stp1), ery <sup>R</sup> , cam <sup>R</sup>	This work
MM92	MH226, but pVL2336-sgRNA(sasG), ery <sup>R</sup> , cam <sup>R</sup>	This work

## Appendix

MM93	MH226, but pVL2336-sgRNA(psm $\alpha$ 1-4), ery <sup>R</sup> , cam <sup>R</sup>	This work
MM94	MH226, but pVL2336-sgRNA(psm $\beta$ 1-2), ery <sup>R</sup> , cam <sup>R</sup>	This work
MM95	MH226, but pVL2336-sgRNA(sdrD), ery <sup>R</sup> , cam <sup>R</sup>	This work
MM96	MH226, but pVL2336-sgRNA(sdrC), ery <sup>R</sup> , cam <sup>R</sup>	This work
MM97	MH226, but pVL2336-sgRNA(fnbB), ery <sup>R</sup> , cam <sup>R</sup>	This work
MM98	MH226, but pVL2336-sgRNA(fnbA), ery <sup>R</sup> , cam <sup>R</sup>	This work
MM99	MH226, but pVL2336-sgRNA(sarA), ery <sup>R</sup> , cam <sup>R</sup>	This work
MM100	MH226, but pVL2336-sgRNA(clpB), ery <sup>R</sup> , cam <sup>R</sup>	This work
MM102	MH226, but pVL2336-sgRNA(icaB), ery <sup>R</sup> , cam <sup>R</sup>	This work
MM103	MH226, but pVL2336-sgRNA(clfB), ery <sup>R</sup> , cam <sup>R</sup>	This work
MM104	MH226, but pVL2336-sgRNA(ftsH), ery <sup>R</sup> , cam <sup>R</sup>	This work
MM105	MH226, but pVL2336-sgRNA(icaD), ery <sup>R</sup> , cam <sup>R</sup>	This work
MM106	MH226, but pVL2336-sgRNA(icaC), ery <sup>R</sup> , cam <sup>R</sup>	This work
MM107	MH226, but pVL2336-sgRNA(capA), ery <sup>R</sup> , cam <sup>R</sup>	This work
MM108	MH226, but pVL2336-sgRNA(Eno), ery <sup>R</sup> , cam <sup>R</sup>	This work
MM109	MH226, but pVL2336-sgRNA(00502), ery <sup>R</sup> , cam <sup>R</sup>	This work
MM110	MH226, but pVL2336-sgRNA(gdpS), ery <sup>R</sup> , cam <sup>R</sup>	This work
MM122	MH226, but pVL2335-sgRNA(clfA), ery <sup>R</sup> , cam <sup>R</sup>	This work

---

<sup>1</sup>ery; erythromycin, spc; spectinomycin, cam; chloramphenicol

**A3 List of sgRNA sequences**

sgRNA sequences were designed by Morten Kjos (NMBU) and Xue Liu (University of Lausanne, Switzerland). The sgRNAs were designed using the genome of *S. aureus* NCTC8325-4.

<b>Accession number</b>	<b>Name</b>	<b>sgRNA sequence</b>
SAOUHSC_00019	<i>purA</i>	CTCCGCCAAATTGAATGGTA
SAOUHSC_00020	<i>walR</i>	AATTCTAAAATATCAGCAAT
SAOUHSC_00114	<i>capA</i>	TGAGTATTAGCTTGATATTT
SAOUHSC_00248	<i>LytM</i>	CATTTGTGTATGTGCTTGTT
SAOUHSC_00411	<i>psmA1-4</i>	CAAGATATATTGGCCACGTG
SAOUHSC_00427	<i>Sle1</i>	ATTGCCCACTGATTCACC
SAOUHSC_00486	<i>ftsH</i>	TGATTATATGTAAGCTGTTT
SAOUHSC_00544	<i>sdrC</i>	GAAAATTTGTTTAATCGATT
SAOUHSC_00545	<i>sdrD</i>	CGAAAATTTATTTAATCGAT
SAOUHSC_00620	<i>sarA</i>	TAACTGCTTTAACAACCTTG
SAOUHSC_00671	Uncharacterized	ATACCAAGTTGTTATCTAAT
SAOUHSC_00705	Uncharacterized	TGACCAGATAAATGTTCTTC
SAOUHSC_00711	<i>mpfA</i>	TTCTGAACCAACAAATACAG
SAOUHSC_00760	<i>gdpS</i>	TTTCTGAATACTGTAAGCGA
SAOUHSC_00762	<i>tagO</i>	TTCGATATTGCAATAACAAT
SAOUHSC_00773	Uncharacterized	GATACATAATTATGTTGAAC
SAOUHSC_00790	<i>clpP</i>	TTTGTGTTTCAATAACTGT
SAOUHSC_00799	<i>eno</i>	GCGTAAACATCTGTAATAAT
SAOUHSC_00812	<i>clfA</i>	ACGTTTGTGTCGTCTGTTTT
SAOUHSC_00912	<i>clpB</i>	TTATCAATTGGTTTGCTTGT
SAOUHSC_00994	<i>atl</i>	AGCGTTAATGCAACCATTGA
SAOUHSC_01008	<i>purE-D</i>	GATACTACTGTTTTTCGTA
SAOUHSC_01135	<i>psmβ1-2</i>	ATTATTAATTGCTGCAGTTA
SAOUHSC_01182	<i>def2</i>	GTTAAAATAGGATGCGATGC
SAOUHSC_01192	<i>fakA</i>	TACAATACCATAACATTCAA
SAOUHSC_01418	<i>sucA</i>	AAATTCGCACCGAAGTTTAC
SAOUHSC_01487	<i>ubiE</i>	ATACCAGTAACCTTCACCTGT
SAOUHSC_01657	<i>ZnuC</i>	ACATTTTTCAATTCAAAGAC
SAOUHSC_01910	<i>pckA</i>	GAAAGTTGAAAATGTGACGT
SAOUHSC_01962	<i>hemE</i>	GCTTGTCGCATAAACCAAAC
SAOUHSC_01983	<i>fumC</i>	GCACCCCAATATTTATCTGC
SAOUHSC_02265	<i>agrA</i>	CATAAGGATTATCAGTTGCG
SAOUHSC_02333	<i>sceD</i>	TAAGTCCGCTTCACTTGCAAT
SAOUHSC_02571	<i>ssaA</i>	CTATATGATGTTGGGTGCTT
SAOUHSC_02576	Uncharacterized	TGTAGGATAGCGCCTTTAGA
SAOUHSC_02647	<i>mgo</i>	ACATTTGAACTCTCTTCGCC
SAOUHSC_02798	<i>sasG</i>	CAATCTTCACTTCTTTTGAT
SAOUHSC_02802	<i>fnbB</i>	GTTACTTGTGTTGATTGTGA
SAOUHSC_02803	<i>fnbA</i>	GTTACTTGTGTTGCGTTTGA
SAOUHSC_02822	<i>fbp</i>	ACGAAATGTTCCGTACCTTT
SAOUHSC_02855	Uncharacterized	CGATTGATGCGTTTGTTCGA
SAOUHSC_02861	Uncharacterized	AAAAGTTCCAATCGTCCTAC
SAOUHSC_02883	Uncharacterized	ATGTCCTGCAAATGCGATAG
SAOUHSC_02887	<i>isaA</i>	GAGCTGCATTTAATTGATCT
SAOUHSC_02963	<i>clfB</i>	TTAGCCGTTGTATTTAATTG

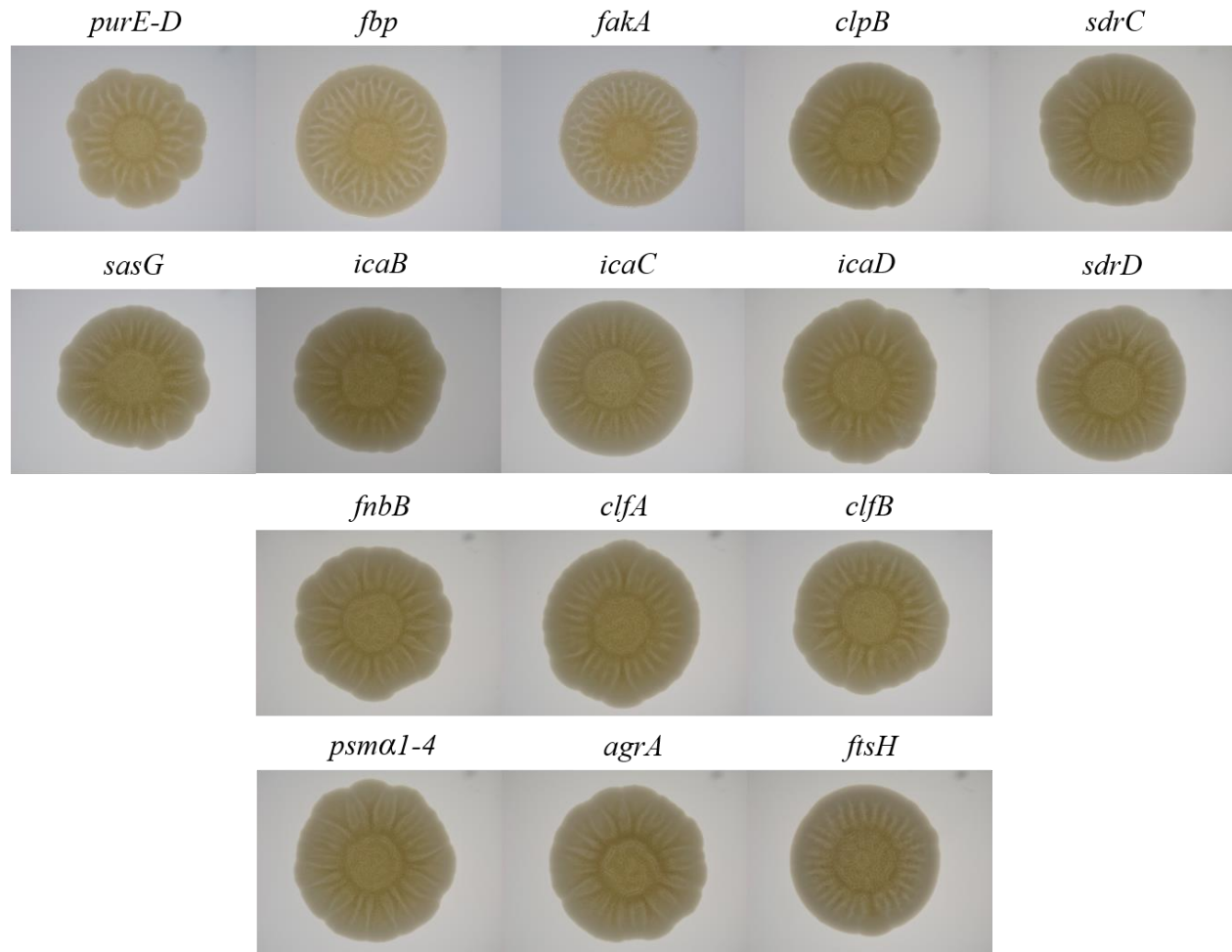
## Appendix

SAOUHSC_03002	<i>icaA</i>	CAGTAAATAGACATAAATAC
SAOUHSC_03003	<i>icaD</i>	GTTGGGTATTCCTCTGTCT
SAOUHSC_03004	<i>icaB</i>	TGACCATCCAGTGTGCTTAC
SAOUHSC_03005	<i>icaC</i>	AATGTAAAATTGTAACACTA

---

#### A4 Macrocolony formation by *S. aureus* Newman CRISPRi strains

Gene expression was knocked down using CRISPRi. Macrocolonies were grown on TSBMg agar and imaged after 5 days.



**A5 Sequence alignments****A5.1 Sequence alignments SAOUHSC\_00671 and SsaA**

57% identity, 68% positives

SAOUHSC_00671	148	SNGNASSFNHQNL	YTAGQCTWYV	FD	RR	AAQAGSP	ISTY	WSDAKY	WAGNA	ANDGYQ	VNNTPS	207
		SNG AS	NLYT+GQCT+YV	FDR		G I + W +A	WA	AA+ GY	VNNTP			
SsaA	144	SNGYASG---	SNLYTSGQCTYV	FDR---		VGGKIGSTWGN	ASNWANA	AAASSG	YTVNNTPK			197
SAOUHSC_00671	208	VGSIMQSTPGPY	GHVAYVERV	NGDGS	SILISEM	NYTYGPY	NMNYRTI	PASEV	SSYAFI	H		265
		VG+IMQ+T G	YGHVAYVE VN	+GS+ +SEM	NY +G	+ RTI	A++ SY	FIH				
SsaA	198	VGAIMQTTQGY	YGHVAYVEG	VNSNGS	SVRSEM	NYGHG	AGVVT	SRTISAN	QAGSYN	FIH		255

**A5.2 Sequence alignment SAOUHSC\_00671 and Sle1**

46% identity, 66% positives

SAOUHSC_00671	29	HTVQSGESLWS	IAQKYNTS	VESIKQ	NNQLD	NNLVFP	GGQVIS	VGGSDA	QNTSNT	-----	SP	83			
		+TVQ+G+SL	IA KY T+ ++I	+ N L+N	++PGQ	+ V G+ + + + +	S								
sle1	93	YTVQAGDSL	S	LIASKY	GTTYQ	NIMRLN	GLNFFI	YPGQ	KLKVS	GTASS	SNAAS	NSSRPST	152		
SAOUHSC_00671	84	QAGSASSHTVQ	AGESLN	IASRYG	VSDQL	MAANL	RGYL	IMP	NQTLQ	IPNGG	SGGTTPT	143			
		+G S +TVQ	AG+SL++IAS	+YG + ++M+	N L + I	P Q L++	S +								
sle1	153	NSGGGSYYT	VQAGDSL	S	LIASKY	GTTYQ	KIMSLN	GLNFFI	YPGQ	KLKVT	GNAST	NSGSA	212		
SAOUHSC_00671	144	ATTG	SNGNASSFNHQ	NLYTAGQ	CTWYV	FD	RR	AAQAGSP	ISTY	WSDAKY	WAGNA	ANDGYQ	VN	203	
		TT N F+HQ	NLYT GQCT++	VF+RRA+ G	ISTYW	+A W	AA DGY	++							
sle1	213	TTTNR	GYNTPV	F	SHQNL	YTWGQ	CTYHVF	NRRAE	IGK	ISTY	W	WNANN	WDNAAA	DGYTID	272
SAOUHSC_00671	204	NTPSVGSIMQ	STPGPYGH	VAYVERV	NGDGS	SILISEM	NYTYGPY	NMNYRTI	PASEV	SSYAF		263			
		N P+VGS	I Q+ G	YGHV +VER	VN DGS	IL+SEM	NY+ P +	YRT+PA	+V++Y +						
sle1	273	NRPTVGS	IAQTDV	GYGHV	M	FVERV	NNDGS	ILVSEM	NYSAAP	GILT	YRTV	PAYQ	VNNYRY	332	
SAOUHSC_00671	264	IH	265												
		IH													
sle1	333	IH	334												

**A5.3 Sequence alignment of NWMN\_RS14065 of *S. aureus* and AdaB of *B. subtilis***

45% identity, 61% positives

NWMN_RS14065	56	YFKGDNPEIT	IPLKPTG	SHFQ	QCVW	NELRQ	VPYGT	LTTYG	AI	AKK	VGKLL	NKPK	MSAQAV	115	
		Y +G	T+P++	G+ FQ	VWN L	++PYG	+Y IA	+ NKP	+ +AV						
AdaB	72	YLEGKRKN	F	TVPEY	AGTQ	FQLAV	WNAL	CEIPY	GQTK	SYSDI	ANDI	----	NKPA-AVR	AV	126
NWMN_RS14065	116	GGAVGSNPL	SII	VPCHR	VVGKT	GS	LTG	FGGT	INN	KIKL	LELE	NID	MSKLY	VP	167
		G A+G+NP+	I	VPCHR	+GK	GS	LTG+ G	K	LL+LE	S++	VP				
AdaB	127	GAAIGAN	PVLIT	VPCHR	VIGK	NGSL	TGYR	GGF	FEMK	TLL	LDLE	KRAS	SEMD	V	178

## **A6 Abbreviations**

ADP	Adenosine diphosphate
AIP	Autoinducing peptide
ATP	Adenosine triphosphate
BHI	Brain heart infusion
Cas	CRISPR associated protein
CFU	Colony forming units
CHAP	Cysteine/histidine-dependent amidohydrolase/peptidase
CIP	Calf intestinal alkaline phosphatase
CLSM	Confocal laser scanning microscopy
CRISPR	Clustered regulatory interspaced short palindromic repeats
CRISPRi	CRISPR interference
crRNA	CRISPR RNA
CV	Crystal violet
CWA	Cell wall anchored
dCas9	Catalytically inactive Cas9 protein
DHNA	Carboxyl of 1,4-dihydroxy-2-naphthoate
DMK	Demethylmenaquinone
dNTP	deoxyribonucleotide triphosphate
ECDC	European Centre for Disease Control
ECM	Extracellular matrix
eDNA	Extracellular DNA
EDTA	Ethylenediaminetetraacetic acid
EEA	European Economic Area
EU	European union
gDNA	genomic DNA
HAI	Hospital acquired infection
HDR	Homology-directed repair

## Appendix

HGT	Horizontal gene transfer
IPTG	Isopropyl- $\beta$ -D-thiogalactosidase
LB	Lysogeny broth
MK	Menaquinone
MRSA	Methicillin resistant <i>Staphylococcus aureus</i>
MSCRAMM	Microbial surface components recognizing adhesive matrix molecules
MSSA	Methicillin sensitive <i>Staphylococcus aureus</i>
NHEJ	Nonhomologous end-joining
OD	Optical density
PAM	Protospacer adjacent motif
PCR	Polymerase chain reaction
PEP	Phosphoenolpyruvate
PIA	Polysaccharide intercellular adhesin
PNAG	Poly-N-acetylglucosamine
PSM	Phenol-soluble modulins
RM	Restriction modification
SDS	Sodium dodecyl sulphate
sgRNA	Single-guide RNA
TCA	Tricarboxylic acid
TCS	Two-component system
TSB	Tryptic soy broth
TSBGN	TSB supplemented with 1% glucose and 1% NaCl
TSBMg	TSB supplemented with 100 mM MgCl <sub>2</sub>
tracrRNA	Target-independent trans-activating crRNA
VISA	Vancomycin intermediate <i>Staphylococcus aureus</i>
VRSA	Vancomycin resistant <i>Staphylococcus aureus</i>
WT	Wild-type
WTA	Wall teichoic acid





**Norges miljø- og biovitenskapelige universitet**  
Noregs miljø- og biovitenskapelige universitet  
Norwegian University of Life Sciences

Postboks 5003  
NO-1432 Ås  
Norway